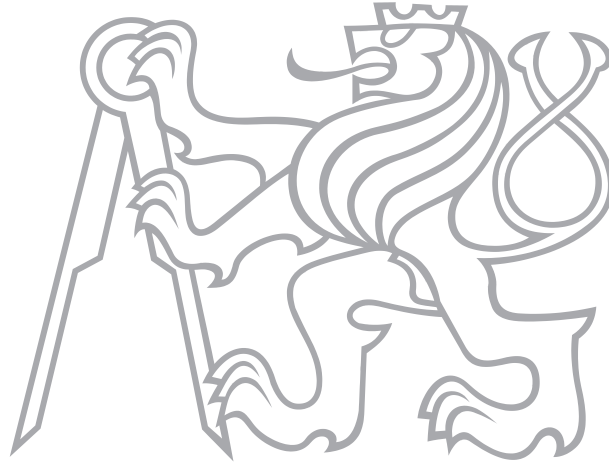Czech Technical University in Prague
Faculty of Electrical Engineering
Department of Electromagnetic Field

Daniel Havelka ~ *Doctoral Thesis*

August 2014

CZECH TECHNICAL UNIVERSITY IN PRAGUE
Faculty of Electrical Engineering ~ Department of Electromagnetic Field

RADIO-FREQUENCY ELECTRIC FIELD GENERATED BY VIBRATION MODES OF A MICROTUBULE

Doctoral Thesis

by

DANIEL HAVELKA

Prague, August 2014

Ph.D. Programme: Electrical Engineering and Information Technology
Branch of Study: Radioelectronics

Supervisor: Prof. Jan Vrba
Supervisor specialist: Dr. Michal Cifra

Institute of Photonics
and Electronics

CONTENTS

ACKNOWLEDGEMENTS

ABSTRACT

MOTIVATION

Previous research on protein dynamics was exclusively aimed at description of mechanical processes. However, it is well known that protein-based structures are usually highly electrically polar. The connection of these mechanical and electrical at phenomena was not studied yet.

AIM

The purpose of this study was to (i) develop a model describing the electromagnetic field generated by longitudinal mechanical vibrations of a microtubule and to (ii) apply this model for analysis of multi-mode excitation of a microtubule and single-mode excitation of microtubule networks.

METHODS

The presented model is based on (i) a coarse-grained structure of a microtubule, (ii) approximation of longitudinal vibration modes of a microtubule by longitudinal modes of inelastic string and (iii) approximation of the electromagnetic field generated by each grain by an oscillating electric dipole.

RESULTS AND CONCLUSIONS

The spatial pattern and temporal evolution of the high-frequency electric field coupled to vibrations of microtubules was calculated. The relevance of the model and described phenomena is discussed. Particularly, it is shown that the reported electromagnetic field of vibrating microtubule may play role in signaling e.g. in neurons or separation of genetic information in dividing cells.

RECOMMENDATION

The presented phenomena have to be confirmed experimentally. Development of more detailed model may verify presented results based on coarse-grained model.

KEYWORDS

microtubule; vibrations; electromagnetic field; mitotic spindle; bioelectrodynamics

ABSTRAKT

MOTIVACE

Ačkoli je známo, že proteinové struktury jsou obvykle vysoce polární, dosavadní výzkum jejich dynamiky se soustředil pouze na popis mechanických procesů. Spojení mezi těmito mechanickými a elektrickými fenomény nebylo dosud důkladně studováno.

CÍL

Účelem této studie bylo (i) vyvinout model popisující elektromagnetické pole generované longitudinálními mechanickými vibracemi mikrotubulu a (ii) použít tento model pro analýzu vícemódové excitace mikrotubulu a jednomódové excitace sítí mikrotubulů.

METODY

Předložený model je založen na (i) hrubozrnné struktuře mikrotubulu, (ii) aproximaci podélných vibračních módů mikrotubulu podélnými módy tuhé struny a (iii) aproximaci elektromagnetického pole vytvářeného jednotlivými zrny pomocí oscilujícího elektrického dipólu.

VÝSLEDKY A ZÁVĚR

Byla spočtena prostorová rozložení a časový vývoj vysokofrekvenčního elektrického pole generovaného mechanickými vibracemi mikrotubulu. Byl diskutován význam modelu a popsaných fenoménů. Jmenovitě bylo ukázáno, že elektromagnetické pole vibrujícího mikrotubulu může hrát roli v signalizaci např. v neuronech a v separaci genetické informace v dělících se buňkách.

DOPORUČENÍ

Prezentované jevy musí být experimentálně ověřeny. Vývoj detailnějšího modelu může ověřit předložené výsledky založené na hrubozrnném modelu.

KLÍČOVÁ SLOVA

mikrotubul; vibrace; elektromagnetické pole; mitotické vřeténko; bioelektrodynamika

PREFACE

Last four years were the happiest in my life up to now. The graduate studies, which I had actually never planned to go through, were very motivating for me and I was given the chance to experience many exciting things. Besides my studies and research, the work in academia provided me the opportunity to work as an occasional clerk, purchasing officer, technician, design engineer, graphic artist, typographer, lab and interior designer, driver, and barkeeper. Moreover, I met many wonderful people and I am glad that I can cooperate with them ever since.

In the course of my studies, I started a family with my marvelous wife Dana, who gave birth to our two children: Kubík and Barunka. Last four years were therefore not only filled in with my studies but also with marriage, making arrangements for our new home and taking care of our children. I would like to express my thanks to my family for making my studies possible in those hectic years, and also to my colleagues who were patient and enabled me to dedicate some time to caring for my family.

When I came to the University as an undergraduate student, I started to study electrical engineering but I was also interested in medicine and life sciences. My mother, and now also my younger sister, are nurses and they care for handicapped people. I have learned from them that the most important thing in one's life are kind people and, indeed, a good health. So, this was my very first motivation to connect my studies somehow with health sciences or biology. The last and the most intensive impulse which directed my professional interest towards life sciences was the death of my very good friend Jakub Filip, who passed away shortly after passing bachelor exams. His death has demonstrated to me how the human knowledge about physiology and diseases is, despite undoubted progress in medicine, still very limited. I would be very contended if results of my and my colleagues' work could have contributed, even if only a little, to better understanding to how the things work in living cells.

1 | INTRODUCTION

The fundamental question in molecular biology concerns the relation between structure and function of bio-macromolecules. Since these molecules are not merely static objects but they interact with the environment, it is also important to study their dynamic behavior. It has been shown that normal mode analysis of bio-macromolecular dynamics has functional relevance in biology [1]. Depending on the size of the macromolecular assemblies, the frequencies of lowest vibration modes lay in the range from MHz to GHz. Proteins and other biomolecules are also electrically polar. It is already known that electrostatics is important for proper function of proteins [2]. Because of the electric polarity, the vibration modes of bio-macromolecules have also the electromagnetic component. In this thesis we illustrate this fact on microtubules, the hollow cylindrical filaments of cytoskeleton. Despite the fact that electromagnetic activity of microtubules has been discussed for almost two decades, no detailed study of electrodynamic effects in microtubules has been ever published with the exception of pioneering estimate by Pokorný [3]. In order to overcome this gap, we developed a numerical model describing the high-frequency electric field connected with vibrations of a microtubule (Chapter 3 and Appendix A, [A1, A5]). We also discussed possible roles of the electromagnetic field of vibrating microtubule in physiology of a cell (Chapters 3 and 5, [A1, A2]).

There are several reasons for choosing microtubules for this pilot study. First of all, microtubules are present in almost every eukaryotic cell where they form a part of the cytoskeleton. Microtubules are structures which represent mechanical support of a cell, provide tracks for the movement of motor proteins, and they also play crucial role during the cell division by forming the mitotic spindle which is responsible for separation of duplicated genetic information. Secondly, tubulin heterodimer, the basic subunit of a microtubule, is highly electrically polar. It means that the microtubules are expected to generate electromagnetic field with higher efficiency compared to other protein-based structures. Last but not least, there are theoretical works which predicted functional relevance of the electromagnetic field of a microtubule in signaling [4], organization [5] and consciousness [6].

The question is whether there exists endogenous electromagnetic field with nontrivial biological role inside cells. Decisive experiments which would confirm the existence of biologically relevant electromagnetic field

were not performed yet but there exist several hypotheses suggesting the role of the filed [7, 8]. Besides intriguing, yet controversial, hypotheses there are also well established physical mechanisms which may explain potential relevance of electromagnetic field of vibrating microtubule. High intensities of the electric field may influence the activation energy of proteins, hydrogen bonding kinetics and it may act by a force on electrically charged, polar or polarizable particles. The magnetic component of the field may also have an effect on singlet and triplet radical pairs. However, the evaluation of these possible effects goes beyond the scope of this thesis. Our main goal was to develop the model of microtubule electrodynamics and estimate the intensities and the shape of the field.

2 | STATE OF THE ART

To avoid duplicity, more detailed overview of the current state of research on cellular electrodynamic phenomena and of microtubules is provided in introductory sections of following Chapters 3, 4, and 5 [A1, A3, A2] and in Appendicies A and B [A5, A4].

2.1 MICROTUBULE STRUCTURE AND ELECTRIC POLARITY

Microtubules, one part of the cytoskeleton, are hollow rods with inner diameter of 17 nm and outer diameter of 25 nm [9]. Length of microtubules may be between tens of nanometers up to several hundreds of micrometers. The body of a microtubule is usually composed of 13 protofilaments but occasionally it may be formed from 8 to 19 protofilaments [10, 11] and thus, smaller or larger radii, were also reported [12, 13]. Besides, the wall of a microtubule creates two types of helix lattices (A and B) [14–16] which have origin in lateral contacts between protofilaments [17]. Protofilament's basic subunit is the protein tubulin heterodimer (dimension of
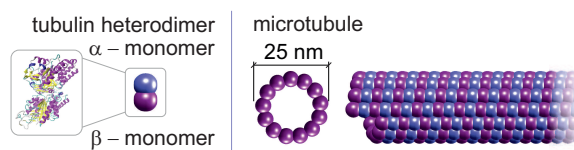
Figure 2.1: From left, the secondary structure of tubulin heterodimer, the schematic depiction of tubulin heterodimer, cross section of a microtubule and schematic depiction of a microtubule.

approximately 8 nm × 6.5 nm × 4.5 nm without C-termini [18]) and is divided into two approximately 55 kDa monomers of α-tubulin and β-tubulin. Nogales et al. [18] described the structure of both tubulins and observed that each monomer has more than 400 amino acids. Furthermore, the tubulin heterodimer (PDB entry: 1TUB) has high total static dipole moment of about 1 714 D [1] and static dipole moment in the direction of the axis of a microtubule of about 337 D as was shown by Tuszyński et al. [19]. Net charge of tubulin heterodimer is in

---

[1] 1 D = 3.3356×10^{-30} Cm and then 1 714 D = 5.7173×10^{-27} Cm

the range from −30 to 5 for pH in range from 8 to 4.5 [19], respectively. Static dipole moments of different α-tubulins and β-tubulins can be in a range from 700 D to 2 000 D and from 1 500 D to 4 000 D [20], respectively. The isoelectric point of the tubulin heterodimer was reported to range between 4.9 [21] and 5.6 [22].

2.2 MECHANICAL PARAMETERS OF A MICROTUBULE

The large discrepancies concern estimations of Young's modulus E, shear modulus G, and flexural rigidity EI of microtubule. The mechanical parameters of a microtubule are summarized in the Table 2.1 and the data are sorted by the year of publication. It can be seen that Young's modulus is in the range from 1 MPa to 2.56 GPa, shear modulus is in the range from 53 Pa to 50 MPa, and flexural rigidity is in the range from $0.02 \cdot 10^{-24}$ Nm^2 to $40 \cdot 10^{-24}$ Nm^2. The investigated lengths of microtubule are in the range from 0.1 μm to 68 μm. Note that (i) some authors estimated the Young's modulus from indentation and bending experiments where the shear between protofilaments also play a role, so the values of the Young's modulus would be valid only under condition that the microtubule is homogeneous and isotropic, that (ii) some of the values are missing due to the fact that they were not specified in the publication.

Equation for rough calculation of frequency range of the first longitudinal mode of mechanical vibrations of a microtubule based on the velocity of acoustic wave is

$$\upsilon = \sqrt{\frac{E}{\rho}} \tag{2.1}$$

$$L \sim \frac{\lambda}{2} \tag{2.2}$$

$$f = \frac{\upsilon}{\lambda} \tag{2.3}$$

where υ is the velocity of acoustic propagation, E is the longitudinal Young's modulus or the shear modulus, ρ is the mass density (around 1 300 ÷ 1 500 kg/m^3 for proteins), L corresponds to dimensions of microtubule and f is the frequency of microtubule vibrations. Using the values of mechanical properties of a microtubule which are shown in Table 2.1 we may estimate the range of the frequency of the first longitudinal mode to lay between 3.47 MHz and 4.23 GHz.[2]

2.3 EXCITATION OF MICROTUBULE VIBRATIONS ACCORDING TO FRÖHLICH AND POKORNÝ

The most influential hypothesis on electromagnetic activity of biological systems was proposed by Fröhlich at the end of 1960s. He proposed (i) the existence of electric polar longitudinal vibrations in biological systems,

---

[2]The lowest estimated frequency is calculated as $f_1 = \sqrt{0.001 \cdot 10^9/1300}/8 \cdot 10^{-6} = 3.47$ MHz and the highest estimated frequency is calculated as $f_2 = \sqrt{0.93 \cdot 10^9/1300}/200 \cdot 10^{-9} = 4.23$ GHz.

	E [GPa]	G [MPa]	EI 10^{-24}[Nm^2]	L [μm]	Stabilization	Method
Gittes [23]	1.20	-	21.5 ± 0.08	25 ÷ 65	Taxol	Thermal Fluctuations
Venier [24]	0.26 ± 0.02	-	4.7 ± 0.4	3 ÷ 8	Taxol	Thermal Fluctuations
	- **	-	4.8 ± 0.4	4 ÷ 9	Taxotere	Thermal Fluctuations
	1.43 ± 0.15	-	26 ± 2.7	9 ÷ 15	BeF$_3^-$	Thermal Fluctuations
	0.51 ± 0.05	-	9.2 ± 0.9	8 ÷ 15	None	Thermal Fluctuations
	1.6 ± 0.3	-	29 ± 5	9.1 ÷ 18.1	BeF$_3^-$	Hydrodynamic Flow
	0.47 ± 0.1	-	8.5 ± 2	9.1 ÷ 19	None	Hydrodynamic Flow
	1.37 ± 0.3	-	25 ± 5	9.5 ÷ 19	AlF$_4^-$	Hydrodynamic Flow
Kurachi [25]	0.60	-	10	10	Taxol	BFOT
	2.40	-	40	10	MAPs	BFOT
Mickey and	1.40	-	26 ± 2	24 ÷ 68	Caps	Thermal Fluctuations
Howard [26]	1.70	-	32 ± 2	24 ÷ 68	Taxol	Thermal Fluctuations
Vinckier [27]	0.001	-	-	4	Taxol	AFM (tapping mode)
	0.003	-	-	4	Taxotere	AFM (tapping mode)
Felgner [28]	-	-	1.0 ± 0.3	6.1 ÷ 14	Taxol	Optical Tweezers – R.
	-	-	3.7 ± 0.8	6.1 ÷ 14	None	Optical Tweezers – R.
	-	-	16 ± 3	6.1 ÷ 14	MAPs	Optical Tweezers – R.
	-	-	1.9 ± 0.1	3.8 ÷ 6.3	Taxol	Optical Tweezers – W.
	-	-	4.7 ± 0.4	3.8 ÷ 6.3	None	Optical Tweezers – W.
	-	-	18 ± 3	3.8 ÷ 6.3	MAPs	Optical Tweezers – W.
Kis [29]	> 0.10	1.4 ± 0.4	> 0.17	4.5	Taxol	AFM (contact mode)
de Pablo [30]	0.80	-	3.2	-	Taxol	AFM (tapping mode)
Needleman [31]	1.30	-	-	10	Taxol	SAXRD
Tuszyński [32]	1.32	53·10^{-6} ÷ 0.5	-	-	None	Simulation
Pampaloni [33]	1.51 ± 0.19	-	-	2.6 ÷ 47.5	Taxol	Thermal Fluctuations
Kikumoto [34]	0.12	-	2	15.7	Taxol	BFOT
	0.46	-	7.90	13.6	None	BFOT
Deriu [35]	0.93	50	3.7 ÷ 8.6	0.1 ÷ 0.32	None	Simulation
Sept [36]	2.20	47	-	-	APO	Simulation
	0.38	48	-	-	Taxol	Simulation
Feng [37]	1.97	-	0.02	-	None	Simulation
Sun [38]	2.56	0.21	-	-	None	Simulation

Table 2.1: Summary of experimental and theoretical findings on microtubule elastic properties. E is the Young's modulus, G is the shear modulus, EI is the flexural rigidity (where E is the Young's modulus and I is the second moment of inertia), and L is the length of microtubule. After polymerization with GTP, microtubules were capped with GMPCPP-tubulin "Caps", or stabilized with taxol, or stabilized with taxotere, or kept in apo state "APO", or stabilized with microtubule associated proteins (MAPs), or stabilized by BeF$_3^-$, or stabilized by AlF$_4^-$. "AFM" stands for the Atomic Force Microscopy, "BFOT" is a Buckling Force with Optical Traps, Optical Tweezers "R." and "W." stand for the RELAX and WIGGLE method, respectively, and "SAXRD" is the Small Angle X-ray Diffraction. "**" – the moment of inertia "I" is $1.820 \cdot 10^{-32}$ m^4 and E is calculated from EI as 0.264 ± 0.02 GPa.

(ii) condensation of energy to the lowest frequency modes, and (iii) coherent vibrational states [39–42].

Electrical and mechanical properties of microtubules were studied separately by several authors in the past three decades, but Pokorný connected these two parts of research together and published his work on biological electromagnetism [5, 43] based on Fröhlich's hypotesis at the turn of new millennium. Few years later

Pokorný summarized his ideas in six postulates [8]: I. "Eukaryotic living cells generate an endogenous electromagnetic field; the field is coherent"; II. "Microtubules are non-linear oscillating structures generating an electromagnetic field in living cells"; III. "Mitochondria establish conditions for generation of the electromagnetic field"; IV. "Synchronization, force effects for transport, interactions, morphology, and information transfer are functions of the electromagnetic field"; V. "Consciousness, instinct of self-preservation, and the central control function of the brain and less developed structures depend on quantum electrodynamic processes" and VI. "Disturbances of the energy processing system and the coherent electrodynamic state far from thermodynamic equilibrium produce pathological states, in particular cancer".

Pokorný and Jelínek [44, 45] analyzed three possibilities of energy supply to microtubules. The energy supply may be provided, firstly, from the guanosine-5'-triphosphate (GTP) hydrolysis if the microtubules grow (tubulin polymerization) or shrink (microtubule depolymerization). Secondly, the movement of motor proteins, if the motor proteins transport cargo along the microtubules or if they help during cell division, could also contribute to excitation of vibrations in microtubules. Finally, the "wasted" energy efflux from the mitochondria, which are "power plants" of the cell and which are generating adenosine triphosphate (ATP), may contribute to energy supply to microtubules. In mitochondrion, less then 50 % of energy is stored in the ATP and more then 50 % of energy is released in the form of heat and emitted radiation to the vicinity of mitochondria. It is worth noting that the mitochondria are spatially correlated with microtubule network (see Figure 2.2). Therefore, the microtubules are exposed to strong electrostatic field of about 10^6 V/m [46], which extends several micrometers from the mitochondrion probably as a result of the creation of a proton gradient across the inner membrane of the mitochondrion. It is expected that this mitochondrial electrostatic field shifts the microtubule vibrations to the non-linear regime of the Fröhlich's hypothesis and enables the excitation of polar vibrations of microtubules above their thermal level and an electromagnetic field can be generated [47].
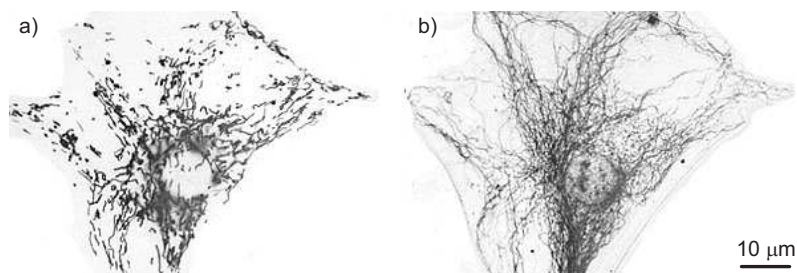
Figure 2.2: "Relationship between mitochondria and microtubules. a) Light micrograph of chains of elongated mitochondria in a living mammalian cell in culture. The cell was stained with a vital fluorescent dye (rhodamine 123) that specifically labels mitochondria. b) Immuno-fluorescence micrograph of the same cell stained (after fixation) with fluorescent antibodies that bind to microtubules. Note that the mitochondria tend to be aligned along microtubules." Alberts et al. [9]

2.4 MECHANICAL VIBRATION MODES OF A MICROTUBULE

Mechanical vibrations of a microtubule have been studied by several authors using several techniques in the past few decades.

Sirenko et al. [48] modeled microtubules by a thin elastic cylindrical shell with isotropic mechanical properties in fluid. Numerical calculations of eigenfrequencies and of eigenmodes of elastic vibrations were based on experimentally measured Young's modulus [24]. This continuum model predicted existence of acoustically non-radiative elastic waves with maximum frequencies of about 10 GHz. There are three types of axisymmetric acoustic waves (longitudinal, torsional and radial) with speed in a range from 200 ms^{-1} to 600 ms^{-1} in the long-wavelength limit $k_z \ll 1/R$ under the condition $m = 0$ (where m is the azimuthal number, k_z is the longitudinal wave vector and R is the central radius of a microtubule).

Pokorný et al. analyzed vibrations of microtubules modeled as one dimensional chain of mass using a method similar to that employed for description of lattice vibrations in solid-state physics [43]. Elastic force constants in the range from 10^{-6} Nm to 10^{-2} Nm were used in calculation of dispersion relations which reveal that vibrations of microtubules could have acoustical branch and optical branch. The highest frequency of vibrations is around 100 MHz while the lowest frequency of the acoustical branch is in the band from 5 MHz to 50 MHz if the length of a microtubule is 10 μm.

Porter et al. [49] described the microscopic dynamical properties of microtubules by a discrete model. Vibration frequencies and velocities are expressed as functions of the elastic constants and of the geometrical characteristics of the microtubules. Results showed that vibrations which propagate along the protofilament do so significantly faster than those along the helix.

Orthotropic and isotropic elastic shell models of microtubule vibrations were developed by Wang et al. [50–52]. The orthotropic model provides detailed analysis of circumferential vibrations of a microtubule and also points out that a parabolic dispersion law does not apply to the circumferential modes. If both models are compared, it appears that the isotropic model substantially overestimates the frequencies of all vibration modes except for axisymmetric longitudinal modes and beam-like bending modes.

Qian et al. [53] modeled orthotropic elastic shell with Young's modulus E_x, circumferential Young's modulus E_θ, shear modulus $G_{x\theta}$ and longitudinal Poisson ratio ν_x along the longitudinal direction identically as Wang [50–52]. It is shown that strong anisotropy of microtubules causes substantially lower velocities of both torsional and radial waves. However, it does not affect longitudinal wave velocity. In many cases, it is found that one of three wave velocities in orthotropic microtubules depends on the wave vector non-monotonically and reaches a minimum velocity around a specific value of the wave vector. In particular, this interesting phenomenon would not exist if microtubules were isotropic.

Vibration analysis of a single microtubule surrounded by cytoplasm was performed by Ghavanloo et al. [54]. The microtubule was modeled as a linear elastic cylindrical tube and the cytosol motion was modeled according to Stokes flow with no-slip condition at the microtubule-cytosol interface. The calculation shows that viscosity

and stiffness of cytoplasm play crucial role in the dynamic behavior of the microtubule. The frequencies increase with decreasing length of the microtubule and increase with increasing Young's modulus.

A mechanical model including the effect of the viscous cytosol and surrounding filaments was developed by Daneshmand and Amabili [55] for analysis of vibrations of a single microtubule immersed in cytoplasm. The model of a microtubule is created by the first-order shear deformation shell theory for orthotropic materials, whereas the cytosol motion is modeled by the Stokes flow. It is shown that the longitudinal modes are the same with or without fluid effect in the first-order shear deformation theory and also in the classic theory.

Deriu et al. [35] developed a coarse-grained elastic network model of the entire 13:3 B-lattice microtubule. In particular, molecular dynamics was used to refine the molecular conformation and composition of the tubulin dimers (the structure is available on the GCSB Protein DataBank - 1TUB code) inside the microtubule lattice. Four main modes are identified: stretching, bending, torsion and circumferential. Figure 2.3 depicts the frequency dependency on the length of microtubule. Frequencies from 1 GHz up to 25 GHz and mode num-
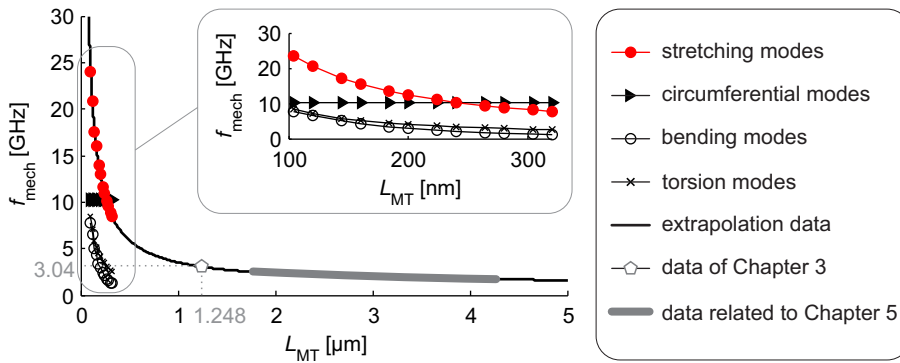

Figure 2.3: Major vibration modes of microtubule are determined by Deriu et al. [35] and recalculated for weight of tubulin heterodimer of 97 kDa. Frequency as a function of the length of a microtubule is shown for stretching modes (solid circles), circumferential modes (solid triangles), bending modes (empty circles) and torsion modes (crosses). The black thin line describes extrapolation of data of stretching modes for longer microtubules up to 350 nm. The pentagon and thick gray line depicts frequencies of stretching modes which would correspond to lengths used in Chapters 3 and 5, respectively. Note that there is a difference between data actually used in Chapters 3 and 5; the Chapter 5 uses exactly the data from ref. [35] while in Chapter 3 there were used data recalculated to correspond to more realistic values of microtubule parameters, namely its mass.

bers of 7 to 30 as a function of radius r_M with respect to length of a microtubule (r_M/L_{MT}) were calculated. Bending stiffness (k_f), torsion stiffness (k_t) and stretching stiffness (k_s) were calculated for length of entire microtubule (100 ÷ 350 nm) and bending modulus (Y_f), stretching modulus (Y_x) and shear modulus (G) were also calculated.

In conclusion, several types of vibration modes (bending, longitudinal, torsional, breathing, etc.) have been identified in above mention works spanning from tens of megahertz to tens of gigahertz. The following Figure 2.4 depicts the comparison of dispersion relations of longitudinal modes calculated in refs. [35, 48, 50–52, 55].
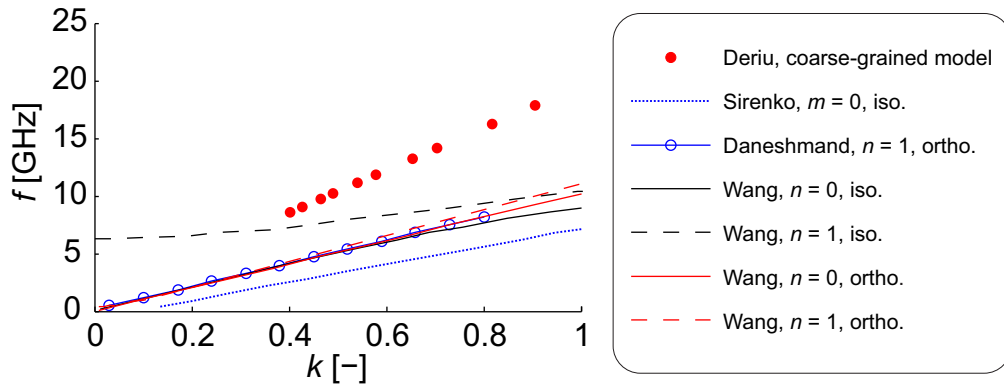
Figure 2.4: Comparison between longitudinal modes of a microtubule according to several models. Parameters of the models are the following. Deriu et al. [35]: average radius r = 10.35 nm, Young modulus E = 0.93 GPa, shear modulus E_θ = 50 MPa. Note, that the data are recalculated for weight of tubulin heterodimer of 97 kDa. Sirenko et al. [48]: r = 12.8 nm, E = 0.5 ± 0.1 GPa, Poisson ratio ν = 0.3, density of mass ρ = 1.47 g/cm^3. Wang et al. [50–52]: r = 12.8 nm, E = 1 GPa, E_θ = 1 MPa, ν = 0.3, ρ = 1.47 g/cm^3, α = 1 and β = 0.35 (iso.), α = β = 0.001 (ortho.). Daneshmand and Amabili [55]: r = 12.8 nm, E = 1 GPa, E_θ = 1 MPa, ν = 0.3, ρ = 1.47 g/cm^3. ("iso." – isotropic shell model, "ortho." – orthotropic shell model, n – wave number, m – azimuthal number, wave vector k = rk_z, where k_z is the axial wave vector).

2.5 Damping of mechanical vibrations of a microtubule

There are no direct measurements which would quantify damping of microtubule vibrations. However, there exists an assumption that the mechanical vibrations of microtubules are viscously overdamped in the cytosol [56,57]. It is worth noting that even the systems which are highly damped could oscillate if driven by an ideal source of force in its vicinity (for example a wave-like movement of an axoneme caused by axonemal motor protein dynein [9]). Nevertheless, there exist several hypotheses according to which the mechanical vibrations of microtubules and other biological nano-objects might not be overdamped.

Liu et al. [58] showed that microwave absorption by virus particles increased when hydrophilicity of virus surface is increased by changing the pH of suspension. In other words, increased viscoelastic transition of hydration shell contributes to decrease of the damping of mechanical vibrations of the viruses. The viral particles were roughly spherical with a diameter of 29.5 ± 0.5 nm and in range of the pH 5.2, 5.95, 6.2 and 7.2 they had the Q-factors of 10.2, 4.0, 4.5 and 5.0, respectively. Moreover, several layers of organized water molecules above the biomolecule interface can be detected and visualized by atomic force microscopy as presented by Fukuma [59] and Kimura et al. [60]. Microtubules, like the majority of proteins in the a cell, have a hydrophilic surface thus the exclusion zones could exist in vicinity of microtubule wall. Stebbings and Hunt [22] observed "clear zones" of width in the range from 5 nm to 20 nm around microtubules fixed at pH 7.6 by cryo-electron microscopy. However, these "clear zones" disappeared at pH 5.6 as microtubules were touching each other and formed bundles.

Pokorný et al. [61–64] proposed that on the surface of the microtubule exists a slip layer which is formed

by attracted ions. The slip layer could have thickness of about 1 nm and shear modulus of 5 Pa and protect vibrations from damping by viscose cytosol.

Fuchs et al. [65] observed that high electric field could organize water. Trombitas et al. [66] found organized water (exclusion zones) near mitochondria. Pokorný et al. [8,67] assumes that the strong electrostatic field from mitochondria organizes water (creates exclusion zones) near the microtubule.

Samarbakhsh and Tuszyński [68] performed theoretical analysis of forced bending-mode vibrations of microtubules in a viscous medium like cytosol. They showed that the Q-factor is frequency dependent and may range from 0.2 to almost 4.[3] Longitudinal modes are expected to be less damped compared to bending modes since they cause only limited displacement of the surrounding cytosol [55,69]

2.6 Electrodynamic models of a microtubule

Pioneering work on the electromagnetic field of vibrating microtubule was performed by Pokorný [3] in 1998. He developed a linear model of mechanical vibrations of a microtubule by using a method which was based on the approximation of the microtubule by a chain of masses connected by springs. He considered the frequency of mechanical longitudinal vibrations to be $f = 100$ MHz, permittivity of ambient medium $\varepsilon' = 81$, length of microtubule $L_m = 3$ µm and the mode number $N = 7$. The intensity of oscillating electric field along microtubule was estimated using multi-pole approximation in some distances (10 nm, 100 nm and 500 nm) from microtubule wall. The intensity of electric field was higher than 10^{-5} V/m in the distance of 10 nm from microtubule wall.

In the model of microtubule with a slip boundary condition [61–63] Pokorný analyzed the effect of the slip ionic layer between the wall of the microtubule and the cytosol in frequency range from 1 MHz to 20 MHz. It was shown that in case of 1 nm thick layer at frequency 10 MHz the relative relaxation time of microtubule vibrations τ_{rel} could be around 100. Pokorný also hypothesized about the role of discussed field in the motion of molecules and charges [5]. He proved that the transport of mass driven by the electric field with omnipresent thermal component has greater probability to reach the target than the transport only by thermal motion itself. No other models have been developed yet.

---

[3]The Q-factor lower than 0.5 corresponds to an overdamped system which shows no oscillatory response.

2.7 Goals of the thesis

This thesis has the following goals:

| To develop a coarse-grained model of high-frequency electric field generated by longitudinal vibration modes of a microtubule.

| To analyze multi-mode excitation of a microtubule.

| To estimate radiated electromagnetic power from symmetrical and asymmetrical network of vibrating microtubules.

| To model oscillating electric field of vibrating mitotic spindle.

| To hypothesize about the role of modeled electric field in cellular physiology and morphogenesis.

3 | MULTI-MODE ELECTRO-MECHANICAL VIBRATIONS OF A MICROTUBULE: IN SILICO DEMONSTRATION OF ELECTRIC PULSE MOVING ALONG A MICROTUBULE

This chapter is a version of:

Author contributions:

| Designed research: O.K. and M.C.

| Performed research: **D.H.**

| Analysed data: **D.H.**, M.C. and O.K.

| Wrote the paper: O.K.

| Candidate's contribution: 50%

The manuscript carries the following acknowledgements:

Multi-mode electro-mechanical vibrations of a microtubule: *In silico* demonstration of electric pulse moving along a microtubule

Daniel Havelka,[1,2] Michal Cifra,[1] and Ondřej Kučera[1,a]

[1]*Institute of Photonics and Electronics, Academy of Sciences of the Czech Republic, Prague, Czechia*
[2]*Department of Electromagnetic Field, Faculty of Electrical Engineering, Czech Technical University in Prague, Prague, Czechia*

Microtubules are known to be involved in intracellular signaling. Here, we show *in silico* that electrically polar collective vibration modes of microtubules form electric oscillating potential which is quasi-periodic both in space and in time. While single mode microtubule vibration excites an electric field with spatially stationary local minima and maxima of the electric field, the multimode excitation causes the formation of an electric pulse and many transient local electric field minima. The biophysical mechanism we describe lends support to the view that microtubules may comprise a substrate for ultra-fast electrical signaling in neurons or other living cells. © 2014 AIP Publishing LLC. [http://dx.doi.org/10.1063/1.4884118]

Microtubules (MTs) are self-assembling protein homo-polymer mesostructures present in virtually every eukaryotic cell, where they form the major components of the cytoskeleton. Microtubules (referred to as MTs in the following) are not merely a passive support of a cell, but they are highly dynamic structures involved in cell motility, intracellular transport, and signaling. MTs represent extensive substrate for biochemical interactions within the cell, because the surface area of MTs inside the cell is roughly comparable with the surface area of the plasma membrane.[1] While biochemical and mechanical signaling pathways involving MTs are the subject of experimental research, here we report *in silico* foundations for electrodynamic signaling pathways along microtubules.

A single MT resembles a tube with its inner and outer diameters of 17 nm and 25 nm, respectively, and its length is in the range of few tens of nanometers to several micrometers. Figs. 1(a)–1(d) show the schematic structure of the MT. The tube consists usually of 13 protofilaments. The building subunits of a MT are the tubulin heterodimers (∼100 kDa) composed of alpha- and beta-tubulin. The tubulin heterodimers have been theoretically calculated to have a rather high electric dipole moment of over 1000 Debye,[2] which may vary among the tubulin isotypes. Any accelerated motion of a MT gives, therefore, rise to electrodynamic phenomena. Unfortunately, only very limited experimental data exists with connection to the electrical properties of MTs. In the low frequency region (cca. <0.5 GHz), there are few published works available which aimed to experimentally verify electric and dielectric properties of MTs,[3–6] but there is no published data on dielectric and electrodynamic properties of microtubules in the range from 230 MHz to 2 THz. A study of the high-frequency electric field generated by MTs is important since (i) it provides better understanding of the role of endogenous and external electromagnetic fields in cell physiology, (ii) it estimates limits of prospective

artificial bio-electronic devices based on MTs,[7] and (iii) it should help to clarify the role of microtubules in intriguing, yet controversial, hypotheses on biological electrodynamic signaling,[8] organization,[9] and consciousness.[10]

Accelerated movement of MTs is connected to the generation of a non-stationary electromagnetic field. Experimentally documented mechanical events involving microtubules take place on rather large time scales where ions provide efficient screening of the generated electromagnetic fields. Nevertheless, this screening is much less efficient at higher frequencies where MTs are expected to have natural vibration modes. Many theoretical works exist which focus on the estimation of MT vibrations using various models.[11–17] Several types of vibration modes (bending, longitudinal, torsional, breathing, etc.) have been identified spanning from several tens of MHz to several hundreds of GHz. There is an ongoing debate on the vibrational properties of MTs, especially on the issue of damping of MT vibrations. It is not clear yet whether MTs are able to accumulate energy in a resonant manner, or if they can transmit the
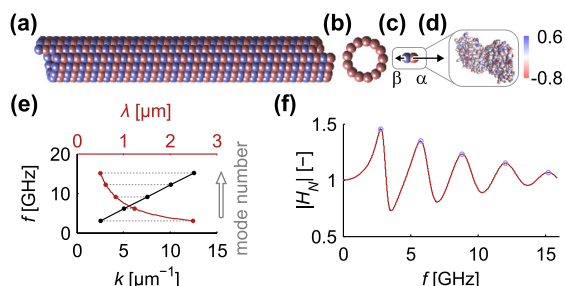
FIG. 1. (a) A schematic depiction of a MT structure and its cross-section (b). A tubulin heterodimer with longitudinal projection of its static dipole moments indicated by arrows (c) is followed by the charge density projected on the atomic structure of the heterodimer (d). (e) Dispersion relation of longitudinal vibration modes of the MT. (f) Transfer function used for calculation of the amplitude spectrum density of thermal vibrations of MT. Data in (e) and (f) are shown for the first five longitudinal vibration modes of the MT with the length of 1.248 μm.

[a]Author to whom correspondence should be addressed. Electronic mail: ondrej.kucera@ufe.cz

excitation only in a dissipative fashion. In the underdamped case, the MTs would be able to accumulate random energy selectively at their resonant frequencies. It was speculated that MTs could likely accumulate the wasted energy from mitochondria, which show co-location with MTs in cells *in vivo*.[18] However, even in the overdamped case, the MT could transmit excitation signals, but with low efficiency. It was shown that there is a wide spectrum of possible oscillatory feeding in living cells,[19] including activity of motor proteins or pulse-like MT-related hydrolysis of guanosine triphosphate (GTP). Theoretical works also exist which predict soliton propagation along MTs.[20,21]

Electromagnetic field generated by a single vibration mode of the MT was the subject of our earlier study.[22] Here, we coarse-grained the atomic model of the MT to calculate the high-frequency electric field generated by the MT's multi-mode vibrations. Our results show that ultra-fast signaling from one end of a MT to another can occur without transfer of signaling molecules by transferring purely the energy in the form of electromechanical pulses excited, e.g., by GTP hydrolysis. In this context, our work may provide physical foundations for the hypothesis that microtubules can comprise substrate for electrodynamic signaling in neurons or other living cells.

We considered longitudinal vibrations of MTs in our calculations. The frequencies of longitudinal modes were estimated using data based on normal mode analysis of a MT[17] adapted to correspond to actual MT mass. The dispersion relation corresponding to such model is shown in Fig. 1(e). For the simplicity of the calculations, the mode shapes of longitudinal vibrations of the MT were approximated by longitudinal vibrations of a string with zero displacement boundary conditions on its ends. It does not fully correspond to structural features of the MT, but since the MT's length is much greater than its width, we do not expect this approximation to substantially alter the result. Biologically relevant amplitudes of vibrations should be comparable to, or higher than, those driven by thermal agitation. We approximated each ith longitudinal mode of the MT with the harmonic oscillator with resonance frequency ω_{oi} in order to estimate the amplitudes of thermal vibrations. Considering a MT with its length L_o, cross section area A_o, and Young modulus in the axial direction E_m, we may write the equivalent spring constant $k = E_m A_o / L_o$. The axial elongation, ΔL_i, of the MT is then equivalent to the displacement, x_i, of the oscillator from its equilibrium position. Considering the dissipation of the energy in the system, we may introduce the quality factor of the oscillator, Q_i. The dissipation (the damping) is represented by mechanical resistance $\beta_i = k/(\omega_{oi}Q_i)$. Let's suppose that the vibrations are not overdamped, so the $Q > 0.5$. The longitudinal response of the MT in the frequency domain is then given as a combination of responses H_i of respective modes

$$H_N(\omega) = \frac{1}{N}\sum_{i=1}^{N}\frac{\mathrm{j}\dfrac{\omega}{Q_i}}{\omega_{oi} + \mathrm{j}\dfrac{\omega}{Q_i} - \dfrac{\omega^2}{\omega_{oi}}}, \qquad (1)$$

if we limit the number of modes to N. The j denotes the imaginary unit. Using Nyquist's and Parseval's theorems, we may write the quadratic mean thermal fluctuation of the MT at the ith resonant frequency as follows:

$$\langle x_i(t)^2\rangle = 4k_B T\beta_i B_i|H_N(\omega_{oi})/k|^2, \qquad (2)$$

where $B_i = \omega_{oi}/4Q_i$ is the effective noise bandwidth of the ith resonance, k_B is the Boltzmann constant, and T is the temperature. Note that the high dissipation in the system leads to a shift of principal frequencies to lower values. The response of the MT used for calculation of the normalized amplitude spectrum density of thermally agitated vibrations of the MT is shown in Fig. 1(f) for five lowest modes. The amplitude of thermal fluctuations for each mode is then used as an estimate of the minimum biologically relevant displacement within the MT from the equilibrium position.

The electric field generated by longitudinal vibrations of MTs was calculated as follows. We summed the effective charge of atomic groups within each tubulin monomer. The result corresponds to the effective charge which is not compensated in the structure of the tubulin. The movement of each nth monomer within vibrating MT was introduced as $\mathbf{r}_n = \mathbf{R}_n + \sum_i A_{n,i}\mathrm{e}^{-\mathrm{j}\omega_i t}\mathbf{e}_l$, where $\mathbf{r}_n$ is the fluctuation vector of the nth monomer, $\mathbf{R}_n$ is the equilibrium position of the nth monomer, $A_{n,i}$ is the vibrational amplitude of the nth monomer for the ith mode, and $\mathbf{e}_l$ is the unit vector with the direction of the MT axis. Since we know the charge density at equilibrium and trajectories of monomers, we may express the charge and current densities as a function of time. These might be directly used for the expression of field quantities using the multipole radiation approach. However, for such a complicated structure—like the microtubule—the straightforward solution is theoretically and numerically rather intractable. Nevertheless, working under the assumption that the system is linear and the reverse coupling of the field to the charge of other atoms is negligible, we may use the superposition principle and treat each vibrating monomer as an elementary oscillating dipole. This simplification can be used since the trajectories of the atoms—which are given, besides other, by electromagnetic interactions—are already known. Denoting the effective charge that can be attributed to the nth monomer as q_n, we may write the oscillating dipole moment of this monomer as

$$\mathbf{p}_n = \sum_i A_{n,i}q_n\mathrm{e}^{-\mathrm{j}\omega_i t}\mathbf{e}_l. \qquad (3)$$

The resulting electric field at point $\mathbf{x}$ around the vibrating microtubule is then given by the superposition of the contributions from all dipoles as $\mathbf{E}(\mathbf{x}) = \sum_n \mathbf{E}_n$, where $\mathbf{E}_n$ is the intensity of the electric field of the oscillating electric dipole with the dipole moment $\mathbf{p}_n$. The intensity of the magnetic field may be evaluated along the same lines.

Our model presented here has some limitations which are given by the necessary simplifications for the description of the mesoscopic system under study. First, the model of mechanical vibrations only approximates movement which would mechanically vibrating MTs actually undergo. More accurate trajectories may be obtained by the normal mode analysis of MT vibrations. Second, the approximation of the oscillating charge density within tubulin proteins by dipoles limits the accuracy of the calculated electric field intensity in the vicinity of the MT. Validity of field quantities calculated according to this model is limited to the area further than the

radial distance of 40 nm from the MT. In order to obtain the values of the electric field in the immediate proximity of the MT, one would need to consider a multipole radiator instead of the dipoles for calculations. However, the general properties of the field would not differ from those obtained by our model. Third, we have not considered explicitly the effect of the counter ion cloud around MT. Instead, we considered homogeneous electrical parameters of MT's surroundings which correspond to macroscopic physiological values. The mobility of ions is low in the frequency range of our interest, so we do not expect counter ions to substantially screen the electric field. Nevertheless, ion-MT interactions are fundamental in electrostatics and low-frequency dynamics of MTs with possible implications in ion-mediated electrical signal transduction.[23,24]

We considered a 1.248 μm long microtubule with a 13:3 B-lattice and a tubulin protein structure based on adopted RCSB Protein Data Bank 1TUB code[17] for the results presented below. Effective charges of α- and β-tubulin monomers in this model were $-17e_o$ and $-21e_o$, respectively, where e_o is the elementary charge. The electrical parameters of the surrounding medium were approximated by complex permittivity of the physiological buffer. The Debye relaxation of the buffer is

$$\epsilon(f) = \epsilon(\infty) + \frac{\epsilon(0) - \epsilon(\infty)}{1 + j\omega\tau}, \tag{4}$$

where $\omega = 2\pi f$ and $\epsilon(0)$ and $\epsilon(\infty)$ are extrapolated low and high frequency permittivities. The real value of $\epsilon(f)$ corresponds to the relative permittivity on frequency f. The conductivity of the buffer may be written as $\sigma(f) = 2\pi f \epsilon_o \, \text{Im}(\epsilon(f))$, where ϵ_o is the absolute permittivity of the vacuum and Im is the operator of the imaginary part of a complex number. The values of permittivity[25] were $\epsilon(0) = 80$ and $\epsilon(\infty) = 5$. Our model does not assume the effect of the tubulin charge compensation by surface effects. The quality factor of vibrations, Q, was 4, which is a realistic compromise between the minimum of theoretically calculated damping for bending modes[26] and the fact that longitudinal modes are expected to be less damped.[27] As stated

above, the shape of modes was considered to follow the longitudinal modes of a string. The axial Young modulus of the MT, E_m, was 100 MPa which lies in the interval of reported mechanical properties of the MT.[28] We considered the physiological temperature of $T = 300\,K$ in the calculations. The maximum amplitude of oscillations calculated according to Eqs. (1) and (2) was approximately 0.28 nm. We considered the first five longitudinal modes. All modes were in phase in our calculations, which corresponds to pulsed excitation on one end of the MT.

The electric field generated by MT vibrations with its parameters described above is shown in Fig. 2. The intensity of the electric field is proportional to the amplitude of mechanical vibrations. Therefore, we plot the values of the intensity of the electric field normalized by the amplitude of vibrations and the total charge of the α-tubulin monomer as

$$|\mathbf{E}_{norm}| = \left| \frac{\mathbf{E}}{17e_o \langle x_1(t) \rangle} 10^{-29} \right|. \tag{5}$$

In general, electrical intensity may reach more than 100 kV/m in the distance of 50 nm from the wall of the microtubule for an amplitude of longitudinal vibrations less than 0.3 nm. We found that the spatial distribution of a high frequency electric field around a MT is nanostructured (contains local minima and maxima) due to the fact that the electro-mechanical vibration propagates with the velocity of an acoustic wave, thus having a wavelength in the range of hundreds of nanometers. The synchronous multimode excitation causes the formation of an electric pulse which propagates along the MT. Such electric pulse could be excited by GTP hydrolysis and is calculated to pass along the microtubule within several picoseconds. This enables ultra fast signal transfer along the microtubule lattice. Oscillating electric potential would be periodic both in space and in time if there was no damping. Dissipation of the energy leads to exponential decay of the pulse, so the resulting field is quasiperiodic.

Biological relevance or function of the described high-frequency electric field is limited by the effects which such a field may have on molecular interactions. An alteration of
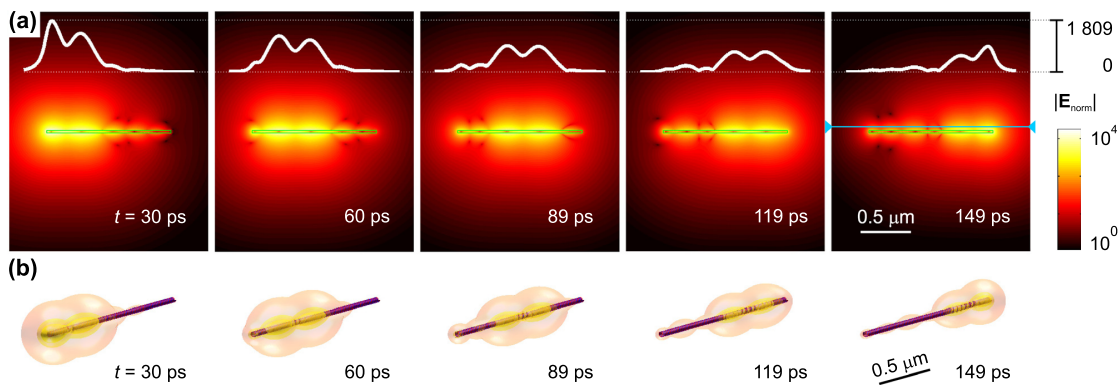
FIG. 2. (a) Propagation of the electric pulse along the microtubule. Normalized intensity of the electric field is depicted in a logarithmic scale according to the presented color-bar. The shape of the pulse, as an electric field intensity along the line parallel to the microtubule axis in the distance of 43 nm from the wall of the microtubule, is shown by the white line, on a linear scale. (b) An isosurface of the electric field intensity is used to visualize the shape of the pulse and its propagation in 3D.

the free activation energy of proteins by the field shown here does not seem realistic within the area of validity of the presented model, because the intensity of the electric field may reach values necessary for the effect[29] only for improbable values of parameters of the excitation. However, this may not be the case in the area directly adjacent to the MT, i.e., within few nanometers around the MT. A more detailed model is therefore required to resolve this question. Other possible effect of the described electric pulse is its action on the hydration layer of the MT and other nearby proteins.[30] Such an interaction would reside in the modification of the behavior of the interfacial water and result in an alteration of the hydrogen bonding kinetics. Since the properties of the hydration layer of the MT are also an important parameter of our calculations, namely, they influence the damping of mechanical vibrations, the analysis of this mechanism would require a more detailed molecular dynamics study which goes beyond the scope of this paper. Beside these specific effects, the electric field also acts on electrically charged, polar and polarizable materials, all being present in living systems; however, the force effects do not exceed those of thermal agitation. The effect of the magnetic component of the calculated field on singlet and triplet radical pairs was not investigated in our research. We may conclude that mechanisms for biological functions of the proposed signaling exist but the assessment of their real involvement requires further study. Experimental verification of the existence of the reported high-frequency electric pulse *in vivo* would be a great challenge even with cutting edge experimental techniques. Nevertheless, *in vitro* spectral characterization of electromechanical coupling in MTs using dielectric spectroscopy and absorption microwave spectroscopy of MTs in liquid phase may shed more light on the reported phenomenon.

In summary, we have shown *in silico* that synchronous multi-mode mechanical excitation of a microtubule generates an electric field in the form of an electric pulse, which propagates from one end of the microtubule to another. The reported phenomenon may serve as a mechanism for an ultra-fast electrodynamic signaling pathway along a microtubule. Such a phenomenon is of general biological importance in the context of microtubule-mediated nucleus-membrane communication[31] and of natural significance in neurophysiology since the modulation of a local electric field of ion channels in neurons and axons, which are packed with microtubules, influences the probability of neuron firing.

[1]G. G. Gundersen and T. A. Cook, Curr. Opin. Cell Biol. **11**, 81 (1999).
[2]J. A. Tuszynski, E. J. Carpenter, J. T. Huzil, W. Malinski, T. Luchko, and R. F. Luduena, Int. J. Dev. Biol. **50**, 341 (2006).
[3]R. Stracke, K. Böhm, L. Wollweber, J. Tuszynski, and E. Unger, Biochem. Biophys. Res. Commun. **293**, 602 (2002).
[4]I. Minoura and E. Muto, Biophys. J. **90**, 3739 (2006).
[5]S. Sahu, S. Ghosh, B. Ghosh, K. Aswani, K. Hirata, D. Fujita, and A. Bandyopadhyay, Biosens. Bioelectron. **47**, 141 (2013).
[6]M. Van den Heuvel, R. Bondesan, M. Cosentino Lagomarsino, and C. Dekker, Phys. Rev. Lett. **101**, 118301 (2008).
[7]S. Sahu, S. Ghosh, K. Hirata, D. Fujita, and A. Bandyopadhyay, Appl. Phys. Lett. **102**, 123701 (2013).
[8]A. Priel, J. A. Tuszynski, and H. F. Cantiello, Electromagn. Biol. Med. **24**, 221 (2005).
[9]J. Pokorný, J. Hašek, and F. Jelínek, J. Biol. Phys. **31**, 501 (2005).
[10]S. Hameroff and R. Penrose, Phys. Life Rev. **10**, 95–96 (2013).
[11]J. Pokorný, F. Jelínek, V. Trkal, I. Lamprecht, and R. Hölzel, J. Biol. Phys. **23**, 171 (1997).
[12]Y. M. Sirenko, M. A. Stroscio, and K. Kim, Phys. Rev. E **53**, 1003 (1996).
[13]A. Kis, S. Kasas, B. Babić, A. Kulik, W. Benoit, G. Briggs, C. Schönenberger, S. Catsicas, and L. Forro, Phys. Rev. Lett. **89**, 248101 (2002).
[14]C. Wang, C. Ru, and A. Mioduchowski, Physica E **35**, 48 (2006).
[15]C. Wang and L. Zhang, J. Biomech. **41**, 1892 (2008).
[16]M. Mallakzadeh, A. Pasha Zanoosi, and A. Alibeigloo, Commun. Nonlinear Sci. Numer. Simul. **18**, 2240 (2013).
[17]M. A. Deriu, M. Soncini, M. Orsi, M. Patel, J. W. Essex, F. M. Montevecchi, and A. Redaelli, Biophys. J. **99**, 2190 (2010).
[18]J. Pokorný, J. Pokorný, and J. Kobilková, Integr. Biol. **5**, 1439 (2013).
[19]O. Kučera and D. Havelka, Biosystems **109**, 346 (2012).
[20]M. Satarić, J. Tuszynski, and R. B. Žakula, Phys. Rev. E **48**, 589 (1993).
[21]D. L. Sekulić, B. M. Satarić, J. A. Tuszynski, and M. V. Satarić, Eur. Phys. J. E **34**, 49 (2011).
[22]M. Cifra, J. Pokorný, D. Havelka, and O. Kučera, Biosystems **100**, 122 (2010).
[23]A. Priel, A. J. Ramos, J. A. Tuszynski, and H. F. Cantiello, Biophys. J. **90**, 4639 (2006).
[24]M. Satarić, D. Ilić, N. Ralević, and J. A. Tuszynski, Eur. Biophys. J. **38**, 637 (2009).
[25]U. Kaatze, Meas. Sci. Technol. **14**, N55 (2003).
[26]A. Samarbakhsh and J. A. Tuszynski, Eur. Biophys. J. **40**, 937 (2011).
[27]F. Daneshmand and M. Amabili, J. Biol. Phys. **38**, 429 (2012).
[28]J. A. Tuszynski, T. Luchko, S. Portet, and J. M. Dixon, Eur. Phys. J. E **17**, 29 (2005).
[29]F. Apollonio, M. Liberti, A. Amadei, M. Aschi, M. Pellegrino, M. D'Alessandro, M. D'Abramo, A. Di Nola, and G. d'Inzeo, IEEE Trans. Microwave Theory Tech. **56**, 2511 (2008).
[30]F. Apollonio, M. Liberti, A. Paffi, C. Merla, P. Marracino, A. Denzi, C. Marino, and G. d'Inzeo, IEEE Trans. Microwave Theory Tech. **61**, 2031 (2013).
[31]P. A. Janmey, Physiol. Rev. **78**, 763 (1998).

4 | HIGH-FREQUENCY ELECTRIC FIELD AND RADIATION CHARACTERISTICS OF CELLULAR MICROTUBULE NETWORK

This chapter is a version of:

Author contributions:

| Designed research: **D.H.**, M.C., J.P., and J.V.

| Performed research: **D.H.**

| Analysed data: M.C. and O.K.

| Wrote the paper: **D.H.**, M.C., and O.K.

| Candidate's contribution: 50%

The manuscript carries the following acknowledgements:

High-frequency electric field and radiation characteristics of cellular microtubule network

D. Havelka [a,*], M. Cifra [b], O. Kučera [b,c], J. Pokorný [b], J. Vrba [a]

[a] *Department of Electromagnetic Field, Faculty of Electrical Engineering, Czech Technical University in Prague, Czech Republic*
[b] *Institute of Photonics and Electronics, Academy of Sciences of the Czech Republic, Czech Republic*
[c] *Department of Circuit Theory, Faculty of Electrical Engineering, Czech Technical University in Prague, Czech Republic*

ABSTRACT

Microtubules are important structures in the cytoskeleton, which organizes the cell. Since microtubules are electrically polar, certain microtubule normal vibration modes efficiently generate oscillating electric field. This oscillating field may be important for the intracellular organization and intercellular interaction. There are experiments which indicate electrodynamic activity of variety of cells in the frequency region from kHz to GHz, expecting the microtubules to be the source of this activity. In this paper, results from the calculation of intensity of electric field and of radiated electromagnetic power from the whole cellular microtubule network are presented. The subunits of microtubule (tubulin heterodimers) are approximated by elementary electric dipoles. Mechanical oscillation of microtubule is represented by the spatial function which modulates the dipole moment of subunits. The field around oscillating microtubules is calculated as a vector superposition of contributions from all modulated elementary electric dipoles which comprise the cellular microtubule network. The electromagnetic radiation and field characteristics of the whole cellular microtubule network have not been theoretically analyzed before. For the perspective experimental studies, the results indicate that macroscopic detection system (antenna) is not suitable for measurement of cellular electrodynamic activity in the radiofrequency region since the radiation rate from single cells is very low (lower than 10^{-20} W). Low noise nanoscopic detection methods with high spatial resolution which enable measurement in the cell vicinity are desirable in order to measure cellular electrodynamic activity reliably.

1. Introduction

Electrodynamic activity of eukaryotic cells is a topic, which is gaining considerable theoretical and experimental support in recent years. In the 1960s Fröhlich postulated and theoretically treated a concept in which he presented the possible existence of the mechanical vibrations of electrically polar structures in living cell causing generation of electric oscillations around and in the cell. Firstly, he proposed electrically polar longitudinal vibrations interacting with an elastic field, giving rise to coherent cellular electric oscillations (Fröhlich, 1968b, 1969). Secondly, he showed that the energy condenses to the lowest frequency mode in his nonlinear model system (Fröhlich, 1968a). Lastly, he estimated that oscillating polar structures are situated in the cellular membrane and their oscillating frequency is in range $10^{11}–10^{12}$ Hz. However, with the advent of deeper understanding of the cellular structure the microtubules emerge as hot candidates for generation of endogenous electrodynamic activity of living cells (Pokorný et al., 1997, 1998).

A possible biological role of the endogenous cellular high-frequency electric field has been analyzed by several authors. Its role has been proposed in long-range protein interactions (Fröhlich, 1972, 1975), in chemical reaction transfer and consequently chemical reaction kinetics (Pokorný and Wu, 1998; Pokorný et al., 2005a, 2005b; Pokorný, 2001), in disrupted cellular organization state such as cancer (Fröhlich, 1978; Pokorný et al., 2008), and in intercellular interactions (Pokorný et al., 1983; Pokorný and Fiala, 1994; Pokorný, 2006; Pohl, 1981, 1980; Rowlands et al., 1981, 1982).

The electrodynamics of cellular structures is inseparably connected to the vibrational dynamics of biomacromolecules. Many marvelous biological functions in proteins and DNA and their profound dynamic mechanisms, such as switch between active and inactive states (Chou, 1984b; Chou et al., 2001; Wang and Chou, 2009), cooperative effects (Chou, 1989), allosteric transition (Chou, 1984a, 1987; Schnell and Chou, 2008), intercalation of drugs into DNA (Chou and Mao, 1988), and assembly of microtubules (Chou et al., 1994), can be revealed by studying their internal motions (Chou, 1988) or terahertz frequency motions. Such inferences have been later observed by NMR (Chou et al., 2001), and applied in medical treatments (Gordon, 2007, 2008;

Madkan et al., 2009). Recently, investigation into the internal motion in biomacromolecules and its biological functions is deemed as a 'genuinely new frontier in biological physics' (Vermont Photonics Technologies Corp, 2011). Likewise, to really understand the action mechanism of microtubules, we should consider not only its static structure but also its dynamical character. The electrodynamic behavior of microtubules inevitably underlies electrodynamic activity of living cells.

Electric oscillations of living cells have been experimentally investigated by several authors in the frequency range from kHz (Jelínek et al., 2008, 2009) through MHz (Pohl et al., 1981; Hölzel and Lamprecht, 1994; Hölzel, 2001; Pokorný et al., 2001) to the GHz (Jelínek et al., 2007; Cifra, 2009) region. These pioneering experiments suggest cellular electrodynamic activity in mentioned frequency region, but the measurement systems used were of the threshold sensitivity. It was recently explained (Kučera et al., 2010) which technical prerequisites must be fulfilled by the measurement system which is designed to detect cellular electrodynamic activity in kHz–GHz region. One of the biophysical aspects underlying the technical prerequisites for high gain and low noise of the first pre-amplifier is the obviously low power radiated from the cell. However, there are few theoretical calculations which provide quantitative evaluation of radiated power from cell and electric field intensity around the cell in the high-frequency region. Pokorný carried out calculations where the source of MHz–THz cellular electric oscillations were assumed to be membrane proteins (Pokorný and Wu, 1998; Pokorný, 1990, 1987) (some selected results are also in Pokorný et al., 1983, 1996; Pokorný, 1985). Shein and Kharlanov (2007) and Kharlanov (2006) represented the whole membrane by discrete dipole layer and considered acoustoelectric vibrations of the membrane in MHz–GHz region. The analysis of Russian authors was inspired by the earlier works of Devyatkov, Golant and Betskii (summarized in books Betskii et al., 1988; Devyatkov et al., 1991) who proposed that the acoustoelectric vibrations of the cell membrane can generate electric oscillations in the region of 30–300 GHz and made the first estimation of radiated electromagnetic power from single cell. Results from both groups of authors show clearly that single cell radiation under most conditions is of the power well below 10^{-20} W, thus hardly detectable in far field at room temperature if the exact frequency of radiation is not known a priori. As can be seen, all of these works considered only cell membrane as the source of the oscillatory electric field, although modern findings suggest that cytoskeleton, especially microtubules, is also very probable source of endogenous cellular high-frequency electric oscillations (Cifra et al., 2010d). Work presented here is filling the gap by calculating electric field and radiation of the whole cellular microtubule network.

2. Microtubules

Cytoskeleton is not only the mechanical support of the cell, but also the dynamic structure responsible for dividing the cell in two, for cellular motion and selforganization of the cell. Cytoskeleton is composed of three types of filaments. One of them are microtubules. Microtubules resemble hollow rods with inner and outer diameter 17 and 25 nm, respectively. These structures are mostly composed of 13 protofilaments, see Fig. 1. The subunits of protofilaments are tubulin heterodimers, which are constituted from α- and β-tubulin. Tubulin heterodimer is very polar structure with static dipole moment $p_{AXIS,STATIC} = 337$ D $(1.12 \times 10^{-27}$C m) (Tuszyński et al., 2005) in the direction of the microtubule axis. In most of eukaroytic cells, microtubule nucleating and organizing center is a centrosome, which is a cell organelle near the nucleus. Microtubules grow up from this center through the cytoplasm to the cell membrane and
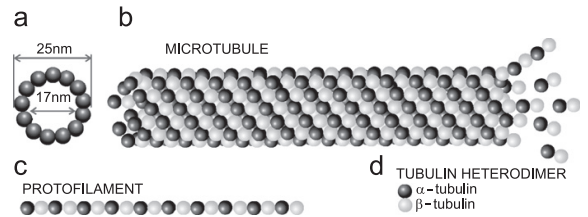

Fig. 1. (a) Cross section of a microtubule. (b) A single microtubule with 13 protofilaments. (c) One protofilament. (d) One tubulin heterodimer.
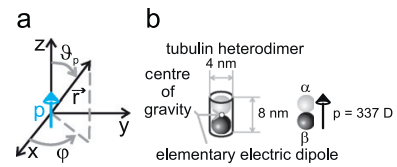
Fig. 2. (a) Dipole moment in the Cartesian coordinate system. (b) Tubulin heterodimer (dimensions and center of gravity).

create intricate network. Together with an extraordinary elasticity, microtubules fulfill all conditions for generation of electric oscillations (Cifra et al., 2010c).

2.1. Electric properties of microtubule

Electric properties of tubulin heterodimer were approximated by an elementary electric dipole (in further text the term "dipole" is used for brevity). Field of such dipole is described by

$$H_{\varphi} = -\frac{Idl}{4\pi}k^2\sin(\vartheta_p)\left(\frac{1}{jkr} + \frac{1}{(jkr)^2}\right)e^{-jkr} \tag{1}$$

$$E_r = -\frac{Idl}{2\pi}Zk^2\cos(\vartheta_p)\left(\frac{1}{(jkr)^2} + \frac{1}{(jkr)^3}\right)e^{-jkr} \tag{2}$$

$$E_{\vartheta} = -\frac{Idl}{4\pi}Zk^2\sin(\vartheta_p)\left(\frac{1}{jkr} + \frac{1}{(jkr)^2} + \frac{1}{(jkr)^3}\right)e^{-jkr} \tag{3}$$

where E is the electric field intensity, H is the magnetic field intensity, I is the equivalent current, dl is the length of the dipole, Z is the wave impedance, k is the propagation constant, ω is the angular frequency, p is the dipole moment, j is the imaginary unit $(j^2 = -1)$ and other symbols are according to Fig. 2a.

All equations include:

$$I\vec{dl} = j\omega\hat{p} \tag{4}$$

In the near zone the dominant components are with $E \sim 1/(jkr)^3$ and $H \sim 1/(jkr)^2$ and the time-averaged Poynting vector (power density, or Poynting vector in further text, for brevity) composed of these components is zero in lossless medium, because the phase shift between E and H is $\pi/2$. Time-averaged Poynting vector $\vec{S}$ is defined as $\vec{S} = \frac{1}{2}\text{Re}\{\vec{E} \times \vec{H}^*\}$, where Re{} denotes real part of complex number and * denotes complex conjugate.

Every tubulin heterodimer in one microtubule is approximated by elementary electric dipole to obtain the model of electrical properties of microtubule (Fig. 3).

Fig. 3. Model of electrical properties of microtubule. Every arrow represents one dipole.
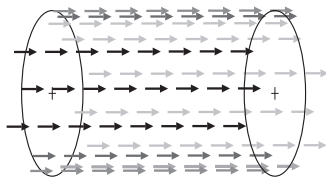

Fig. 4. Location of microtubule in coordinate system and sense of the angles ϑ and ϕ.

3. Method of calculation

Scripts for calculation of electromagnetic field generated by microtubule network were written in Matlab. It had to be dealt with three problems during calculations. The first is the distribution of points on the sphere with the smallest potential energy—to obtain the most symmetric distribution of arbitrary number of microtubules. The second is the rotation of microtubules and then creation of microtubule network. The last problem to deal with was a summation of small and great numerical values. The first problem was analyzed by Bulatov (1996). The solution of problem of microtubule rotation will be described in the following: The microtubule is situated in Cartesian coordinate system (Fig. 4) and coordinates of vector of elementary electric dipoles (both position and direction) are known.[1]

These coordinates were rotated according to the points distributed on the sphere[2] with the smallest potential energy. Two representative models of microtubule network were created in this way. The first model (symmetric) represents the microtubule network of nondividing cell. End points of microtubules' axes are distributed symmetrically and uniformly on the sphere in this model (the axes of microtubules are situated along radius vectors from center of the sphere to end points which are uniformly distributed on the sphere. Uniform distribution was obtained by an algorithm which calculates coordinates of point charges uniformly distributed on sphere—distributed according to their total smallest potential energy) (Fig. 5). This uniform and symmetric distribution of microtubules simulates complete (phase and geometric) symmetry in the cell. The second model (asymmetric) is the model of asymmetric distribution of microtubules (Fig. 6). This model represents microtubule network during mutual cellular interaction or during cellular interaction with solid substrates when cytoskeleton is redistributed. Both models are composed of 100 microtubules, which is reasonable estimate based on electron microscopy studies of eukaryotic cells (Sobel, 1997; Winey et al., 1995; May and Hyams, 1998). Each microtubule in our model is constituted of 1950 heterodimers.[3] We assumed that the ends of microtubules are in direct contact with the cell membrane, i.e. diameter of the model cell is 2.8 µm (0.4 µm diameter of the centrosome $+2 \times 1.2$ µm of microtubule length).

The problem of summation of small and large numeric values occurred in calculations of power mainly in lossless medium, because the value of field calculated only from near field
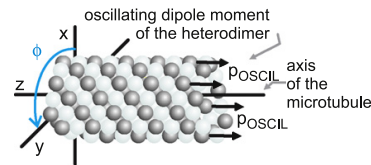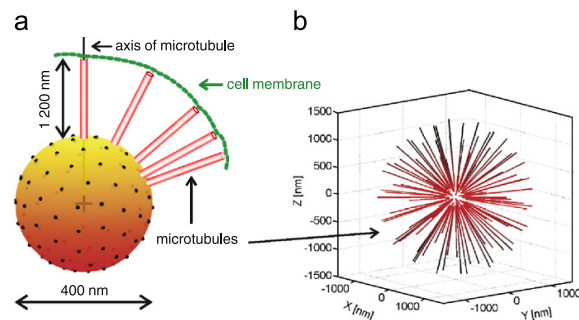

Fig. 5. (a) Model of centrosome with nucleation centers (black points) uniformly and symmetrically distributed on the sphere. (b) The symmetric model of a simple microtubule network with 100 microtubules. The ends of microtubules are distributed according to (a). Each red line represents one microtubule. Centrosome is in no way involved in the generation of mechanical or electric oscillations in the current calculations model, it is depicted here only for clarity and explanation of the geometrical distribution of microtubules. (For interpretation of the references to color in this figure legend, the reader is referred to the web version of this article.)
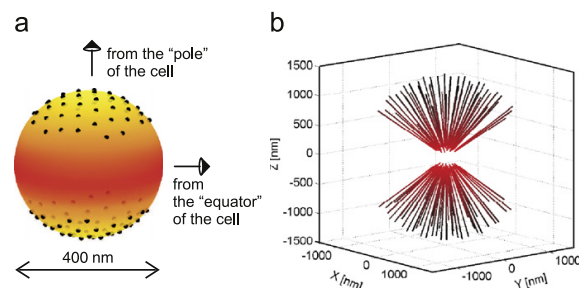
Fig. 6. (a) Model of centrosome with nucleation centers (black points). There are 50 points on each pole. (b) The asymmetric model of a simple microtubule network with 100 microtubules. The ends of microtubules are distributed according to (a). Each red line represents one microtubule. Centrosome is in no way involved in the generation of mechanical or electric oscillations in the current calculations model, it is depicted here only for clarity and explanation of the geometrical distribution of microtubules. (For interpretation of the references to color in this figure legend, the reader is referred to the web version of this article.)

components is much greater than value of field calculated from far field components. This was solved by decomposition of Eqs. (1)–(3) into parts $1/jkr$, $1/(jkr)^2$ and $1/(jkr)^3$ and by calculation of small and large values separately. All three problems and their solutions were described closely by Havelka (2010).

The calculation is executed by vector summation of contributions from all dipoles in the point of space in which the value of electric and/or magnetic field (in further text the term "point" is used for brevity) has to be calculated and then this procedure is repeated for all points in the chosen set (sets included either plane, coaxial surface of microtubule or spherical surface around

---

[1] Coordinates of the initial point of dipole vector are in the center of gravity of tubulin heterodimer and coordinates of the endpoint of dipole vector depend on angle ϑ. ϑ is the angle between the axis of dipole vector and the axis of microtubule. Thus, $\vartheta = 0$ corresponds to case when the dipole vector is parallel with the microtubule axis. In other words, when we consider longitudinal axial oscillations of microtubule (and heterodimer from which it consists), only component of the dipole vector which oscillates significantly is the one which is parallel with the microtubule axis.

[2] Sphere with radius 200 nm represents simple approximation of spherical surface of centrosome, from where the microtubules grow.

[3] Thirteen protofilaments $\times$ 150 heterodimers in one protofilament, corresponds to the length of 1.2 µm of a single microtubule.

cell). This method was used for calculation of the power radiated from models and electric intensity in radiant distance from a cell membrane. The effect of the cell membrane is neglected in our calculations. To obtain the radiated power P, numerical integration of Poynting vector (power density) was performed over the sphere concentric to cell center using summation $P = \sum_i^N S_i \cdot A_i$ (N, number of elementary surfaces, A_i, i-th surface with S_i power density flowing through it) which is discrete equivalent of continuous integration $P = \int \vec{S} \, d\vec{A}$, where P is the power flowing through the surface A and S is the Poynting vector (power density). Electric field of the whole microtubule network was calculated along the radius vector, either in the direction from the "pole" or from the "equator" (Fig. 6).

4. Parameters used for calculations

Calculations were performed in frequency regions in which various workers have been attempting to measure electric oscillations of cells (Jelínek et al., 2007, 2008, 2009; Pelling et al., 2005; Pohl et al., 1981; Hölzel and Lamprecht, 1994; Hölzel, 2001; Pokorný et al., 2001; Cifra, 2009). Two different surrounding media were taken into account: lossy and lossless. The parameters of surrounding media are in Table 1 (ε_r and σ have subscript 1 for lossy medium and subscript 2 for lossless medium). Longitudinal shift between neighboring protofilaments is 4.92 nm (corresponds to the microtubule lattice A, Tuszyński et al., 2005) as can be seen in Fig. 4. Longitudinal oscillations of tubulin heterodimers are represented by oscillating dipole moment in the direction of microtubule axis ($p_{AXIS,STATIC} = 337$ D static part of dipole moment). We note for clarity that every tubulin in microtubule is oscillating. This follows from the fact that oscillations of microtubules as wholes are considered in this paper. Amplitude of oscillatory component of the tubulin dipole moment around kHz was estimated based on Pelling et al. (2004, 2005). In this work Pelling measured oscillations of yeast cell wall, likely connected with cytoskeleton oscillations, in the amplitude range 1–10 nm, so the amplitude of 1 nm was accepted. Amplitudes of oscillations for higher frequencies are assumed to be of the level of thermal motion amplitude of proteins (Chou, 1988), which is around 0.1 nm. Thus, taking ratio of the oscillatory amplitude (1 and 0.1 nm) and the length of the dipole (tubulin heterodimer length of 8 nm) amplitude of the dipole oscillatory component were estimated: for kHz $p_{OSCIL1} = \frac{1}{8} p_{AXIS,STATIC}$ and for higher frequencies $p_{OSCIL2} = \frac{0.1}{8} p_{AXIS,STATIC}$.

Oscillations of tubulin heterodimers in one protofilament were approximated by longitudinal oscillations of the chain of rigid particles of two types, optical branch (Kittel, 1976). Optical branch is able to generate and absorb electromagnetic field effectively. Movement of particles (tubulin heterodimers) and corresponding oscillations of the dipole moment are described by spatial modulation function:

$$p_m = p_{OSCIL} \cdot \sin(m\nu) \tag{5}$$

Table 1
Parameters of surrounding medium around microtubules and cell model for eight frequencies. ε_r and σ have subscript 1 for lossy medium and subscript 2 for lossless medium.

f (Hz)	1 k, 1 M, 10 M, and 100 M	1 G	10 G	42 G	100 G
ε_{r1} (−) (relative permittivity)	81	81	71	20	10
σ_1 (S/m) (conductivity)	1	1.33	17.22	39.67	68.50
ε_{r2} (−) (relative permittivity)	81	81	71	20	10
σ_2 (S/m) (conductivity)	0	0	0	0	0

where p_m is the modulated dipole moment, p_{OSCIL} is the oscillatory component of the dipole moment and $m\nu$ is basically distance along the microtubule. Modulation function is specific for each mode, minimal mode number is zero, maximal mode number (max) depends on the number of tubulin heterodimers, i.e. length of microtubule. The mode zero represents oscillations of all dipoles in phase and the max mode represents oscillations of neighboring dipoles in antiphase.

For the illustration, modulation function of the 1st protofilament is depicted in Fig. 7 for the mode 3. Modulation functions of other protofilaments (2nd–13th) are axially shifted, according to the position of protofilaments in the real microtubule A lattice. Each circle in Fig. 7 represents the value of dipole moment of one heterodimer. Modulation function represents effect of a vibrational longitudinal wave on dipole moments of individual tubulin heterodimers. This wave can be described as the wave which has the same phase in the cutting plane orthogonal to the axis of the microtubule (Fig. 8—mode 3). Integer values of mode numbers correspond to boundary conditions of rigidly bound ends of microtubule. It is important to note that in our models of microtubule network, phase difference between oscillations of individual microtubules is zero, i.e. microtubules oscillate in phase. The distribution of electric field around microtubule excited by vibration modes min (mode 0) and max (mode 50, in this case) can be seen in Fig. 9. The intensity of
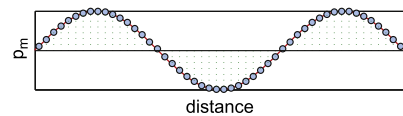

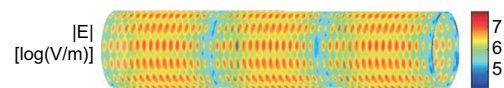**Fig. 7.** The modulation function of the 1st protofilament (mode 3).

Fig. 8. The intensity of electric field in logarithmic scale on the coaxial surface 1 nm above the microtubule wall (mode 3).
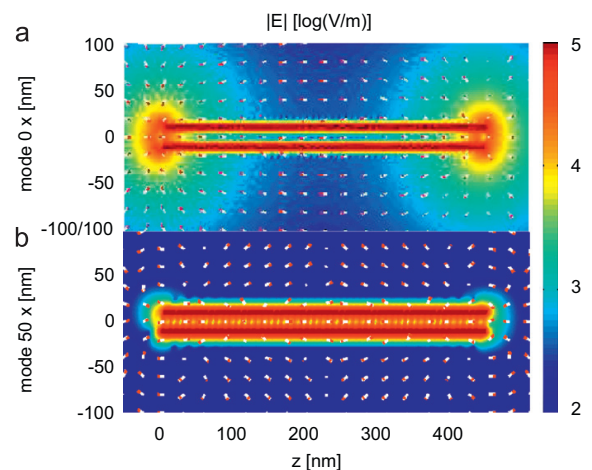

Fig. 9. The intensity of electric field in logarithmic scale in section through axis of the microtubule, which is excited by (a) mode 0 (min mode) and by (b) mode 50 (max mode).

Table 2
Total radiated power from the whole cellular microtubule network for different frequencies of the microtubule oscillations, lossless medium. The radiated power is the same both from symmetric and asymmetric model.

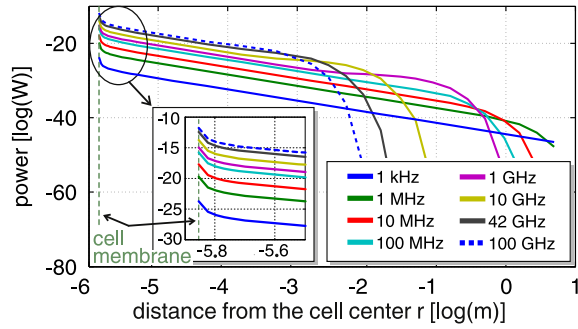| f (Hz)	1 k	1 M	10 M	100 M	1 G	10 G	42 G	100 G
P [log(W)]	−52.22	−40.22	−36.22	−32.22	−28.22	−24.25	−22.03	−20.68

Fig. 10. Power calculated from the cell membrane to the distance of 1 m for eight frequencies (asymmetric model, mode 0 and lossy medium).

electric field around microtubule generated by mode 50 is smaller by several orders of magnitude compared to electric field intensity generated by mode 0.

5. Results

At first, selected results of calculations of power of asymmetric microtubule network are presented. Eight frequencies (Table 2) and mode 0 were used for excitation of microtubules. The mode 0 is the most effective for generation of electric oscillations. Lossy and lossless medium was considered. The calculated results show that the values of radiated power from microtubule network generated by oscillations of mode min and of mode max are negligibly different (see Figs. 1–4 in supplementary material) and the values of power radiated from asymmetric and symmetric model are the same (see Figs. 5 and 6 in supplementary material). Therefore, from the calculations of radiated power results from asymmetric model only are shown. Poynting vector computed from near-field components ($E \sim 1/(jkr)^3$ and $H \sim 1/(jkr)^2$) has zero value in lossless medium. In contrast, the Poynting vector calculated from far field components ($E \sim 1/(jkr)$ and $H \sim 1/(jkr)$) is not zero. The values of power radiated from asymmetrical model in lossless medium for all eight frequencies are in Table 2.

The phase shift between near field components of intensity of electric and magnetic field is not $\pi/2$ but $\pi/2 + 2\phi_k$ in lossy medium (ϕ_k is a phase of propagation constant k of electromagnetic field in lossy medium, in lossless medium $\phi_k = 0$). Consequently, the values of Poynting vector calculated from components of near field are not zero and are higher than Poynting vector calculated from other components in lossy medium. On the one hand the values of power near the membrane in lossy medium are higher than in lossless medium but on the other hand the values of power in lossy medium decrease steeply with distance from cell membrane. Fig. 10 shows the dependence of power generated by asymmetric microtubule network in lossy medium for all eight frequencies on radial distance. The value of power is the highest in the proximity of the cell membrane and decreases fast with growing distance.

Further results are from the calculations of intensity of electric field depending on radial distance from the pole or equator of cell (Fig. 6) for both models (Fig. 11). Fig. 12 depicts intensity of electric
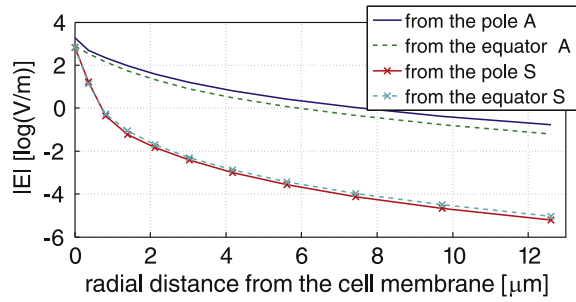
Fig. 11. Radial dependence of the electric intensity from the cell membrane in the direction from the equator (dashed lines) and from the pole (full lines) up to 12.6 μm. A and S stands for the asymmetric and the symmetric model, respectively (mode 0, $f = 100$ GHz, lossy medium).
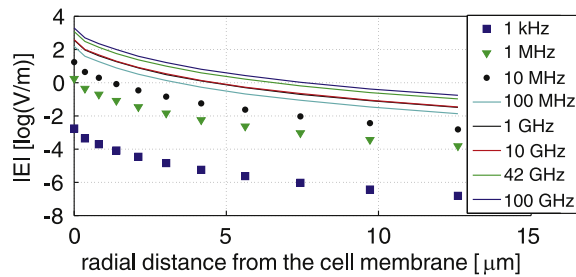
Fig. 12. Radial dependence of the electric intensity from the pole of the cell membrane—comparison of frequencies which are in the legend of the figure in Hz (asymmetric model, mode 0 and lossy medium).
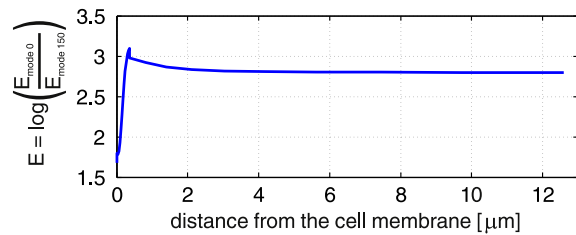
Fig. 13. Logarithm of the ratio of the electric intensity generated by mode 0 and that generated by mode 150 in dependence on radial distance from the pole of the cell membrane ($\log_{10}(E_{mode0}(r)/E_{mode150})(r)$). Electric intensity generated by mode 0 has higher values (asymmetric model, $f = 100$ GHz and lossy medium).

field depending on the distance from pole of the cell membrane for all eight frequencies. The difference between the electric intensity ΔE generated by mode 0 and that by mode 150 (maximal mode for the 1.2 μm long microtubule) in dependence of radial distance from the pole of asymmetric model in lossy medium and for frequency 100 GHz is shown in Fig. 13. The intensity of electric field on the border (at the cell membrane) of asymmetric model of the microtubule network is depicted in Fig. 14.
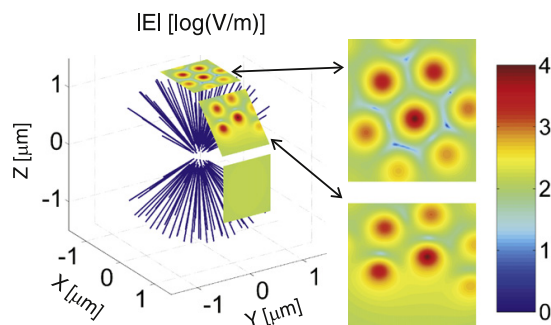
Fig. 14. The electric intensity on the border (at the cell membrane) of asymmetric model of the microtubule (mode 0, $f = 42$ GHz, lossy medium).

6. Discussion

6.1. Approximations and assumptions on the level of the single microtubule

On the level of the single microtubule approximations and assumptions used include:

- integer mode numbers used;
- magnitude of oscillating dipole moment;
- shift of protofilaments in microtubule;
- microtubule protofilament approximated by chain of rigid particles, usage of axial longitudinal vibration modes, optical branch;
- coherent or at least quasi-coherent oscillations of individual dipoles, which require low damping of microtubule vibrations.

All of these points were discussed in the previous works of current authors (Cifra, 2009; Cifra et al., 2010d) where electric field generated by vibrations of single microtubule was already analyzed, so they are touched only briefly here.

Integer values of vibration mode number is related to boundary conditions of rigidly bound ends of microtubule. In real physiological conditions all microtubules grow from centrosome or other microtubule organizing center and can be considered to be bound rigidly (or quasi-rigidly) on the centrosome connected end (minus end). However, not all microtubules are capped and bound on its other end, the plus end. Substantial number of microtubules (exact fraction depends on the cell state and the phase of the cell cycle) undergoes dynamic instability and perpetual growth and shrinkage (Alberts et al., 2008). Vibrations of microtubules with one free end could assume infinite number of noninteger mode numbers.

Value of oscillating dipole moment used in calculations presented here represents the lower boundary of the possible values. This means that in real conditions the oscillating dipole moment can be also higher and consequently the generated electric field intensity may be higher, by approximately one order of magnitude. Axial shift of protofilaments in microtubule which was used in the model presented here corresponds to the real arrangement of protofilaments in microtubule lattice and is called lattice A, as already mentioned in Section 4. Another arrangement of protofilaments also often found in microtubules in vivo is lattice B (Tuszyński et al., 2005).

Vibrations of microtubule protofilament were approximated by vibrations of chains of rigid two-type particles, optical branch. A similar model of microtubule vibrations was used by Pokorný et al. (1997). On the level of the whole microtubule, this corresponds to axial longitudinal vibration modes of microtubules, such as treated

by Wang et al. (2006), but is a special case in which neighboring tubulin particles oscillate against each other (optical branch). Vibrations of single microtubules were treated based on tubulin atomic coordinates obtained from crystallography (Deriu et al., 2010) but this approach is not computationally feasible for the whole cellular microtubule network. Therefore the approximation of tubulin as single rigid particles is considered reasonable for the current purpose.

Calculations presented here assume that there are coherent or at least quasi-coherent oscillations of individual dipoles (tubulin heterodimer). Coherent excitation can be provided by external coherent electromagnetic radiation or can be provided endogenously if system of oscillators fulfills conditions such as described by Fröhlich (1968a,b, 1980). Microtubules fulfill necessary conditions of the Fröhlich system (Cifra, 2009). Recently, Reimers et al. (2009) and McKemmish et al. (2009) performed computational studies of Fröhlich system based on using Wu–Austin Hamiltonian. They concluded that condensation of energy in certain modes strong enough to provide coherent excitations (one of the main features of Fröhlich system) is not feasible in biological systems. It is not necessary to go into details here but it has been pointed out (Cifra et al., 2010a,b) that the studies of Reimers and McKemmish treat incomplete Fröhlich system (nonlinear temperature dependence of coupling coefficients is missing) and contains several further flaws. Also another group of authors (Salari et al., 2011) noticed several errors in Reimers' study. Thus, conclusion of Reimers et al. (2009) and McKemmish et al. (2009) that the "…coherent Fröhlich condensates are not biologically feasible,…" cannot be fully accepted and definitely cannot be used for overgeneralization.

6.2. Damping of microtubule vibrations

Regardless of the mechanism for selective excitation of certain microtubule mode, it is necessary that the modes to be excited have low damping so the energy may be stored quasi-coherently in them. This requires that the energy supplied to microtubules is not dissipated rapidly to surrounding medium. Physically the problem is related to the damping of microtubule vibrations. If the microtubule vibrations are treated classically like for a cylinder immersed into bulk water, the result will be that the vibrations will be overdamped (Foster and Baish, 2000), i.e. $Q < 1$ (Q, quality factor of oscillations). This may not be the case if one considers ions on the microtubule surface behaving as a slip layer (Pokorný, 2005), especially for longitudinal vibrations where negligible or no water at all will be displaced as for example in the case of standing waves with a zero vibration amplitude at the ends of microtubule. The quality factor (and the lifetime) of the biomolecule vibrations depends also on the organization of the water around the biomolecule surface: the higher the ability of the surface to attract water molecules (i.e. the higher the hydrophilicity of the surface), the higher is the Q (and lifetime) of the vibrations (Liu et al., 2009a,b). The physical mechanism is such that the water due to the electric polarity of its molecules is organized by the electric field of the surface charge of the hydrophilic biomolecule and the water undergoes visco-elastic transition (Van Zandt, 1986, 1987). There is extensive experimental evidence that the water is organized at the hydrophilic surfaces. Several layers of organized water molecules above the biomolecule interface can be detected and visualized by atomic force microscopy (Fukuma, 2010; Kimura et al., 2010). However, ordering of the water is not a matter of only a few molecular layers but can extend to macroscopic distances from strongly hydrophilic interfaces, e.g. few hundreds of micrometers as in the case of exclusion zone found by Zheng and Pollack (2003) and Zheng et al. (2006). These zones carry their name "exclusion zones" after the process they are

visualized with; the zones exclude micrometer sized particles (e.g. latex particles) in such a manner that two distinct water phases (zones) are visible at the hydrophilic interface observed under the microscope. The zone of water adjacent to the surface contains no particles (they are excluded to the outer zone), while beyond rather sharp boundary, particles are present in the second, outer water zone. It was experimentally proved that the organized water in the exclusion zone has different physical properties compared to bulk water including higher viscosity (Pollack et al., 2006), lowered thermal motion of molecules (Zheng et al., 2006), further it exhibits separation of charge, different pH (Chai et al., 2009), different spectroscopic properties (Chai et al., 2008), solvent exclusion (Zheng and Pollack, 2003; Zheng et al., 2006) and that infrared radiation promotes formation of the exclusion zones (Chai et al., 2009), etc. (Pollack et al., 2006, 2009).

Direct evidence of damping can be obtained from spectroscopy. While some spectroscopic and theoretical studies suggest that collective vibrations of proteins are overdamped by the water (Hayward et al., 1993) which is a major constituent of the cytosol, there are indications (Romanovsky et al., 2003) that the broadening of the spectral lines (a physical signature of a damping) may not be solely due to the damping but also due to inhomogeneous broadening of the spectral line—slight difference in the mode frequency due to conformational differences in the protein molecules in the ensemble under study. Actually, nonlinear spectroscopy already brought experimental evidence that lifetime (similar to quality factor Q of the oscillating system—inversely proportional to damping) of certain protein modes can be rather large, over 1000 (Xie et al., 2001). Currently, published data from direct spectroscopic studies on microtubules in MHz–GHz region are very limited. Hameroff et al. (1986) reported 8 GHz acoustic mode of microtubules with Brillouin spectroscopy, from the sole figure they provided the half width of the peak (Δf) is about 2 GHz, giving Q factor ($f/\Delta f$) about 4. Pizzi et al. (2011) measured very weak microwave absorption (0.5 dB) of in vitro microtubules with mean length of 2 μm at 1510 MHz which probably corresponds to some bending modes of microtubules which are overdamped (Samarbakhsh, 2010). Regarding these two past and any future experiments, it needs to be noted that inhomogeneous broadening contributes to broadening of the peak, thus leads to underestimation of the real Q factor. If the spectral resolution of the spectroscopy technique used is low, multiple spectral peaks will be merged into one broad peak, additionally clouding the real Q factor of oscillations. Further, longitudinal axial modes (which are most electromagnetically active in comparison with twisting or bending modes because the "stretching" of the tubulin dipole moment is greatest for longitudinal axial wave on microtubule) which conserve microtubule length will be damped much more weakly since they do not cause any displacement of the surrounding water. It is also important to realize that microtubules are naturally present in a cellular environment where the surrounding water is strongly organized due to numerous interfaces (Pollack, 2001) and by strong static electric field of mitochondria (Tyner et al., 2007). It can be expected that the in vivo damping of microtubule elastic vibrations will be lower than that measured on extracted microtubules. This can be reasonable if the amplitude of oscillations is small and comparable to size of damping units (water molecules or water clusters). In such case, classical hydrodynamic treatment of the damping (Stokes' formula) fails (Mitrofanov et al., 2006) and it underestimates the Q factor of protein oscillations especially in the THz region.

6.3. Related works on microtubule and protein vibrations (low-frequency phonons)

It may be of interest for readers to discuss several related works of Sinkala (2006) and Chou et al. (1994) and their relation to the topic of the current paper. Sinkala analyzed possibility of soliton/exciton transport in proteins which would enable non-dissipative transport of energy and related his model to the model of Resonant Recognition Model of Cosic (1994). The main connection with the current work is that solitons treated in Sinkala's paper are having low-frequency phonon (vibrational) component. In the current work, low frequency (low compared to higher frequencies of the protein vibrations) collective vibrations of the whole microtubules are the basis for the calculation of distribution of the electric field around them. However, vibrations considered in the current paper are not of the soliton type but of simple standing harmonic wave of longitudinal axial type, optical branch, as described in our earlier paper focused on the field calculation around single microtubules (Cifra et al., 2010d). Chou et al. (1994) has focused on the soliton-like solution of the kink waves generated by the GTP hydrolysis and the possible role of these waves in the regulation of the microtubule polymerization dynamics. In the current paper, we focus on the electric field characteristic of the whole microtubule network. Regarding Davydov's solitons in proteins (namely the α-helix) and its relation to the generation of electromagnetic field we can refer reader to the works of Brizhik (Brizhik and Eremko, 2001, 2003; Brizhik, 2003), where emission of electromagnetic waves due to acceleration of the soliton involving charge transfer has been studied. The connecting work between microtubule soliton propagation and electric field generation seems to be in work of Satarić and Tuszyński. They carried out analysis of propagation of soliton type (kink) of tubulin dipole moment tilt on protofilament, which can have effect on microtubule polymerization kinetics (Satarić et al., 1992), energy transfer along microtubules (Satarić et al., 1993; Trpisová and Tuszyński, 1997), provide a possible elucidation of the unidirectional transport of cargo via motor proteins (Sataric and Tuszyński, 2005; Sataric et al., 2008). To summarize this paragraph regarding microtubules, soliton propagation and intrinsic microtubule electric field, it can be said that another approach to the problem treated in this paper could be based on calculation of electric field around microtubules generated by propagation of solitons on microtubules involving phonon–charge or phonon–dipole interaction.

6.4. Approximations and assumptions on the level of the whole cellular microtubule network

Regarding the model of the whole cellular microtubule network there are following approximations in the models in the study presented here:

- geometry of the models,
- in phase and single frequency oscillations of individual microtubules,
- size of the cell.

Geometry of the symmetric model was chosen to correspond to geometry of nondividing cell (interphase). Asymmetric model cannot be attributed to specific phase of the cell cycle, although it resembles the position of astral microtubules during the cell division. Asymmetric model was constructed in order to study influence of simple asymmetry of cytoskeleton distribution on radiation and electric field characteristic. Current work of the present authors involves modeling of complete mitotic spindle—microtubule formation during the cell division. It should be also noted that the microtubule organizing center (centrosome in many eukaryotic cells) is not always located in the center of the cell, so the microtubules do not grow exactly radially from the cell center.

In the model used in the study presented here the mutual phase difference between oscillations of individual microtubules is zero, i.e. microtubules oscillate in phase. This situation is probably very natural. Oscillations of individual microtubules can be coupled mechanically through the centrosome (or other microtubule organizing center) from which microtubules grow and coupling can be also established via microtubule electrodynamic field. From the time of Huygens it is known and nowadays very well established that coupled oscillators tend to synchronize each other (Bennett et al., 2002) in frequency (see Maffezzoni, 2010 for illustration) under certain conditions. In principle, even if the microtubules are of different length, they can support oscillations of the same frequencies (same modes). The condition of in phase oscillations of microtubules also corresponds to the requirement of minimal energy of the system. The radiation rate is lowest for such configuration since geometrical symmetry together with in phase oscillations causes effective canceling of radiative component of generated electromagnetic field. In the case when the minimum energy state is perturbed, models using random or quasi-random phase distribution of microtubules on the one hand or models using opposite phases of microtubule on opposite hemispheres on the other hand could be used.

Size of the cell (diameter 2.8 μm) used in models presented here corresponds to a rather small cell since typical diameter e.g. of standard eukaryotic model cell, yeast *Saccharomyces Cerevisiae* is 5−10 μm. Nevertheless, the total amount of microtubules used in current model corresponds to amounts present in larger cells. Work in progress includes parametric analysis of influence of number of microtubules and cell sizes on radiated power and electric field intensity at the cell membrane.

6.5. Discussion of results

Intensity of electric field and magnitude of the radiated power are comparable with the results obtained from the calculations using membrane proteins as the sources of the electric oscillations (Pokorný and Wu, 1998). Models presented here give good quantitative estimates of power and intensity of the cellular microtubule network unperturbed and unloaded by the detection electrodes. However, few other biophysical aspects influencing the technical requirements for measurement system (Kučera et al., 2010) could not be covered in current models. Electrodynamic activity probably arises from coupled oscillatory system of polar cellular structures, i.e. cytoskeleton coupled to membrane. Vibrations excited at various points of the membrane (e.g. where the cytoskeleton binds to the cell membrane) would create very complex interference pattern of multiple standing waves on the membrane. In such general case, spatial distribution of electric field intensity associated with the vibrations of the membrane will resemble high order spherical harmonics, having closely spaced regions of opposite orientation of the electric field vector. In order to resolve the spatial minima and maxima, detector electrode needs to have tip with radius of few hundreds of nanometers, ideally units of nanometers. Another aspect is related to the "softness" of the source. Providing the Q factor of oscillating system is high, energy accumulates in the system. Once the system is loaded by the detector and the energy is drained, the effective power supplied to the detector drops to the value of power delivered by the metabolism.

Models presented here do not take into account the effect of the cell membrane. It should be noted that the cell membrane behaves due to its capacitive character as a high pass filter. Therefore electric oscillations up to few MHz (or up to few hundreds of kHz only, depending on the cell type and effective capacitance of its membrane) (Asami and Yonezawa, 1996; Wang et al., 1993) which originate inside the cell cannot pass through the membrane. However, if there are mechanical vibrations present in cytoskeleton, they can be transferred into cell membrane through the cytoskeleton-membrane protein junctions. Consequently, electric oscillations can be generated by vibrations of the polar cell membrane.

7. Conclusion

Electromagnetic radiation and electric field of the whole cellular network consisting of 100 microtubules have been calculated for microtubule oscillations in the frequency region from 1 kHz to 100 GHz. Two basic models have been used for microtubule distribution, symmetric and asymmetric model. Microtubules are uniformly distributed in the symmetric model and they are distributed toward the poles of the cell in the asymmetric model. Total radiated power of the single cell for the lossless medium from the symmetric model is the same as from asymmetric model, being highest (10^{-20} W) for the highest frequency (100 GHz) calculated and lowest (10^{-52} W) for the lowest frequency (1 kHz) calculated. Electric field intensity of the symmetric model decreases steeper with the distance from the cell membrane than that of the asymmetric model, the difference is 4 orders of magnitude at the distance of 10 μm.

From current results, there are serious implications for the measurement system which is aimed to detect cellular electrodynamic activity. It is clear that macroscopic detection of the cellular far field radiation at room temperature with classical antennas is very doubtful. Cellular electrodynamic activity in radiofrequency region will be detectable under most conditions only within 10 μm from the cell membrane, conditions are more favorable when the symmetry (both phase and geometrical symmetry) of the microtubule network is perturbed. Further requirements for detectors, which cannot be quantitatively evaluated from the current models but have been enumerated and reasoned by Kučera et al. (2010), include minimal draining of the energy from biological nanosource (oscillating microtubule) and spatial resolution of hundreds to tens of nanometers. Development of sensors with these parameters is necessary to elucidate the biological role of the cellular electrodynamic activity.

Acknowledgments

Appendix A. Supplementary data

Supplementary data associated with this article can be found in the online version at doi:10.1016/j.jtbi.2011.07.007.

References

Alberts, B., Johnson, A., Lewis, J., Raff, M., Roberts, K., Walter, P., 2008. Molecular Biology of the Cell, fifth ed. Garland.

Asami, K., Yonezawa, T., 1996. Dielectric behavior of wild-type yeast and vacuole-deficient mutant over a frequency range of 10 kHz to 10 GHz. Biophysical Journal 71 (4), 2192–2200. URL ⟨http://www.sciencedirect.com/science/article/B94RW-4V8X9KV-1T/2/e7bf9e4fe3509087f10582c611c6ec1b⟩.

Bennett, M., Schatz, M., Rockwood, H., Wiesenfeld, K., 2002. Huygens's clocks. Proceedings of the Royal Society A: Mathematical, Physical and Engineering Sciences 458 (2019), 563–579.

Betskii, O.B., Golant, M.B., Devyatkov, N.D., 1988. Millimeter waves in biology, in Russian, Millimetrovye volny v biologii. In: Fizika. Znanie, Moskva, No. 6.

Brizhik, L.S., 2003. Dynamical properties of Davydov solitons. Ukrainian Journal of Physics 48 (7), 611–622.

Brizhik, L.S., Eremko, A.A., 2001. Soliton induced electromagnetic radiation and selfregulation of metabolic processes. Physics of the Alive 12 (1), 5–11.

Brizhik, L.S., Eremko, A.A., 2003. Nonlinear model of the origin of endogenous alternating electromagnetic fields and selfregulation of metabolic processes in biosystems. Electromagnetic Biology and Medicine 22 (1), 31–39.

Bulatov, V., 1996. Distributing points on the sphere by electrostatic repulsion. ⟨http://www.math.niu.edu/~rusin/known-math/96/repulsion⟩.

Chai, B., Yoo, H., Pollack, G., 2009. Effect of radiant energy on near-surface water. The Journal of Physical Chemistry B 113, 13953–13958.

Chai, B., Zheng, J., Zhao, Q., Pollack, G., 2008. Spectroscopic studies of solutes in aqueous solution. Journal of Physical Chemistry A 112 (11), 2242–2247.

Chou, J.J., Li, S., Klee, C.B., Bax, A., 2001. Solution structure of Ca2+-calmodulin reveals flexible hand-like properties of its domains. Nature Structural & Molecular Biology 8 (11), 990–997.

Chou, K.C., 1984a. The biological functions of low-frequency vibrations (phonons): 4. Resonance effects and allosteric transition. Biophysical Chemistry 20 (1–2), 61–71.

Chou, K.C., 1984b. Biological functions of low-frequency vibrations (phonons). III. Helical structures and microenvironment. Biophysical Journal 45 (5), 881–889.

Chou, K.C., 1987. The biological functions of low-frequency phonons: 6. A possible dynamic mechanism of allosteric transition in antibody molecules. Biopolymers 26 (2), 285–295.

Chou, K.C., 1988. Low-frequency collective motion in biomacromolecules and its biological functions. Biophysical Chemistry 30 (1), 3–48.

Chou, K.C., 1989. Low-frequency resonance and cooperativity of hemoglobin. Trends in Biochemical Sciences 14 (6), 212.

Chou, K.C., Mao, B., 1988. Collective motion in DNA and its role in drug intercalation. Biopolymers 27 (11), 1795–1815.

Chou, K.C., Zhang, C.T., Maggiora, G.M., 1994. Solitary wave dynamics as a mechanism for explaining the internal motion during microtubule growth. Biopolymers 34 (1), 143–153.

Cifra, M., 2009. Study of Electromagnetic Oscillations of Yeast Cells in kHz and GHz Region. Ph.D. Thesis, Czech Technical University in Prague.

Cifra, M., Havelka, D., Kučera, O., 2010a. Biophysical role of oscillatory electric field generated by undamped microtubule vibrations. In: 6th International Workshop on Biological Effects of Electromagnetic Fields. Bogazici University, Istanbul.

Cifra, M., Havelka, D., Kučera, O., 2010b. Electric oscillations generated by collective vibration modes of microtubule. In: Kinnunen, M., Myllylä, R. (Eds.), Laser Applications in Life Sciences. Proceedings of SPIE, vol. 7376, p. 73760N.

Cifra, M., Havelka, D., Kučera, O., Pokorný, J., 2010c. Electric field generated by higher vibration modes of microtubule. In: 15th Conference on Microwave Techniques—COMITE 2010.

Cifra, M., Pokorný, J., Havelka, D., Kučera, O., 2010d. Electric field generated by axial longitudinal vibration modes of microtubule. BioSystems 100 (2), 122–131.

Cosic, I., 1994. Macromolecular bioactivity: Is it resonant interaction between macromolecules?—theory and applications. IEEE Transactions on Biomedical Engineering 41 (12), 1101–1114.

Deriu, M.A., Soncini, M., Orsi, M., Patel, M., Essex, J.W., Montevecchi, F.M., Redaelli, A., 2010. Anisotropic elastic network modeling of entire microtubules. Biophysical Journal 99 (7), 2190–2199. URL ⟨http://www.sciencedirect.com/science/article/B94RW-515K8MN-V/2/b04f67bbda5123dade8927db98c5cb93⟩.

Devyatkov, N.D., Golant, M.B., Betskii, O.B. (Eds.), 1991. Millimeter waves and their role in life processes, in Russian Millimetrovye volny i ikh rol v processakh zhiznedeyatelnosti. Moskva, Radio i svyazi.

Foster, K.R., Baish, J.W., 2000. Viscous damping of vibrations in microtubules. Journal of Biological Physics 26 (4), 255–260.

Fröhlich, H., 1968a. Bose condensation of strongly excited longitudinal electric modes. Physical Letters A 26, 402–403.

Fröhlich, H., 1968b. Long-range coherence and energy storage in biological systems. International Journal of Quantum Chemistry 2, 641–649.

Fröhlich, H., 1969. Quantum mechanical concepts in biology. In: Marois, M. (Ed.), Proceedings of First International Conference on Theoretical Physics and Biology 1967, pp. 13–22.

Fröhlich, H., 1972. Selective long range dispersion forces between large systems. Physics Letters A 39 (2), 153–154. URL ⟨http://www.sciencedirect.com/science/article/B6TVM-46TY34W-18T/2/a9809a742a843a5ac0f1380c5b616209⟩.

Fröhlich, H., 1975. The extraordinary dielectric properties of biological materials and the action of enzymes. Proceedings of the National Academy of Sciences of the United States of America 72 (11), 4211–4215. URL ⟨http://www.pnas.org/content/72/11/4211.abstract⟩.

Fröhlich, H., 1978. Coherent electric vibrations in biological systems and the cancer problem. IEEE Transactions on Microwave Theory and Techniques 26 (8), 613–618.

Fröhlich, H., 1980. The biological effects of microwaves and related questions. Advances in Electronics and Electron Physics 53, 85–152.

Fukuma, T., 2010. Water distribution at solid/liquid interfaces visualized by frequency modulation atomic force microscopy. Science and Technology of Advanced Materials 11 (3), 033003. URL ⟨http://stacks.iop.org/1468-6996/11/i=3/a=033003⟩.

Gordon, G., 2007. Designed electromagnetic pulsed therapy: clinical applications. Journal of Cellular Physiology 212 (3), 579–582.

Gordon, G., 2008. Extrinsic electromagnetic fields, low frequency (phonon) vibrations, and control of cell function: a non-linear resonance system. Journal of Biomedical Science and Engineering 1, 152–156.

Hameroff, S., Lindsay, S., Bruchmann, T., Scott, A., 1986. Acoustic modes of microtubules. Biophysical Journal 49(2 Pt 2), 58a, thirtieth Annual Meeting 9–13 February 1986, Brooks Hall/Convention Center, San Francisco, CA, Monday, February 10, 1986, 1:30 - 5:00 p.m., Polk Hall, Part 1.

Havelka, D., 2010. Electromagnetic field of microtubule network of the cell, in czech Elektromagnetické pole mikrotubulárního systému buňky. Master's Thesis, Czech Technical University in Prague.

Hayward, S., Kitao, A., Hirata, F., 1993. Effect of solvent on collective motions in globular protein. Journal of Molecular Biology 234 (4), 1207–1217.

Hölzel, R., 2001. Electric activity of non-excitable biological cells at radiofrequencies. Electro- and Magnetobiology 20 (1), 1–13.

Hölzel, R., Lamprecht, I., 1994. Electromagnetic fields around biological cells. Neural Network World 3, 327–337.

Jelínek, F., Cifra, M., Pokorný, J., Hašek, J., Vaniš, J., Šimša, J., Frýdlová, I., 2009. Measurement of electrical oscillations and mechanical vibrations of yeast cells membrane around 1 kHz. Electromagnetic Biology and Medicine 28 (2), 223–232.

Jelínek, F., Pokorný, J., Vaniš, J., Hašek, J., Šimša, J., 2008. Measurement of electrical and mechanical oscillations of yeast cells membrane in acoustic frequency range. In: 14th Conference on Microwave Techniques, 2008. COMITE 2008, April, pp. 1–4.

Jelínek, F., Šaroch, J., Kučera, O., Hašek, J., Pokorný, J., Jaffrezic-Renault, N., Ponsonnet, L., 2007. Measurement of electromagnetic activity of yeast cells at 42 GHz. Radioengineering 16 (1), 36–39.

Kharlanov, A.V., 2006. Acoustoelectric Vibrations of Cell, in Russian Akustoelektricheskie kolebaniya kletki. Ph.D. Thesis, Volograd State Technical University.

Kimura, K., Ido, S., Oyabu, N., Kobayashi, K., Hirata, Y., Imai, T., Yamada, H., 2010. Visualizing water molecule distribution by atomic force microscopy. The Journal of Chemical Physics 132, 194705.

Kittel, C., 1976. Introduction to Solid State Physics. John Wiley & Sons.

Kučera, O., Cifra, M., Pokorný, J., 2010. Technical aspects of measurement of cellular electromagnetic activity. European Biophysics Journal 39 (10), 1465–1470.

Liu, T., Chen, H., Wang, L., Wang, J., Luo, T., Chen, Y., Liu, S., Sun, C., 2009a. Microwave resonant absorption of viruses through dipolar coupling with confined acoustic vibrations. Applied Physics Letters 94, 043902.

Liu, T., Chen, H., Yeh, S., Wu, C., Wang, C., Luo, T., Chen, Y., Liu, S., Sun, C., 2009b. Effects of hydration levels on the bandwidth of microwave resonant absorption induced by confined acoustic vibrations. Applied Physics Letters 95 (17), 173702.

Madkan, A., Blank, M., Elson, E., Chou, K.C., Geddis, M.S., Goodman, R., 2009. Steps to the clinic with ELF EMF. Natural Science 1 (3), 157–165.

Maffezzoni, P., 2010. Synchronization analysis of two weakly coupled oscillators through a PPV macromodel. IEEE Transactions on Circuits and Systems I 57 (3), 654–663.

May, K.M., Hyams, J.S., 1998. The yeast cytoskeleton: the closer we look, the more we see. Fungal Genetics and Biology 24 (1–2), 110–122. URL ⟨http://www.sciencedirect.com/science/article/B6WFV-45K17FP-10/2/07a53e5685075a04b75af212f3dc46df⟩.

McKemmish, L.K., Reimers, J.R., McKenzie, R.H., Mark, A.E., Hush, N.S., 2009. Penrose–Hameroff orchestrated objective-reduction proposal for human consciousness is not biologically feasible. Physical Review E 80 (2), 021912-1–021912-6.

Mitrofanov, V., Romanovsky, Y., Netrebko, A., 2006. On the damping of the fluctuations of atomic groups in water environment. Fluctuation and Noise Letters 6 (2), L133–L145.

Pelling, A.E., Sehati, S., Gralla, E.B., Gimzewski, J.K., 2005. Time dependence of the frequency and amplitude of the local nanomechanical motion of yeast. Nanomedicine: Nanotechnology, Biology and Medicine 1, 178–183.

Pelling, A.E., Sehati, S., Gralla, E.B., Valentine, J.S., Gimzewski, J.K., 2004. Local nanomechanical motion of the cell wall of *Saccharomyces cerevisiae*. Science 305, 1147–1150.

Pizzi, R., Strini, G., Fiorentini, S., Pappalardo, V., Pregnolato, M., 2011. Evidences of new biophysical properties of microtubules. In: John, A. Flores (Ed.), Focus on Artificial Neural Networks. Nova Science Publisher, ch. 9, pp. 191–208.

Pohl, H.A., 1980. Oscillating fields about growing cells. International Journal of Quantum Chemistry: Quantum Biology Symposium 7, 411–431.

Pohl, H.A., 1981. Electrical oscillation and contact inhibition of reproduction in cells. Journal of Biological Physics 9 (4), 191–200.

Pohl, H.A., Braden, T., Robinson, S., Piclardi, J., Pohl, D.G., 1981. Life cycle alterations of the micro-dielectrophoretic effects of cells. Journal of Biological Physics 9, 133–154.

Pokorný, J., 1985. Biological effects of microwaves and cancer treatment. Mikrowellen Magazin 11 (3), 240–242.

Pokorný, J., 1987. Coherent excitation and electromagnetic field generated by living cells. In: Fiala, J., Pokorný, J. (Eds.), Biophysical Aspects of Cancer, pp. 102–110.

Pokorný, J., 1990. Electromagnetic field generated by living cells, in Czech, Elektromagnetické pole generované živými buŏkami. Ph.D. Thesis. Faculty of Mathematics and Physics, Charles University.

Pokorný, J., 2001. Endogenous electromagnetic forces in living cells: implication for transfer of reaction components. Electro- and Magnetobiology 20 (1), 59–73.

Pokorný, J., 2005. Viscous effects on polar vibrations microtubules. In: URSI GA Delhi Proceedings.

Pokorný, J., 2006. The role of Fröhlich's coherent excitations in cancer transformation of cells. In: Herbert Frohlich FRS: A Physicist Ahead of his Time. University of Liverpool, pp. 177–207.

Pokorný, J., Fiala, J., 1994. Condensed energy and interaction energy in Fröhlich systems. Neural Network World 94 (3), 299–313.

Pokorný, J., Fiala, J., Skála, L., Jelínek, F., Šrobár, F., Trkal, V., 1996. Biohysical aspects of coherence and Fröhlich's theory, in Czech Biofyzikální aspekty koherence a Fröhlichovy teorie. Československý časopis pro fyziku 46 (3), 139–156.

Pokorný, J., Hašek, J., Jelínek, F., 2005a. Electromagnetic field in microtubules: effects on transfer of mass particles and electrons. Journal of Biological Physics 31 (3–4), 501–514.

Pokorný, J., Hašek, J., Jelínek, F., 2005b. Endogenous electric field and organization of living matter. Electromagnetic Biology and Medicine 24 (3), 185–197.

Pokorný, J., Hašek, J., Jelínek, F., Šaroch, J., Palán, B., 2001. Electromagnetic activity of yeast cells in the M phase. Electro- and Magnetobiology 20 (1), 371–396.

Pokorný, J., Hašek, J., Vaniš, J., Jelínek, F., 2008. Biophysical aspects of cancer—electromagnetic mechanism. Indian Journal of Experimental Biology 46 (May), 310–321.

Pokorný, J., Jandová, A., Kobilková, J., Heyberger, K., Hraba, T., 1983. Fröhlich electromagnetic radiation from human leukocytes: implications for leukocyte adherence inhibition test. Journal of Theoretical Biology 102 (2), 295–305.

Pokorný, J., Jelínek, F., Trkal, V., 1998. Electric field around microtubules. Bioelectrochemistry and Bioenergetics 48, 267–271.

Pokorný, J., Jelínek, F., Trkal, V., Lamprecht, I., Hölzel, R., 1997. Vibrations in microtubules. Journal of Biological Physics 23, 171–179.

Pokorný, J., Wu, T.-M., 1998. Biophysical Aspects of Coherence and Biological Order. Academia, Springer, Praha, Czech Republic, Berlin, Heidelberg, New York.

Pollack, G., 2001. Cells, Gels and the Engines of Life. Ebner Seattle, WA.

Pollack, G., Cameron, I., Wheatley, D., 2006. Water and the Cell. Springer, Dodrecht, The Netherlands.

Pollack, G., Figueroa, X., Zhao, Q., 2009. Molecules, water, and radiant energy: new clues for the origin of life. International Journal of Molecular Sciences 10 (4), 1419–1429.

Reimers, J.R., McKemmish, L.K., McKenzie, R.H., Mark, A.E., Hush, N.S., 2009. Weak, strong, and coherent regimes of Fröhlich condensation and their applications to terahertz medicine and quantum consciousness. Proceedings of the National Academy of Sciences 106 (11), 4219–4224. URL ⟨http://www.pnas.org/content/106/11/4219.abstract⟩.

Romanovsky, Y., Netrebko, A., Chikishev, A., 2003. Are the subglobular oscillations of protein molecules in water overdamped? Laser physics 13 (6), 827–838.

Rowlands, S., Sewchand, L., Enns, E., 1982. Further evidence for a Fröhlich interaction of erythrocytes. Physics Letters A 87 (5), 256–260.

Rowlands, S., Sewchand, L., Lovlin, R., Beck, J., Enns, E., 1981. A Fröhlich interaction of human erythrocytes. Physics Letters A 82 (8), 436–438.

Salari, V., Rahnama, M., Tuszynski, J.A., 2011. On the theoretical possibility of quantum visual information transfer to the human brain. ⟨arXiv.org/quant-phys:0809.0008v4⟩.

Samarbakhsh, A., 2010. Mechanical Properties of Bio- and Nano-filaments. Ph.D. Thesis. University of Alberta.

Sataric, M., Budinski-Petkovic, L., Loncarevic, I., Tuszyński, J., 2008. Modelling the role of intrinsic electric fields in microtubules as an additional control mechanism of bi-directional intracellular transport. Cell Biochemistry and Biophysics 52 (2), 113–124.

Sataric, M., Tuszyński, J., 2005. Nonlinear dynamics of microtubules: biophysical implications. Journal of Biological Physics 31 (3), 487–500.

Satarić, M., Tuszyński, J., Žakula, R., 1993. Kinklike excitations as an energy-transfer mechanism in microtubules. Physical Review E 48(1), 589.

Satarić, M., Żakula, R., Tuszyński, J., 1992. A model of the energy transfer mechanisms in microtubules involving a single soliton. Nanobiology 1 (4), 445–456.

Schnell, J.R., Chou, J.J., 2008. Structure and mechanism of the M2 proton channel of influenza A virus. Nature 451 (7178), 591–595.

Shein, A.G., Kharlanov, A.V., 2007. Dipole representation of the membrane, in Russian Dipolnoe predstavlenie membrany. Biomedtsinskie tekhnologii i radioelektronika (5), 15–19.

Sinkala, Z., 2006. Soliton/exciton transport in proteins. Journal of Theoretical Biology 241, 919–927.

Sobel, S.G., 1997. Mini review: mitosis and the spindle pole body in saccharomyces cerevisiae. The Journal of Experimental Zoology 277 (2), 120–138.

Trpisová, B., Tuszyński, J.A., 1997. Possible link between guanosine 5' triphosphate hydrolysis and solitary waves in microtubules. Physical Review E 55 (3), 3288.

Tuszyński, J., Brown, J., Crawford, E., Carpenter, E., Nip, M., Dixon, J., Sataric, M., 2005. Molecular dynamics simulations of tubulin structure and calculations of electrostatic properties of microtubules. Mathematical and Computer Modelling 41 (10), 1055–1070. URL ⟨http://www.sciencedirect.com/science/article/B6V0V-4HBSKN3-2/2/696be29f0574687723502f8017c628c5⟩.

Tyner, K.M., Kopelman, R., Philbert, M.A., 2007. "Nano-sized voltmeter" enables cellular-wide electric field mapping. Biophysical Journal 93, 1163–1174.

Van Zandt, L.L., 1986. Resonant microwave absorption by dissolved DNA. Physical Review Letters 57 (16), 2085–2087.

Van Zandt, L.L., 1987. Why structured water causes sharp absorption by DNA at microwave frequencies. Journal of Biomolecular Structure & Dynamics 4 (4), 569.

Vermont Photonics Technologies Corp., 2011. URL ⟨http://homepages.sover.net/~bell/newfrontierpics.htm⟩.

Wang, C., Ru, C., Mioduchowski, A., 2006. Vibration of microtubules as orthotropic elastic shells. Physica E: Low-dimensional Systems and Nanostructures 35 (1), 48–56. URL ⟨http://www.sciencedirect.com/science/article/B6VMT-4KJTNT4-2/2/c937e65ac2d9b1c7e4f0449b66f544b0⟩.

Wang, J.F., Chou, K.C., 2009. Insight into the molecular switch mechanism of human Rab5a from molecular dynamics simulations. Biochemical and Biophysical Research Communications 390 (3), 608–612.

Wang, X.B., Huang, Y., Hölzel, R., Burt, J.P.H., Pethig, R., 1993. Theoretical and experimental investigations of the interdependence of the dielectric, dielectrophoretic and electrorotational behaviour of colloidal particles. Journal of Physics D: Applied Physics 26, 312.

Winey, M., Mamay, C., O'Toole, E., Mastronarde, D., Giddings Jr, T.H., McDonald, K., McIntosh, J., 1995. Three-dimensional ultrastructural analysis of the Saccharomyces cerevisiae mitotic spindle. Journal of Cell Biology 129 (6), 1601–1615. URL ⟨http://jcb.rupress.org/cgi/content/abstract/129/6/1601⟩.

Xie, A., van der Meer, A., Austin, R., 2001. Excited-state lifetimes of far-infrared collective modes in proteins. Physical Review Letters 88 (1), 18102-1–18102-4.

Zheng, J., Chin, W., Khijniak, E., Khijniak Jr., E., Pollack, G.H., 2006. Surfaces and interfacial water: evidence that hydrophilic surfaces have long-range impact. Advances in Colloid and Interface Science 127 (1), 19–27.

Zheng, J., Pollack, G., 2003. Long-range forces extending from polymer-gel surfaces. Physical Review E 68 (3), 31408-1–31408-7.

5 | ELECTRO-ACOUSTIC BEHAVIOR OF THE MITOTIC SPINDLE: A SEMI-CLASSICAL COARSE-GRAINED MODEL

This chapter is a version of:

Author contributions:

| Designed research: M.C., **D.H.**, and O.K.

| Performed research: **D.H.**

| Analysed data: O.K., **D.H.** and M.C.

| Wrote the paper: O.K., M.C. and **D.H.**

| Candidate's contribution: 60%

The manuscript carries the following acknowledgements:

Erratum:

| The equations (6) and (7) are in error and should read as follows:

$$\mathbf{E_z} = -\frac{\omega |\mathbf{p_m}| Z k^2}{4\pi r'''^2}\Bigg[2z'''\left(-y'''\sin\xi + z'''\cos\xi\right)\left((\mathrm{j}kr''')^{-2} + (\mathrm{j}kr''')^{-3}\right)$$

$$+ \left(-y'''z'''\sin\xi - (x'''^2 + y'''^2)\cos\xi\right)\left((\mathrm{j}kr''')^{-1} + (\mathrm{j}kr''')^{-2} + (\mathrm{j}kr''')^{-3}\right)\Bigg]e^{-\mathrm{j}kr'''}\mathbf{z_0}$$

$$\begin{pmatrix} x''' \\ y''' \\ z''' \end{pmatrix} = \begin{pmatrix} 1 & 0 & 0 \\ 0 & \cos\xi & -\sin\xi \\ 0 & \sin\xi & \cos\xi \end{pmatrix}\begin{pmatrix} \cos\eta_r & -\sin\eta_r & 0 \\ \sin\eta_r & \cos\eta_r & 0 \\ 0 & 0 & 1 \end{pmatrix}\begin{pmatrix} x_x - x_0 \\ y_x - y_0 \\ z_x - z_0 \end{pmatrix}$$

PLOS ONE

Electro-Acoustic Behavior of the Mitotic Spindle: A Semi-Classical Coarse-Grained Model

Daniel Havelka[1,2]*, Ondřej Kučera[1], Marco A. Deriu[3], Michal Cifra[1]

1 Institute of Photonics and Electronics, Academy of Sciences of the Czech Republic, Prague, Czechia, 2 Department of Electromagnetic Field, Faculty of Electrical Engineering, Czech Technical University in Prague, Prague, Czechia, 3 Institute of Computer Integrated Manufacturing for Sustainable Innovation, Department of Innovative Technologies, University of Applied Sciences and Arts of Southern Switzerland (SUPSI), Manno, Switzerland

Abstract

The regulation of chromosome separation during mitosis is not fully understood yet. Microtubules forming mitotic spindles are targets of treatment strategies which are aimed at (i) the triggering of the apoptosis or (ii) the interruption of uncontrolled cell division. Despite these facts, only few physical models relating to the dynamics of mitotic spindles exist up to now. In this paper, we present the first electromechanical model which enables calculation of the electromagnetic field coupled to acoustic vibrations of the mitotic spindle. This electromagnetic field originates from the electrical polarity of microtubules which form the mitotic spindle. The model is based on the approximation of resonantly vibrating microtubules by a network of oscillating electric dipoles. Our computational results predict the existence of a rapidly changing electric field which is generated by either driven or endogenous vibrations of the mitotic spindle. For certain values of parameters, the intensity of the electric field and its gradient reach values which may exert a not-inconsiderable force on chromosomes which are aligned in the spindle midzone. Our model may describe possible mechanisms of the effects of ultra-short electrical and mechanical pulses on dividing cells—a strategy used in novel methods for cancer treatment.

Competing Interests: The authors have declared that no competing interests exist.

* E-mail: havelka@ufe.cz

Introduction

Mitosis is a crucial step in cell division of eukaryotic cells, *i.e.* those forming animals, plants, fungi, and protists. During mitosis a cell separates its duplicated genetic information encoded in its chromosomes into two identical ensembles. Errors in this process may lead to genetic disorders and are also supposed to play a role in cancer and aging [1,2]. The main part of the apparatus involved in the mitosis process is formed by microtubules, tubular cytoskeletal polymers, arranged in a so-called mitotic spindle.

Microtubules (MTs in following) are most frequently formed by 13 protofilaments organized in a hollow cylinder. Each protofilament comprises of a chain of alternating alpha- and beta-tubulin monomers. MTs can be found either stable or highly dynamic. Dynamic instability of MTs resides in rapid switching between growth and shrinkage. These MTs are structurally polar and the charge bound in their structure (see models in refs. [3–5]) is also responsible for their electrical polarity, which is generally supposed to play an important role in the function of proteins [6]. MTs can be moved and oriented both in static and alternating electric fields as a result of electrophoresis and dielectrophoresis [7–12]. Also, it has been proved that a high magnetic field effects the alignment of MTs [13–15], due to diamagnetic anisotropy. Experimental data about mechanical properties of MTs vary over several orders of magnitude [16]. Dynamic mechanical properties of MTs have been studied only on a theoretical level [17–30]. MTs should be

able to vibrate at their natural frequency according to these studies. In combination with their electrical properties, basic electrodynamic models of MTs have been recently introduced [31–34]. These models have enabled the calculation of spatial distribution and time evolution of high-frequency electric fields generated by the single vibration mode of microtubule and MT networks. It has been predicted that MTs should exhibit such electrodynamic activity *in vivo*. The importance of this activity resides in the fact that it (i) may provide an intracellular signaling mechanism [35], (ii) may locally change the chemical reaction rates by attracting or rotating the molecular reaction partners [36].

Microtubules assemble mitotic spindles in a way resembling field lines of an electric dipole. MTs grow from one microtubule organizing center (MTOC, the pole) towards the other. In the spindle midzone (equatorial plane), where chromosomes are arranged, the MTs are either linked to each other (polar microtubules) or bounded to chromosomes (kinetochore microtubules). MTs which ray from MTOC and do not grow towards the equatorial plane are also present (astral microtubules). The mitotic spindle is a dynamic structure which undergoes permanent remodeling in order to capture and segregate chromosomes between daughter cells.

Due to their polarity and involvement in mitosis (and also in other crucial physiological processes), MTs are often targets of research connected to chemical and physical treatment of various diseases. In general, medical strategies aimed at microtubules

32

which form the mitotic spindle are useful in those cases when the rapid rate of cell division is to be interrupted or when an apoptosis triggered by a disruption of the mitotic spindle is to be initiated. Chemical anti-microtubule agents, which cause the aggregation of tubulin or dissociation of MTs, are therefore in widespread clinical use against various types of cancer [37]. Thanks to the electrical polarity of microtubule subunits, it was shown that tumor growth may be inhibited by alternating the electric field which disrupts proper formation of mitotic spindles in cells [38]. While the effect of the external electromagnetic field of 94 GHz on microtubule dynamics within cells seemed to be purely due to heating [39], other authors found small but significant effects on dividing cells which were exposed to 935 MHz which they interpreted as effects of MT polymerization [40]. These examples are, however, not efficient enough or they have drastic side effects. Better understanding of how the formation and function of the mitotic spindle is controlled is, therefore, important for a general biophysical insight as well as for the development of novel diagnostic methods and therapeutic strategies.

Despite this importance, only a few models addressing the dynamics and physical properties of the mitotic spindle exist. The importance of motor proteins for the assembly of the mitotic spindle was analyzed in ref. [41]. The biochemical model addressing control pathways of Mitotic Spindle Assembly Checkpoint was also published [42]. The relation between mechano-chemical factors and their contribution to the generation of forces within the mitotic spindle was reviewed in [43]. Authors of ref. [44] developed the physical theory of mechanical second-scale oscillations of the mitotic spindle which takes place during asymmetric cell division and which is attributed to force imbalances produced by assemblies of molecular motors. Mechanical oscillations, with no reference to electrical, with respect to interruption of mitosis by the ultrasound were also subjects of the rough model [45], which predicts the effective range of frequencies to produce such effect as tens of kHz. Electrical oscillations of the mitotic spindle were considered as a speculative mechanism controlling the chromosome separation [46]. However, no qualitative analysis of this phenomenon was shown. In this context, the study of the electric field coupled to mechanical oscillations of mitotic spindles may comprise one of the missing links in comprehension of the dynamic functionality of mitotic spindles (Preliminary conference report on this topic [33] does not cover all necessary features. Furthermore, it considers only optical branch of vibrations of mitotic spindle, which is very special case selected for convenience of calculation in this [33] pioneering study. Moreover, no analysis is provided.).

In this research paper, we present an electromechanical model of mitotic spindle vibrations based on the Microtubule Resonance Dipole Network Approximation (MRDNA) [34]. It estimates the generation of an electromagnetic field and its force effects as a result of either endogenous or forced vibrations of mitotic spindles. This model has relevance for the assessment of

- influence of external electromagnetic and mechanical stimuli on cell division, especially on the process of chromosome segregation,
- role of the hypothetical endogenous electrodynamic phenomena in mitosis regulation and control,
- possible role of electric fields in cancer treatment, and
- general assessment of the dynamic properties of the mitotic spindle.

We report on how a pulsed electric field, which is used for therapeutic strategies against cancer [47] and is common to contemporary electronic devices, may influence the electric field distribution within the equatorial plane where chromosome separation takes place. Our results also clarify the relevance of the endogenous vibrations for regulatory mechanisms in cells. We provide experimentally testable predictions of spectroscopic data for the purpose of validation of the model. Generally, our model provides a framework for the evaluation of driven or endogenous electro-acoustic behavior of the mitotic spindle.

Results

We performed computational predictions of the intensity of the electric field generated by acoustic vibrations of the mitotic spindle. In our model, we started with a molecular model of a microtubule (Fig. 1–A), from which we extracted the positions of atoms which form one heterodimer. Since one heterodimer of tubulin contains about 9,000 atoms and the mitotic spindle includes hundreds of thousands of heterodimers, computational demands allow only coarse-grained modeling of the mitotic spindle dynamics. From different combinations of atomic weights and positions we calculated the position of the center of gravity of each monomer of tubulin. We positioned an electric dipole which corresponds to the dipole moment of charge distribution within the monomer into the gravity center of each monomer (Fig. 1–D). Next, we calculated the spatial positions of MTs which form the mitotic spindle and within them coordinates of the centers of gravity for each monomer. Finally, we let the elementary dipoles, representing the electrical polarity of heterodimers, oscillate according to the first natural longitudinal vibrational mode of corresponding MT [23]. We considered two boundary conditions: (i) both ends of all MTs are fixed and (ii) all astral MTs are fixed while equatorial ends of polar and kinetochore MTs are free. We considered two situations in our calculations: (i) synchronized vibrations of the mitotic spindle after pulsed excitation and (ii) vibrations with a random phase and a constant amplitude. The first may come from an externally pulsed electromagnetic or mechanical signal (Note that the pulse duration is bounded with its frequency content. The shorter the pulse, the broader the frequency spectrum.), the latter corresponds to the accumulation of noise and vibrational energy from the inside of a cell [34]. We studied the time evolution of the intensity of the electric field generated by damped and undamped mechanical vibrations of the mitotic spindle for both situations. The notation in figures is as follows: P stands for pulsed excitation; R – random excitation; Fx – fixed-ends; Fe — free-ends; U – undamped vibrations; D – damped vibrations. For example, PFxU denotes undamped vibrations of MTs with fixed-ends driven by pulse.

We used ellipsoidal cell models. We positioned 300 microtubules within each cell: 100 astral, 100 kinetochore and 100 polar microtubules. We calculated detailed time and space evolution of the intensity of the electric field for cells with volume equivalent to a sphere with a radius of 3.3 μm (Fig. 2). The equivalent sphere may be understood as the non-dividing version of the ellipsoidal cell. This size was chosen for two reasons. Firstly, such cell has very high microtubule density, so this size of the model may act as an upper estimate of the intensity of electric field in cells. Secondly, small size of the cell reduces the computational demands while sufficient resolution is preserved. We also calculated the spectroscopic properties of this model and of cells with a radius equivalent to 7, 30 and 65 μm to show how the spectrum of vibrations depends on the cell size. The summary of values of specific parameters used in our calculations, as well as mathematical details of the model, are provided in the Models section.
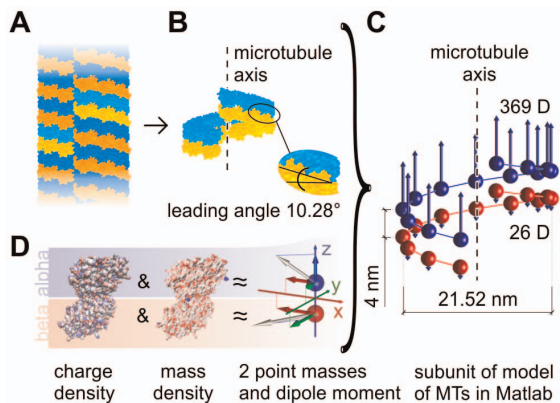
33

Figure 1. Method of approximation of electric properties of microtubules. The MT (A) is divided into so called MT rings (B) forming the spiral, where corresponding dipoles were placed in the center of gravity of respective monomer (C). Center of gravity and dipoles were calculated from molecular structure of tubulin (D).
doi:10.1371/journal.pone.0086501.g001

Figure 2. Model of mitotic spindles and corresponding intensities of electric field. The model of mitotic spindle of ellipsoidal cell with equivalent radius 3.3 µm (A). The position of equatorial plane is marked by red dashed line. Magnitude of intensity of electric field in three main plains of the ellipsoidal cell (boundary of the cell is depicted by white circle) in time $t = 27$ ps after pulsed excitation is shown in (B–D). The plane shown in (D) is the equatorial plane. All pictures have the same spatial and intensity scale and the same quality factor of vibrations, $Q = 4$. All time locks were taken in $t = 27$ ps after pulsed excitation. Presented data correspond to boundary conditions with fixed ends.
doi:10.1371/journal.pone.0086501.g002

Spectroscopic properties

The essential parameter of oscillatory behavior of MTs is the quality factor of oscillations, which shows how the oscillations are damped. There have been theoretical discussions whether any microtubule vibration modes can be underdamped and thus sustain coherence [48,49]. Theoretical analysis [30] of forced bending-mode vibrations of MTs in a viscous medium like cytosol revealed that the quality factor of vibrations is frequency dependent and may range from 0 to almost 4. However, there are no experimental works which would quantify the damping coefficient or the quality factor and resolve this discussion. We used values of the quality factor ranging between 0.1 and 50.0 within the parametric space of our model. Values lower than 0.5 correspond to an overdamped system where the responses to impulse driving show no oscillatory behavior but rather exponential decay. We restricted the lower boundary to 0.1 since such a dynamic system becomes too slow and our model might not be appropriate. The upper boundary of 50 reflects the fact that we do not expect microtubule oscillations with higher quality to take place *in vivo*. If it was not so, the oscillations would accumulate a rather large amount of energy which might cause destruction of the system. The upper limit of 50 is higher than that reported in [30] because we consider longitudinal vibration modes in our model. Longitudinal modes are expected to be less damped compared to bending modes since they cause only limited displacement of the surrounding cytosol [31,50]. The value of the quality factor influences the shape of the frequency spectrum of oscillations: the lower the quality factor, the broader the bandwidth of each MT. The resulting spectrum of the mitotic spindle (see Fig. 3–A) is therefore smooth and broad for smaller values of the quality factor and it shows distinct narrow spectral lines only for higher values of the quality factor. The shape of the spectrum comprises of two bands: the lower one corresponding to relatively longer kinetochore and polar MTs and the higher one corresponding to astral MTs, which are relatively shorter in the considered model. In conclusion, the spectrum of vibrations resembles a histogram of lengths of microtubules with the number of bins proportional to the quality factor.

The bandwidth of the vibrations is given by modes excited in individual MTs. We considered only the lowest longitudinal mode
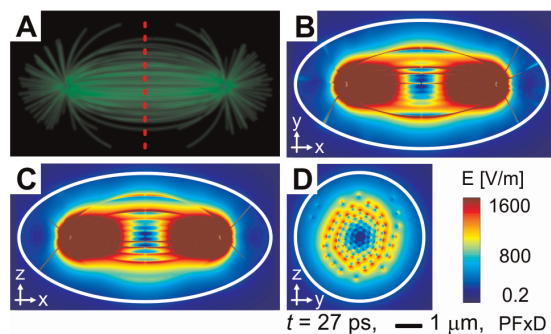
for which we may expect the highest coupling of the driving electric field. The boundary conditions limit the number of half-waves on MT and thus the frequency content. MTs with fixed ends vibrate with a higher frequency than those with one end free. The spectra of the models with different boundary conditions are therefore also different. The other parameter which influences the bandwidth of the spectrum is the size of the model because with increasing size of the spindle the corresponding frequencies become lower. For the largest considered model cell the maximal response occurs at a frequency of approx. 1 GHz while for the smallest cell the spectrum covers a range between approx. 8 and 18 GHz. The shape of the spectrum remains similar and appears to be relatively wider, although the ratio of bandwidth to the central frequency remains unaffected (see Fig. 3–B).

The amplitude of oscillations was set to 1 nm in our simulation, which roughly corresponds to the amplitude predicted by molecular modeling [23]. It means that the maximal longitudinal displacement of the center of gravity of one monomer in the position of the vibration anti-node was 1 nm. Displacements of other monomers within the MT was lower according to the shape of the mode.

Intensity of the electric field

The high-frequency electric field generated by the vibrations of the mitotic spindle has a very complex structure with high intensity fixed maxima around MTs and other moving local minima and maxima, which are given by destructive and constructive interferences of contributions from all MTs. Generally, the shape of the field changes very rapidly within few nanoseconds as a results of high frequencies involved in vibrations. The intensities of the field vary on very small distances within few orders of magnitude, which leads to gradients as large as 10^5 V/m on the distance of few hundred nanometers. The field either pulsates if the vibrations are synchronized to some extent, or has a rather runny character if the phases of vibrations are highly desynchronized. Videos of time evolution of the field are provided in the supplementary material.
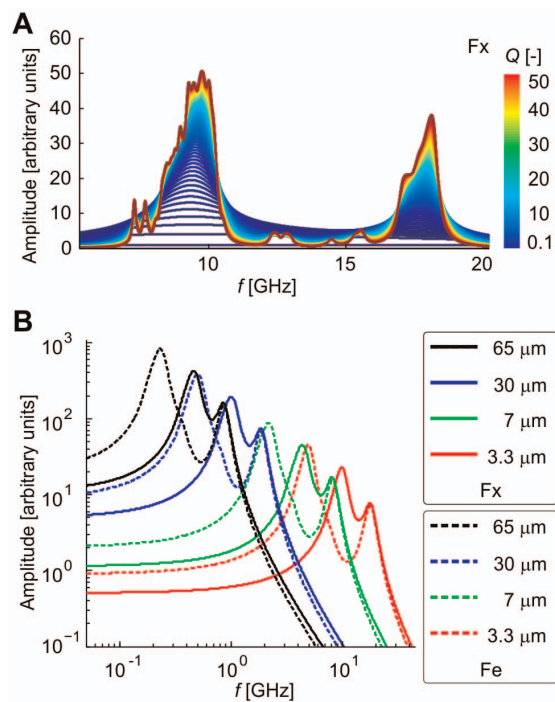
34

Figure 3. Spectrum of vibrations of mitotic spindle. Spectrum as a function of the quality factor (A) and size of model cell (B). The value of quality factor is coded according to the colorbar in A. Solid line in B corresponds to boundary conditions with fixed ends, dashed line to free ends in equatorial plane.
doi:10.1371/journal.pone.0086501.g003

Since the most important activity of the mitotic spindle takes place in the spindle midzone where chromosomes are aligned, we analyzed mainly the intensities of the field in the equatorial plane of our model cell, which corresponds to the spindle midzone. The model of the mitotic spindle and examples of time-locks of intensity of the electric field in equatorial and other main plains of the ellipsoid forming the model cell are shown in Fig. 2. The electrical intensity is coded according to the provided scale-bar. In order to show the influence of the chosen parameters of calculations on the resulting intensity, we analyzed the behavior of the model for different boundary conditions and the feeding of vibrations.

It is clearly visible in Fig. 2 that the magnitude of intensity of the electric field has the highest values in the immediate vicinity of MTs. Therefore, the smaller model cells with denser MT networks show higher average intensities of electric fields (data not shown). Very high intensities of electric field are around the MTOCs for the same reason.

Due to synchronization, pulse-driven oscillations generate higher intensity electric fields at the beginning. This synchronization is lost in the course of time due to different lengths and therefore different frequencies of individual MTs. The oscillatory behavior of the resulting intensity therefore vanishes after few periods. The amplitude of intensity decreases due to damping and to lesser extent also due to desynchronization (*i.e.* lower probability of constructive interferences). It is clearly visible how oscillations driven by pulse die out within 1 ns (Fig. 4). The time scale of vibrations, which is given by their frequencies, therefore leads to

events much faster than the dynamic functionality which is visible in microscopic experiments.

Free ends of MTs generate higher electrical intensity in the equatorial planes of cells. The reason for this behavior resides in the fact that there is higher displacement of dipoles in free ends of MTs within the equatorial plane. The higher the displacement, the higher the generated intensity of the electric field. Compared to fixed-end conditions, free ends generate an electric field which is stronger by a few orders of magnitude (Fig. 4).

Endogenous undamped vibrations with random phases create more unstable structures of the field which, however, looks similar to the previous one in its time-locks. The time evolution does not show any regularity since interferences occur randomly. We therefore analyzed the statistical distribution of the intensity of the electric field in time and space using the Monte Carlo approach, *i.e.* by statistical analysis of many simulations with random initial conditions. The maximum, minimum and mean values of electrical intensity within the equatorial plane are shown in Fig. 5 (A–F). Data were collected from 5 periods of vibrations of the longest MT for 100 random initial conditions. 300 samples were statistically analyzed from each realization. Again, free-end boundary conditions lead to much higher electrical intensities in the equatorial plane compared to fixed-end boundary conditions. Despite no distinctive regularity in terms of the field shape, there was only a little variation from run to run in terms of average intensity of electric field. The same type of data calculated for the pulse driven vibrations are shown in Fig. 5 (G–L) for comparison. The differences in the time evolution of the electric field in the equatorial plane between pulsed and random excitation is illustrated in Fig. 6. The pulsed excitation leads to higher amplitudes of electric intensity, while the mean value at the point of evaluation is almost identical for both feedings due to constructive interference.

In summary, the maximal intensities of the electric field are achieved (i) in the vicinity of MTs (ii) in the area of the highest amplitude of vibrational displacement and (iii) shortly after excitation due to maximum displacement of dipoles. We may generally conclude that the absolutely highest magnitude of intensity of the electric field within the equatorial plane is achieved after synchronized excitation in cells with high density of the MT network, where MTs are not fixed in the midzone. However, the mean value of the intensity does not depend on the type of excitation.

Discussion

This is the first documented report of a model concerning the electro-acoustic behavior of the mitotic spindle. This model provides valuable data for future research of mitotic spindle dynamics. It also provides foundations for assessment of the role of large scale bio-electrodynamic phenomena in cell physiology. In the following section, we discuss the limitations of our model, the selection process of used parameters, physical and biological relevance of results and possibilities of verification of the model and its computational predictions.

Limitations of the model

The model provides the very first insight into electro-acoustic behavior of the mitotic spindle. In this section, we will analyze the limitations of the model and discuss possible biological and biophysical implications of the results.

The limitations of the model are caused by simplifications which were necessary for efficient calculation. First of all, the real atomic arrangement of MTs was replaced with a coarse-grained
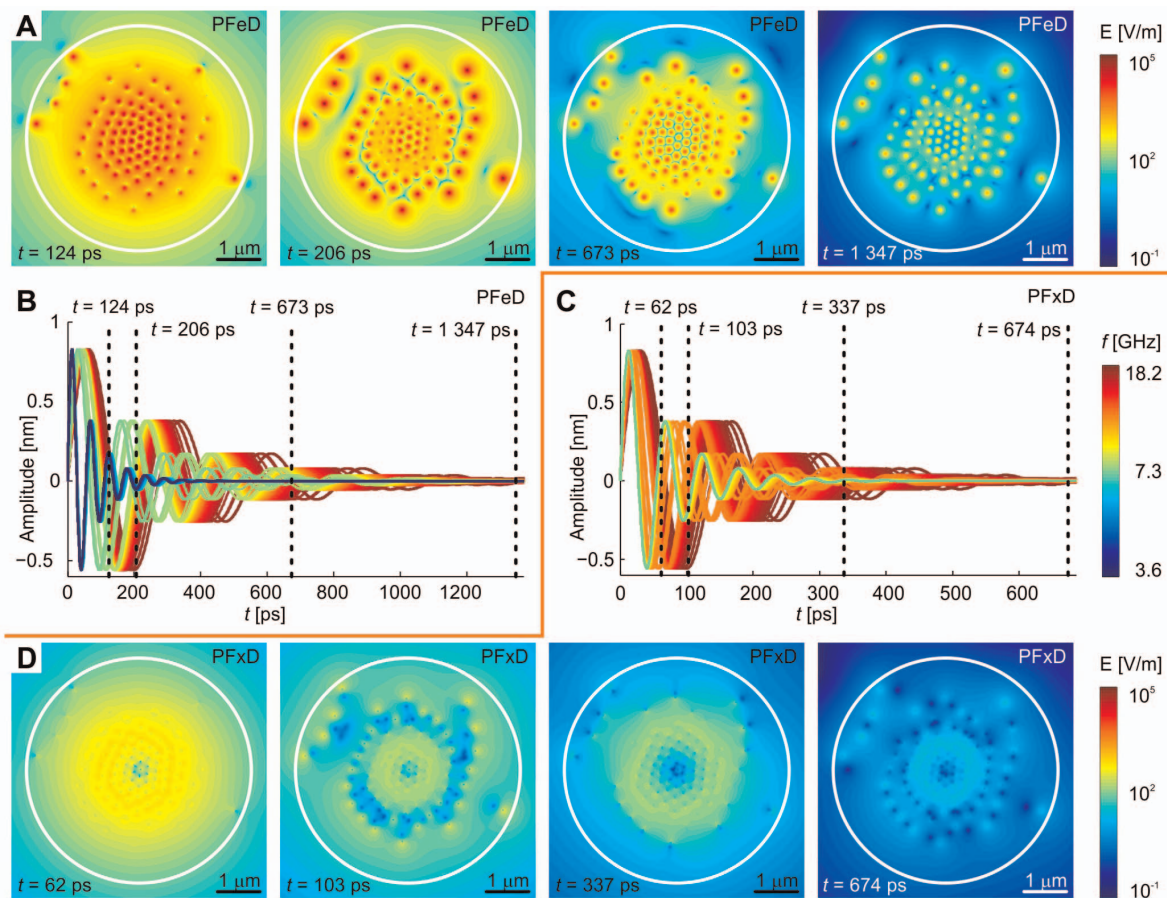
35

Figure 4. Time evolution of intensity of electric field in equatorial plane for different boundary conditions. The magnitude of intensity of electric field depends on time and boundary conditions. It undergoes exponential decay due to damping after pulsed excitation. Map of electrical intensities (A) and amplitude of mechanical oscillations of all MTs (B) are shown for free ends of MTs in equatorial plane. Data for fixed boundary conditions are shown in (C) and (D). Data correspond to ellipsoidal cell with equivalent radius of 3.3 m. Note different time scales in (A, B) and (C, D). Quality factor of vibrations, $Q = 4$, is the same for all examples.
doi:10.1371/journal.pone.0086501.g004

representation where each monomer was approximated with its mass and a dipole moment. Such an approximation leads to loss of details of the consequently generated field on the scales which is comparable to the size of one monomer. However, since the field for each point in space is a summation of the total contribution from all dipoles, the loss of details is not so dramatic. Moreover, it may be considered as an advantage because it provides averaged values which may allow more general conclusions (they are less sensitive to the nanometer-detailed spatial arrangement of the mitotic spindle). A more detailed structure of the field would probably not have such an effect on the chromosomes with dimensions much larger than one tubulin heterodimer.

The second limitation resides in the fact that our model is based on the assumption that there is no back-coupling of the oscillating field to mechanical oscillations. We allowed ourselves to neglect any back- coupling because we suppose that mechanical oscillations of a single MT already take the coupling into account since mechanical properties are, besides other forces, given by the electromagnetic interaction between atoms constituting the MT. The interaction between MTs was neglected because of compu-

tational demands. From the results we may say that it does not affect the resulting field in the equatorial plane because MTs are rather far from each other with respect to the intensity of the field they generate. A different situation is near the MTOC, where the microtubules' network is dense. Coupling in this region should be analyzed in future research.

Thirdly, the oscillations of individual MTs were calculated with boundary conditions independent from oscillations of other MTs. It means that MTOCs were considered absolutely rigid. As a result, the overall vibrations of the MTs in our model probably do not correspond to natural vibrations of the mitotic spindle. However, it is not to the detriment of generality of our results because the parameters of the coupling between MTs forming the mitotic spindle are not known anyway. Also, no boundary conditions can be generally stated.

Parameters used in calculations

Like in any other model or rather a complicated system, our model of the mitotic spindle has a large number of degrees of freedom, *i.e.* a large number of parameters which we had to
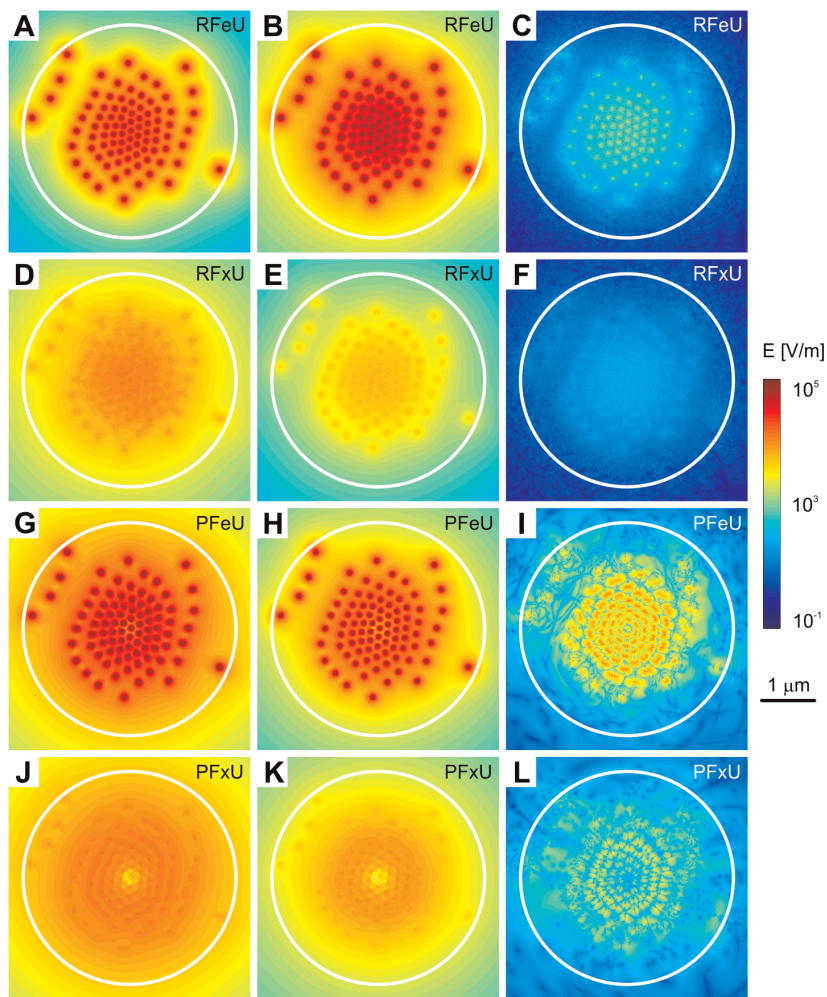
36

Figure 5. Statistical analysis of electric field generated by random and fixed undamped vibrations. Data are shown for free-ends boundary conditions (A–C, G–I) and for fixed-ends in equatorial plane (D–F, J–L). Maximal values (left column A, D, G, J), mean values (middle column B, E, H, K) and minimum values (right column C, F, I, L) of the intensity of electric field in equatorial plane are shown. Data corresponding to random vibrations are shown in (A–F), results for pulse-driven vibrations are displayed in (G–L).
doi:10.1371/journal.pone.0086501.g005

choose. Some values of the used parameters are either simply unknown or subject to biological variability.

The size, geometry and number of MTs forming the spindle vary for diverse cells and it is not possible to generalize this variability in one model. However, our model is rather robust in this sense and enables modifications thanks to possible separation of the geometrical model and electromagnetic computations. The vibrational properties are the most speculative part of our model. The damping of vibrations, type of excited modes, excitation itself and boundary conditions may be only estimated. The frequency of the lowest vibration mode of MT was extrapolated from the molecular dynamics and normal model analysis data, the most accurate up to date model available. The selection of the longitudinal type of modes was based on their highest efficiency for generation of an electric field and assumed low damping. Bending modes involve much greater displacement of surrounding mass and therefore are likely much more damped. Torsional

modes involve much smaller total electric dipole moments due to cylindrical symmetry and therefore their efficiency of generation and absorption of electric field is likely low. There is only a single report which allows estimates of microtubule vibration damping [51] and yields $Q \approx 4$ from halfwidth Δf of the spectral peak at the central frequency f assuming $Q = f/\Delta f$. Homogenization of electrical properties of the remaining cells was necessary for obtaining generalized results. Other approximations do not influence the fundamental behavior of the model.

Discussion of results

Our *in silico* experiments have shown that mechanical vibrations of microtubules which form the mitotic spindle generate an oscillating high frequency electromagnetic field. The relevance of an electromagnetic field in cell biology resides in the force by which it may act on the matter. The electromagnetic field may influence particles which are electrically charged, polarized or
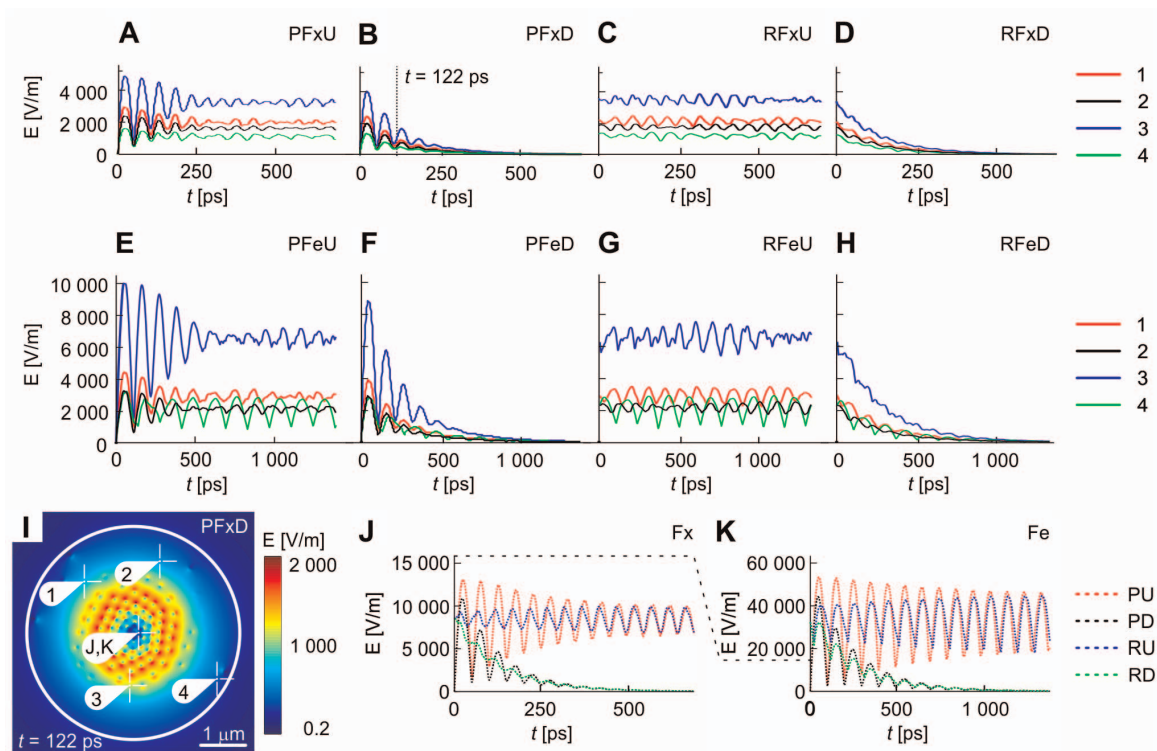
37

Figure 6. Time evolution of intensity of electric field in equatorial plane for different feeding. Time versus electric intensity plots are shown for fixed-ends and pulsed undamped (A), pulsed damped (B), random undamped (C) and random damped (D) excitation followed by free-ends and pulsed undamped (E), pulsed damped (F), random undamped (G) and random damped (H) excitation shown in points 1–4 of equatorial plane specified in time-lock (I). (J and K) show time versus electric intensity plots in central point of the equatorial plane. Fixed-end boundary condition is displayed in (J), free-end boundary condition is displayed in (K). Dashed curves show data for pulsed undamped, pulsed damped, random undamped and random damped conditions.
doi:10.1371/journal.pone.0086501.g006

polarizable. Since the magnetic component of the field is very low in our simulations (data not shown), we may limit the following discussion to only the effects of the electric component in the field.

The intensity of the electric field has reached the highest magnitude in the surroundings of microtubules' vibration anti-nodes, within the area with high microtubule density and, to lesser extent, also in cases of constructive interference of contributions from more MTs. The position of the regions of high intensity of the field is therefore dependent on the boundary conditions of microtubules' vibrations. The question whether MTs have a vibration node or anti-node in their equatorial plane is therefore important for further evaluation of possible effects of the generated field. We may expect that the free-end condition (anti-node in the equatorial plane) is closer to reality because the MTs in the spindle midzone are either free searching for chromosomes (kinetochore MTs) or bound to each other by motor proteins (polar MTs). The binding of MTs to motor proteins can not be definitely represented by only free MT ends, but we may expect that the binding is either (i) stiff or (ii) pliant. In the first case, the vibrations will be effectively coupled between MTs and, therefore, there will not be a single node in the spindle midzone. In the second case, the weak coupling between MTs will most likely lead to the formation of a local anti-node. We may, therefore, expect that the intensity of the electric field would be reaching a higher range of values presented in our results. The intensity also depends on the

amplitude of mechanical vibrations. We used maximum amplitude in anti-nodes of 1 nm, which is comparable to the amplitude of vibrations measured on single cells [52]. These vibrations have much lower frequency than those discussed here, but such an amplitude may be reached after artificial excitation.

Generally, vibrations excited by pulse generate the same mean intensity as random vibrations, both without damping. The issue of damping is very important in our model but its relevance for random vibrations is questionable, because it is extremely difficult to estimate thermal excitation of the mitotic spindle. The relevance of the presented data is in comparison with pulsed excitation. Since the mean value of generated intensities is the same, the question of phase synchronization was proved to be not of much importance for the evaluation of driven vibrations. It means that external feeding does not need to take into account the space/time/phase properties of vibrations in order to be excited. Only the constructive interference, which has limited effect, will disappear while the main behavior features exhibited by our model will not be affected.

Since the functional role of the mitotic spindle takes place within the spindle midzone, we were mostly interested in the field properties in the equatorial plane of our model cell. The intensities of the field in the equatorial plane were as large as $4.4 \cdot 10^7$ V/m. The intensity may vary within several orders of magnitude in space and time. Differences up to 5 orders of magnitude of V/m

Table 1. List of parameters.

Symbol	Description	Value	Units
D_α	dipole moment of α monomer	369	D
D_β	dipole moment of β monomer	26	D
s	axial shift between protofilamnets	0.92	nm
ζ	diameter of MT rings	10.76	nm
Ξ	leading angle of MT rings	10.28	degrees
a	major axis of ellipsoid cell	5.16	μm
b	minor axis of ellipsoid cell	2.64	μm
R	radius of non-dividing spherical cell	3.3	μm
V	volume of spherical cell with radius R	0.15	μm^3
c	position of MTOC on the x-axis	2.64	μm
ρ	diameter of MTOC	200	nm
N	number of MTs	300	-
N_a	number of nucleations centers, astral MTs, one MTOC	50	-
N_k	number of nucleations centers, kinetochore MTs, one MTOC	50	-
N_p	number of nucleations centers, polar MTs, one MTOC	50	-
κ_a	equivalent number of nucleation centers	120	-
Ω_a	spatial angle for division of MTOC, astral MTs	2.8212	sr
κ_{p+k}	equivalent number of nucleation centers	225	-
Ω_{p+k}	spatial angle for division of MTOC, polar and kinetochore MTs	2.9154	sr
m_q	arbitrary constant	1	-
u	index of polar and kinetochore MTs	1, 2,…, 200	-
π	mathematical constant	3.14159…	-
n	index denoting n^{th} MT	1,2,…,N	-
$p_{a\alpha}$	oscillating part of dipole moment of α-tubulin	$(3.8)^{-1}$	-
$p_{a\beta}$	oscillating part of dipole moment of β-tubulin	$(3.8)^{-1}$	-
Q	quality factor	0.5÷100	-
k_1	coefficient of extrapolation	$2.5304\cdot10^{12}$	-
r	radius of outer wall of MT	12.5	nm
k_2	coefficient of extrapolation	$9.0966\cdot10^{8}$	-
l_{TH}	length of tubulin heterodimer	8	nm

The list of symbols (in the order of appearance) representing variables of the model and their values used for calculations.
doi:10.1371/journal.pone.0086501.t001

may be found on the distance of hundreds of nanometers and even larger differences occur in one point of space within hundreds of picoseconds.

The quantitative analysis of possible force effects of electromagnetic fields presented in this research go beyond the scope of this paper. Briefly, the field with comparable frequencies and intensities as large as those shown in this research was experimentally shown to produce observable translational effect on the free MTs. Since chromosomes are also electrically polarizable [53] and larger in size in two more dimensions than MTs, we may also expect them to be more profoundly susceptible to the reported field due to polarization. The idea that the field exerts translational movements of chromosomes for larger distances is rather far-fetched, but the rotational or small scale translational movement may be possible. Such a small scale movement may, however, have a significant effect on the proper binding of chromosomes to MTs. Whether this effect would be constructive or destructive for proper chromosome separation remains unknown, but we may expect that destructive effects are much more probable, because such a complex field could be driven externally for specific purposes only with extreme technical difficulties. Picosecond time-scale of vibrations leads to ultra-fast events which are much faster than standard dynamics of the mitotic spindle. Biological events with this time-scale are explored only a little.

We see the presented model to have relevance for elucidation of the effects of electric pulses during mitosis, especially for cancer treatment. The effects of short nanosecond pulses, be it of electric or acoustic nature, can be described using our model by pulse excitation of the mitotic spindle vibrations. Such pulse excitation of the mitotic spindle generates strong electric field intensity at the centromere searching ends of MTs. This high intensity may have disrupting influence on (i) the kinetochore-microtubule binding process or on (ii) the chromatid separation with consequence in disrupting mitosis. Cancer cells would be especially sensitive to mitosis disruptions due to their high division rate. A more selective targeting process of microtubule-kinetochore binding or chromatid separation could be developed, once the details of microtubule electro-mechanical coupling and vibrational properties are disclosed by experiments.
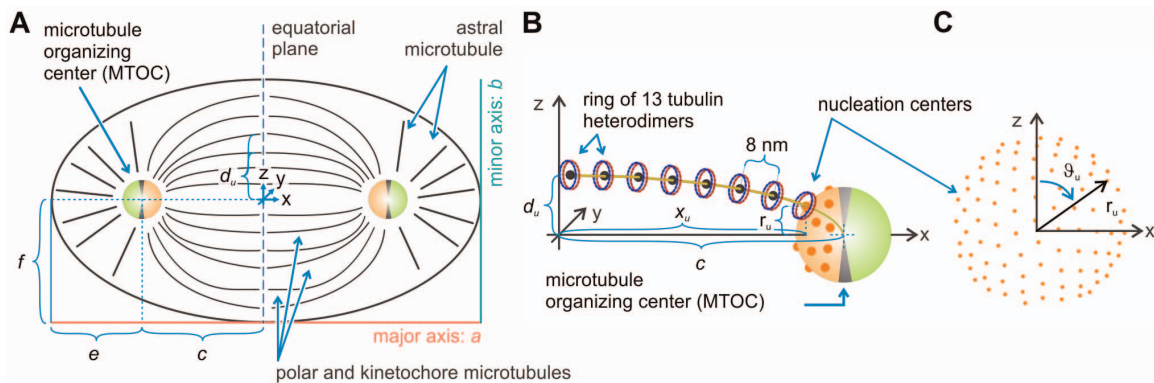
39

Figure 7. Detailed geometry of the model. The overall structure of mitotic spindle in the model (A). Kinetochore and polar microtubules grow from MTOC along ellipsoidal trajectory towards the equatorial plane (B). The MTOC is devided into two parts. One serves as a base for kinetochore and polar MTs (orange), the second for astral MTs (green). Nucleation centers of MTs are distributed uniformly on the surface of the MTOC (C).
doi:10.1371/journal.pone.0086501.g007

Further, our model represents a tool for quantification of the role of endogenous cellular high frequency electric field upon which further theoretical and experimental development can be built. High frequency electric oscillations can mediate force interactions between molecules and supramolecular structures over a longer range than electrostatic interactions [54,55]. This is because any screening of an electric field by ions gets much less effective for higher frequencies of electric oscillations due to limited ion mobility in cytoplasm [55]. This fact opens a new view on possible endogenous mechanisms for recruitment of molecular partners in cells where diffusion is restricted due to macromolecular crowding. Namely, the fluctuating high frequency electric field of microtubule network could provide the long range searching and steering mechanism needed for microtubule-based kinetochore and centromere location and subsequent chromosome segregation.

Future directions and conclusions

Our model predicts the existence of a rapidly changing electric field generated by either driven or endogenous vibrations of the mitotic spindle. The existence of this field is subject to experimental verification. Well defined *in vitro* spindle models [56] or well described model cells can be used for electrical spectroscopic measurements which could reveal absorption on frequencies corresponding to lengths of MTs. Direct measurement of the MT generated field is considered extremely challenging even with currently available nanotechnologies [57], but fluorescent probes sensitive to electric fields [58] may bring some initial insight.The biological relevance of electro-acoustic vibrations of microtubules and the mitotic spindle remains to be experimentally tested.

In conclusion, our model enables the analysis of the effects of electro-acoustic vibrations of the mitotic spindle for the very first time. We believe that all the necessary approximations and simplifications did not have a significant effect on the fundamental outputs of our model. The results of our simulations revealed that the electric field coupled to mechanical vibrations of microtubules forming the mitotic spindle has a very complex spatial and temporal structure. For certain values of our parameters, the intensity of the electric field and its gradient reached values which may have a significant effect when subject to biological conditions. For instance, to exert a force on chromosomes aligned within the spindle midzone or on the microtubules which do not undergo

vibrations. The model may be applied in various fields dealing with the effects of electric fields on dividing cells, especially in cancer treatment. Future research should pursue (i) experimental verification of predicted behavior and (ii) a more detailed modeling of the mitotic spindle of real model cells. Our key contribution in this research has been to provide our model for future research, showing the biological relevance of the processes it describes.

Models

The details of the model are described in this section. All the parameters of the model are first shown as variables. The values of these variables which were chosen for our calculations are then summarized in Table 1. The model was developed in Matlab. The code is freely available upon request.

The center of gravity of tubulin monomers

The spatial arrangement of atoms within a molecular model of one heterodimer in polymerized MT was used. Each ith atom within one monomer has its position $\mathbf{P}_i(x_i,y_i,z_i)$ and weight m_i. The center of gravity of one monomer was determined as $\mathbf{P}_c = \frac{1}{m}\sum (m_i\mathbf{P}_i)$, where m is the total mass of the corresponding monomer.

Dipole approximation of tubulin monomers

The charge distribution within heterodimers is included in the above mentioned molecular model. The total dipole moment was assessed similarly to the determination of the center of gravity. The charge q_i in position $\mathbf{P}_i$ (relatively to the center of gravity) has its dipole moment $\mathbf{D}_i = q_i(\mathbf{P}_i - \mathbf{P}_c)$. The total dipole moment of one monomer is then given as $\mathbf{D} = \sum \mathbf{D}_i$ (see Fig. 1).

MT rings

The parallel arrangement of protofilaments in lattice leads to axial shift s between neighboring protofilaments. The microtubule may be seen as being formed by periodically arranged rings of heterodimers in axial direction. These so called MT rings have the shape of a spiral (see Fig. 1) with a diameter ζ (distance of the center of gravity from the axis) and leading angle of Ξ degrees.
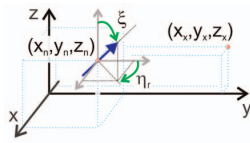
Figure 8. Transformation of coordinates used for calculation of radiation of a dipole. The schematics explains the geometrical meaning of parameters in Eqs. 4–7.
doi:10.1371/journal.pone.0086501.g008

The arrangement of microtubules

The geometry of the mitotic spindle was calculated in the coordinates shown in Fig. 7–A. The spindle occupies space of an ellipsoid with dimensions $a = \dfrac{3V}{4\pi b^2}$ and $b = 0.8R$, where V is the volume of a spherical cell with a radius R (this radius corresponds to a non-dividing spherical cell with the same volume like a dividing ellipsoidal cell considered here). Microtubule organizing centers (MTOCs) were placed on the x-axis in distance $c = \pm\dfrac{a}{2}\left(\dfrac{1+\sqrt{5}}{2}\right)$ from the origin of the coordinate system. MTOC, the pole, was represented by a sphere with a diameter ρ from which MTs grow tangentially. In order to efficiently distribute $N/2$ microtubule nucleation centers (N_a astral, N_k kinetochore and N_p polar microtubules, corresponding to $N = N_a + N_k + N_p$ microtubules in our model) on MTOC without any intersections we placed them uniformly according to the following algorithm. We used the equation of symmetrical distribution $\{\tau_s\}_{s=1}^{\kappa}$ of κ electrically charged particles on a sphere under the condition of the smallest potential energy [59]

$$\{\tau_n\}_{s=1}^{\kappa} = \arg\min \frac{1}{2}\sum_{i=1}^{\kappa}\sum_{j=1,j\neq i}^{\kappa} |\mathbf{g}_i - \mathbf{g}_j|^{-m_q} \qquad (1)$$

where $\mathbf{g}_i$ is the position of the ith particle and m_q is an arbitrary constant (we used 1). Since we assume that there are more kinetochore and polar MTs than astral MTs, we divided MTOC into two parts given by spatial angles Ω_a for astral MTs and Ω_{p+k} for kinetochore and polar MTs (the corresponding κ of the model is increased proportionally to the surface of the whole MTOC). Therefore, there are different densities of nucleation centers on each part, so the resulting number of centers of corresponding parts represents $N_a/2$ and $(N_p + N_k)/2$ MTs, respectively.

Astral MTs grow from each MTOC radially towards the cell membrane. Kinetochore and polar microtubules grow along the ellipsoidal trajectory which is given by 3 points: the center of MTOC, nucleation center and the magnified projection of nucleation centers to the equatorial plane. The magnification is given by factor

$$\frac{d_u}{r_u} = \left(\sqrt{1 - \left(\frac{x_u}{c}\right)^2}\right)^{-1} \qquad (2)$$

where parameters r_u is the distance of the nucleation center of uth kinetochore or polar MT from the x-axis, d_u is its magnified projection to the equatorial plane and x_u is its x-coordinate (for details see 7–B, C).
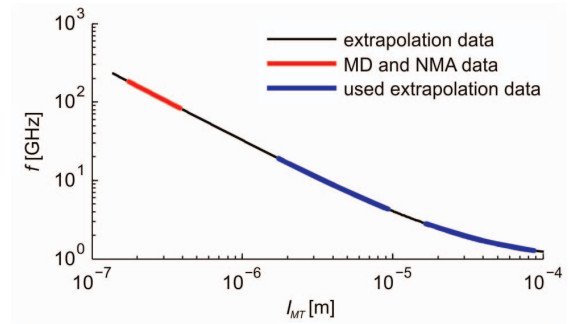

Figure 9. Frequency of vibrations of MT as a function of its length. Molecular dynamics and normal mode analysis models of MT (red) were extrapolated (black) for this purpose to the region of lengths relevant to this model (blue).
doi:10.1371/journal.pone.0086501.g009

MT ring positions

Once the equations of microtubules' axes were defined, the dipoles representing tubulin monomers were placed along these trajectories. The length of these trajectories, l_{MT}, was divided into 8 nm long sections (potential differences were rounded) corresponding to the longitudal size of one heterodimer. MT rings were placed coaxially with the MTs' trajectories at the beginning of each section (see Fig. 7).

Excitation of vibrations

Finally, the dipole moments of all monomers were modulated both in space and time. These modulations correspond to oscillations of dipoles along the trace of a given vibration mode in the course of time. All dipoles were modulated by the function $\sin(2\pi f_n t + \phi_n)$, which represents the frequency of vibrations of respective n^{th} MT ($n = 1,\ldots,N$), where f_n is the frequency of vibration, t is time and ϕ_n is the phase of nth MT. The amplitude and phase of vibrations depends, for each dipole, on its position
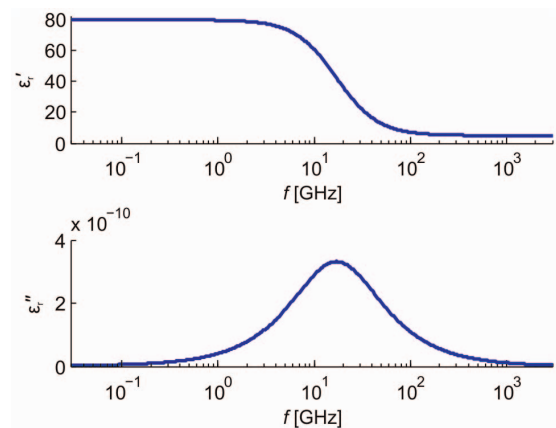
Figure 10. Electrical parameters of the cytosol. We used homogeneous electrical properties of the surroundings of the MTs in our model. The figure shows frequency versus complex permittivity plot. The real part of the complex permittivity (up) represents the value of the relative electrical permittivity, and therefore energy stored in the material, and the imaginary part (down) corresponds to dielectric losses.
doi:10.1371/journal.pone.0086501.g010

41

within the MT. Therefore the dipole moment was also modulated by the function $\mathbf{p_m} = 2\pi f_n p_a \sin(d_n)\mathbf{D}$, where $\mathbf{p_m}$ is the modulated dipole moment, p_a is the oscillating part of the dipole moment of the corresponding monomer ($p_{a\alpha}$ for α-tubulin and $p_{a\beta}$ for β-tubulin) and d_n is the amplitude of monomer's displacement given by the wave number.

Calculation of the intensity of the electric field

The resulting intensity of the electric field in a point $\mathbf{x}(x_x, y_x, z_x)$ of space was calculated as a vector summation of all the contributions as

$$\mathbf{E(x)} = \sum_{n=1}^{N} \sum_{v=1}^{13h_n} \left(\mathbf{E_x(x)}_{n,v} + \mathbf{E_y(x)}_{n,v} + \mathbf{E_z(x)}_{n,v} \right) \quad (3)$$

where v is the index of the electric dipole (tubulin monomer) in n^{th} MT, h_n is the number of electric dipoles in one protofilament of nth MT (all n_u in u^{th} MT are equal), $\mathbf{E_x(x)}_{n,v}$, $\mathbf{E_y(x)}_{n,v}$ and $\mathbf{E_z(x)}_{n,v}$ are components of the electrical intensity of electric dipole with indexes n and v in the direction of respective axes. The relation between $\mathbf{p_m}$ and $\mathbf{E_x(x)}, \mathbf{E_y(x)}$ and $\mathbf{E_z(x)}$ is given by standard equations of dipole radiation. Those equations stand, in Cartesian coordinates and after rotation and translation of the dipole to its proper position, as follows

$$\mathbf{E_x} = -\frac{\omega |\mathbf{p_m}| Z k^2}{4\pi r'''^2} \left[2z'''(x''' \cos\eta_r + y''' \cos\xi \sin\eta_r + z''' \sin\xi \sin\eta_r)\left((jkr''')^{-2} + (jkr''')^{-3}\right) \right.$$
$$+ \left(x'''z''' \cos\eta_r + y'''z''' \cos\xi \sin\eta_r - (x'''^2 + y'''^2)\sin\xi \sin\eta_r\right)$$
$$\left. \cdot \left((jkr''')^{-1} + (jkr''')^{-2} + (jkr''')^{-3}\right)\right]e^{-jkr'''}\mathbf{x_0} \quad (4)$$

$$\mathbf{E_y} = -\frac{\omega |\mathbf{p_m}| Z k^2}{4\pi r'''^2} \left[2z'''(-x''' \sin\eta_r + y''' \cos\xi \cos\eta_r + z''' \sin\xi \cos\eta_r)\left((jkr''')^{-2} + (jkr''')^{-3}\right) \right.$$
$$\left. + \left(-x'''z''' \sin\eta_r + y'''z''' \cos\xi \cos\eta_r - (x'''^2 + y'''^2)\sin\xi \cos\eta_r\right) \cdot \left((jkr''')^{-1} + (jkr''')^{-2} + (jkr''')^{-3}\right)\right]e^{-jkr'''}\mathbf{y_0} \quad (5)$$

$$\mathbf{E_z} = -\frac{\omega |\mathbf{p_m}| Z k^2}{4\pi r'''^2} \left[2z'''(-y''' \sin\xi + z''' \cos\eta_r)\left((jkr''')^{-2} + (jkr''')^{-3}\right) \right.$$
$$\left. + \left(-y'''z''' \sin\xi - (x'''^2 + y'''^2)\cos\eta_r\right)\left((jkr''')^{-1} + (jkr''')^{-2} + (jkr''')^{-3}\right)\right]e^{-jkr'''}\mathbf{z_0} \quad (6)$$

where $r''' = \sqrt{x'''^2 + y'''^2 + z'''^2}$, x_x, y_x, z_x are coordinates of the point of evaluation $\mathbf{x}$. $j = \sqrt{-1}$ denotes the imaginary constant. $Z = \omega\mu/k$ is the impedance of the environment, where ω is angular frequency of oscillations, μ is permeability and k is the wave number. Auxiliary coordinates x''', y''', z''', are given as

$$\begin{pmatrix} x''' \\ y''' \\ z''' \end{pmatrix} = \begin{pmatrix} 1 & 0 & 0 \\ 0 & \cos\xi & -\sin\xi \\ 0 & \sin\xi & \cos\xi \end{pmatrix} \begin{pmatrix} \cos\eta_r & \sin\eta_r & 0 \\ -\sin\eta_r & \cos\eta_r & 0 \\ 0 & 0 & 1 \end{pmatrix} \begin{pmatrix} x_x - x_0 \\ y_x - y_0 \\ z_x - z_0 \end{pmatrix} \quad (7)$$

where x_n, y_n and z_n denote axial coordinates of the position of the dipole and ξ and η_r are angles between the dipole and axes z and y, respectively (see Fig. 8).

Estimation of the spectra of vibrations

The spectra of vibrations were estimated by summation of the Lorentzian curves placed at principal vibrational frequencies of

each MT. Assuming each MT to have the principal frequency f_n and quality factor Q, then the resulting spectrum is given by the following equation:

$$S(f) = \sum_{n=1}^{N} \frac{\left(\frac{\gamma_n}{2}\right)}{(2\pi f - 2\pi f_n)^2 + \left(\frac{\gamma_n}{2}\right)^2} \quad (8)$$

where $\gamma_n = \frac{2\pi f_n}{Q}$, f is frequency and f_n is the resonance frequency of the nth microtubule.

Parameters of the model

Specific values of parameters of the model are given below.

The molecular model of tubulin was taken from the RCSB Protein Data Bank (1TUB code) and adopted as described in [23]. The resulting model corresponds to structure of heterodimers within polymerized MTs with 13:3 B lattice.

The model cells we used in our calculations have an equivalent radius, R, of 65 μm, 30 μm, 7 μm and 3.3 μm. We positioned 300 microtubules within these cells: 100 astral, 100 kinetochore and 100 polar MTs. For positioning of $N_a/2 = 50$ nucleation centers of astral MTs on one MTOC we used $\kappa_a = 120$ symmetrically distributed points corresponding to a solid angle $\Omega_a = 2.8212$ sr (see Fig. 7–A, green part of MTOC). Correspondingly, we used $\kappa_a = 225$ and $\Omega_{p+k} = 2.9154$ sr (see Fig. 7, orange part of MTOC) for $(N_p + N_k)/2 = 100$ nucleation centers of kinetochore and polar MTs.

The dependency of the resonance frequency on the length of the microtubule was extrapolated from molecular dynamics and normal mode analysis models [23] as

$$f_n = \frac{k_1 \cdot r}{l_{TH} \cdot h_n} + k_2 \quad (9)$$

where k_1 and k_2 are coefficients of extrapolation ($k_1 = 2.5304 \cdot 10^{12}$ and $k_2 = 0.90966 \cdot 10^9$), l_{TH} is the length of tubulin heterodimer. This extrapolation (black thin curve) is shown in Fig. 9. The thick red curve was calculated by MD (molecular dynamics) and NMA (normal mode analysis). The frequency range used in our model is depicted by the thick blue line. We used the principal longitudinal vibration mode for excitation of MT. All astral MTs were

considered with zero boundary conditions, i.e. with fixed ends on the cell membrane and MTOC. We used two different boundary conditions for kinetochore and polar MTs

1. fixed on both ends of MT and
2. fixed on MTOC and free in equatorial plane.

The quality factor of vibrations ranging between 0.1 and 50 was used. The maximum amplitude of displacement of the monomer's center of gravity within one MT (in anti-node) was set to 1 nm. The displacements of all other monomers within MT are described by the shape of the vibration mode. The electrical parameters of the surroundings of MTs were considered homogeneous within the volume of the cell. The dielectric permittivity spectrum of the model cytosol is shown in Fig. 10, [60]. All other parameters and their values are summarized in Table 1.

Resolution

The volume of model cells was segmented into the Cartesian grid of voxels, *i.e.* points of evaluation, with equal dimensions. The edge length of each cubic voxel was 8 nm for cell with equivalent radius of 3.3 µm.

The time resolution in time-evolution simulations was given by the duration of the periods of vibration of MTs. We used time series covering 5 periods of the vibration of longest MT sampled into 300 time steps. This range and sampling together cover a variety of possible interference products, still ensure that the highest vibration frequency is not under-sampled and is computationally affordable.

The Monte Carlo analysis

The Monte Carlo analysis was used for statistical evaluation of random vibrations. Maximal, mean and minimal value of the intensity of the electric field was estimated in each point of evaluation within the equatorial plane. The analysis was performed for 100 random initial conditions. As is stated above,

data were collected from 5 periods of vibrations of the longest MT. 300 equidistant samples were taken from the time of these 5 periods.

Supporting Information

Video S1 Time evolution of intensity of electric field in equatorial plane for pulsed feeding and free ends.
(AVI)

Video S2 Time evolution of intensity of electric field in equatorial plane for pulsed feeding and fixed ends.
(AVI)

Video S3 Time evolution of intensity of electric field in three major planes of the model cell for pulsed feeding and fixed ends.
(AVI)

Video S4 Time evolution of intensity of electric field in XY plane for pulsed feeding and fixed ends.
(AVI)

Video S5 Time evolution of intensity of electric field in XZ plane for pulsed feeding and fixed ends.
(AVI)

Video S6 Time evolution of intensity of electric field in equatorial plane for random feeding and free ends.
(AVI)

Video S7 Time evolution of intensity of electric field in equatorial plane for random feeding and fixed ends.
(AVI)

Author Contributions

Conceived and designed the experiments: MC DH OK. Performed the experiments: DH. Analyzed the data: OK DH MC. Contributed reagents/materials/analysis tools: MAD. Wrote the paper: OK MC DH.

References

1. Rajagopalan H, Lengauer C (2004) Aneuploidy and cancer. Nature 432: 338–341.
2. Postnikoff S, Harkness T (2012) Mechanistic insights into aging, cell-cycle progression, and stress response. Frontiers in physiology 3.
3. Nogales E, Wolf SG, Downing K (1998) Structure of the alpha beta tubulin dimer by electron crystallography. Nature 391: 199–203.
4. Mershin A, Kolomenski AA, Schuessler HA, Nanopoulos DV (2004) Tubulin dipole moment, dielectric constant and quantum behavior: computer simulations, experimental results and suggestions. Biosystems 77: 73–85.
5. Tuszyński J, Brown J, Crawford E, Carpenter E, Nip M, et al. (2005) Molecular dynamics simulations of tubulin structure and calculations of electrostatic properties of microtubules. Mathematical and Computer Modelling 41: 1055–1070.
6. Simonson T (2003) Electrostatics and dynamics of proteins. Reports on Progress in Physics 66: 737.
7. Vassilev PM, Dronzine RT, Vassileva MP, Georgiev GA (1982) Parallel arrays of microtubles formed in electric and magnetic fields. Bioscience reports 2: 1025–1029.
8. Ramalho R, Soares H, Melo L (2007) Microtubule behavior under strong electromagnetic fields. Materials Science and Engineering: C 27: 1207–1210.
9. Stracke R, Böhm K, Wollweber L, Tuszynski J, Unger E (2002) Analysis of the migration behaviour of single microtubules in electric fields. Biochemical and biophysical research communications 293: 602–609.
10. Böhm KJ, Mavromatos NE, Michette A, Stracke R, Unger E (2005) Movement and alignment of microtubules in electric fields and electric-dipole-moment estimates. Electromagnetic Biology and Medicine 24: 319–330.
11. Minoura I, Muto E (2006) Dielectric measurement of individual microtubules using the electroorientation method. Biophysical Journal 90: 3739–3748.
12. Van den Heuvel M, Bondesan R, Cosentino Lagomarsino M, Dekker C (2008) Single-molecule observation of anomalous electrohydrodynamic orientation of microtubules. Physical review letters 101: 118301.
13. Bras W, Diakun GP, Diaz J, Maret G, Kramer H, et al. (1998) The susceptibility of pure tubulin to high magnetic fields: a magnetic birefringence and x-ray fiber diffraction study. Biophysical journal 74: 1509–1521.
14. Glade N, Tabony J (2005) Brief exposure to high magnetic fields determines microtubule self-organisation by reaction-diffusion processes. Biophysical chemistry 115: 29–35.
15. Liu Y, Guo Y, Valles JM, Tang JX (2006) Microtubule bundling and nested buckling drive stripe formation in polymerizing tubulin solutions. Proceedings of the National Academy of Sciences 103: 10654–10659.
16. Tuszyński JA, Luchko T, Portet S, Dixon JM (2005) Anisotropic elastic properties of microtubules. The European Physical Journal E 17: 29–35.
17. Kasas S, Cibert C, Kis A, De Los Rios P, Riederer BM, et al. (2004) Oscillation modes of microtubules. Biol Cell 96: 697–700.
18. Portet S, Tuszyński JA, Hogue CWV, Dixon JM (2005) Elastic vibrations in seamless microtubules. European Biophysics Journal 34: 912–920.
19. Wang C, Ru C, Mioduchowski A (2006) Vibration of microtubules as orthotropic elastic shells. Physica E: Low-dimensional Systems and Nanostructures 35: 48–56.
20. Qian XS, Zhang JQ, Ru CQ (2007) Wave propagation in orthotropic microtubules. Journal of Applied Physics 101: 084702.
21. Wang C, Zhang L (2008) Circumferential vibration of microtubules with long axial wavelength. Journal of Biomechanics 41: 1892–1896.
22. Ghavanloo E, Daneshmand F, Amabili M (2010) Vibration analysis of a single microtubule surrounded by cytoplasm. Physica E: Low-dimensional Systems and Nanostructures 43: 192–198.
23. Deriu MA, Soncini M, Orsi M, Patel M, Essex JW, et al. (2010) Anisotropic elastic network modeling of entire microtubules. Biophysical Journal 99: 2190–2199.
24. Shen HS (2011) Nonlinear vibration of microtubules in living cells. Current Applied Physics 11: 812–821.
25. Xiang P, Liew K (2012) Free vibration analysis of microtubules based on an atomistic-continuum model. Journal of Sound and Vibration 331: 213–230.

43

26. Taj M, Zhang J (2012) Analysis of vibrational behaviors of microtubules embedded within elastic medium by pasternak model. Biochemical and Biophysical Research Communications 424: 89–93.
27. Mohrbach H, Johner A, Kulić IM (2012) Cooperative lattice dynamics and anomalous fluctuations of microtubules. European Biophysics Journal 41: 217–239.
28. Mallakzadeh M, Pasha Zanoosi A, Alibeigloo A (2013) Fundamental frequency analysis of microtubules under different boundary conditions using differential quadrature method. Communications in Nonlinear Science and Numerical Simulation 18: 2240–2251.
29. Li H, Xiong J, Wang X (2013) The coupling frequency of bioliquid-fillled microtubules considering small scale effects. European Journal of Mechanics-A/Solids 39: 11–16.
30. Samarbakhsh A, Tuszynski JA (2011) Vibrational dynamics of bio-and nano-filaments in viscous solution subjected to ultrasound: implications for microtubules. European Biophysics Journal 40: 937–946.
31. Cifra M, Pokorný J, Havelka D, Kučera O (2010) Electric field generated by axial longitudinal vibration modes of microtubule. BioSystems 100: 122–131.
32. Havelka D, Cifra M, Kučera O, Pokorný J, Vrba J (2011) High-frequency electric field and radiation characteristics of cellular microtubule network. Journal of Theoretical Biology 286: 31–40.
33. Havelka D, Cifra M, Vrba J (2011) What is more important for radiated power from cells-size or geometry? In: Journal of Physics: Conference Series. IOP Publishing, volume 329, p. 012014.
34. Kučera O, Havelka D (2012) Mechano-electrical vibrations of microtubules–link to subcellular morphology. Biosystems 109: 346–355.
35. Priel A, Tuszynski J, Cantiello H (2005) Electrodynamic signaling by the dendritic cytoskeleton: toward an intracellular information processing model. Electromagnetic Biology and Medicine 24: 221–231.
36. Pokorný J (2001) Endogenous electromagnetic forces in living cells: implication for transfer of reaction components. Electro- and Magnetobiology 20: 59–73.
37. Pellegrini F, Budman DR (2005) Review: tubulin function, action of antitubulin drugs, and new drug development. Cancer investigation 23: 264–273.
38. Kirson E, Dbalý V, Tovaryš F, Vymazal J, Soustiel J, et al. (2007) Alternating electric fields arrest cell proliferation in animal tumor models and human brain tumors. Proceedings of the National Academy of Sciences 104: 10152–10157.
39. Samsonov A, Popov SV (2013) The effect of a 94 ghz electromagnetic field on neuronal microtubules. Bioelectromagnetics 34: 133–144.
40. Pavicic I, Trosic I (2008) In vitro testing of cellular response to ultra high frequency electromagnetic field radiation. Toxicology in vitro 22: 1344–1348.
41. Walczak CE, Vernos I, Mitchison TJ, Karsenti E, Heald R, et al. (1998) A model for the proposed roles of different microtubule-based motor proteins in establishing spindle bipolarity. Current biology 8: 903–913.
42. Ibrahim B, Diekmann S, Schmitt E, Dittrich P (2008) In-silico modeling of the mitotic spindle assembly checkpoint. PLoS One 3: e1555.
43. Dumont S, Mitchison TJ (2009) Force and length in the mitotic spindle. Current Biology 19: R749–R761.
44. Grill SW, Kruse K, Jülicher F (2005) Theory of mitotic spindle oscillations. Physical review letters 94: 108104.
45. Naruse Y (2002) Mechanical vibration model for chromosomes in metaphase of mitosis and possible application to the interruption of cell division. Biosystems 66: 55–63.
46. Zhao Y, Zhan Q (2012) Electric fields generated by synchronized oscillations of microtubules, centrosomes and chromosomes regulate the dynamics of mitosis and meiosis. Theor Biol Med Model 9: 26.
47. Breton M, Mir LM (2012) Microsecond and nanosecond electric pulses in cancer treatments. Bioelectromagnetics 33: 106–123.
48. Foster KR, Baish JW (2000) Viscous damping of vibrations in microtubules. Journal of Biological Physics 26: 255–260.
49. Pokorný J (2003) Viscous effects on polar vibrations in microtubules. Electromagnetic Biology and Medicine 22: 15–29.
50. Daneshmand F, Amabili M (2012) Coupled oscillations of a protein microtubule immersed in cytoplasm: an orthotropic elastic shell modeling. Journal of Biological Physics 38: 429–448.
51. Hameroff S, Lindsay S, Bruchmann T, Scott A (1986) Acoustic modes of microtubules. Biophysical journal 49: 58a.
52. Pelling AE, Sehati S, Gralla EB, Valentine JS, Gimzewski JK (2004) Local nanomechanical motion of the cell wall of saccharomyces cerevisiae. Science 305: 1147–1150.
53. Holzel R (2009) Dielectric and dielectrophoretic properties of dna. Nanobiotechnology, IET 3: 28–45.
54. Preto J, Floriani E, Nardecchia I, Ferrier P, Pettini M (2012) Experimental assessment of the contribution of electrodynamic interactions to long-distance recruitment of biomolecular partners: Theoretical basis. Physical Review E 85: 041904.
55. Preto J, Pettini M (2013) Resonant long-range interactions between polar macromolecules. Physics Letters A 377: 587591.
56. Uppalapati M, Huang YM, Aravamuthan V, Jackson TN, HancockWO(2011) artificial mitotic spindle generated by dielectrophoresis and protein micro-patterning supports bidirectional transport of kinesin-coated beads. Integrative Biology 3: 57–64.
57. Kučera O, Cifra M, Pokorný J (2010) Technical aspects of measurement of cellular electromagnetic activity. European Biophysics Journal 39: 1465–1470.
58. Tyner KM, Kopelman R, Philbert MA (2007) "Nano-sized voltmeter" enables cellular-wide electric field mapping. Biophysical Journal 93: 1163–1174.
59. Frickel R, Bronk B (1988) Symmetries of configurations of charges on a sphere. Canadian journal of chemistry 66: 2161–2165.
60. Kaatze U (2003) Logarithmic derivative complex permittivity spectrometry. Measurement Science and Technology 14: N55.

44

6 | RESULTS

Results of the research presented in this thesis were published in a number of papers in scientific journals and conference proceedings (see the list of author's publications). The core of the dissertation is composed of three papers [A1 - A3] in the main part of the dissertation, and two papers [A4] and [A5] in the Appendix. Full bibliographic citation, contribution of the candidate, and acknowledgments are stated at the beginning of each chapter.

Chapter 3 describes the calculation of high-frequency electric field coupled to collective vibration modes of a microtubule. First five acoustical longitudinal modes of the microtubule vibrations are considered in the model. The frequencies of these modes were taken from the coarse-grained mechanical model of a microtubule. The multi-mode excitation causes the formation of an electric pulse which propagates from one end of a microtubule to the other. This field has many transient local electric field minima. The reported phenomenon may serve as a mechanism for an ultra-fast electrodynamic signaling pathway along a microtubule without transfer of signaling molecules.

Chapter 4 deals with calculations of the electromagnetic radiation and field characteristics of the mechanically vibrating microtubule network in dividing and non-dividing cells. First optical longitudinal mode of microtubule vibrations is considered in the model and the field characteristics are analyzed at several frequencies in the range between kHz and GHz. The results show that (i) the field has a complex spatial structure and (ii) the intensity of electric field and the radiated power decrease fast with the distance from the cell wall. Therefore, low noise nanoscopic detection methods with high spatial resolution which enable measurement in the cell vicinity are desirable in order to measure cellular electrodynamic activity reliably.

Chapter 5 presents electromechanical model which for the first time enables calculation of the electromagnetic field coupled to acoustic vibrations of the microtubules which form the mitotic spindle. This electromagnetic field originates from the electric polarity of microtubules. The model is based on the approximation of resonantly vibrating microtubules by a network of oscillating electric dipoles. We focused on equatorial plane in our calculation as a place where the chromosomes are segregated. The computational results predict the existence of a rapidly changing electric field which is generated by either driven or endogenous vibrations of the mitotic spindle. These types of excitations are (i) synchronized vibrations of the mitotic spindle after pulsed

excitation and (ii) vibrations with a random phase and a constant amplitude in the equatorial plane. The intensities of the generated field vary on very small distances within few orders of magnitude, which leads to gradients as large as 10^5 V/m on the distance of few hundreds of nanometers. Such a high intensity of the generated field may in consequence disrupt the mitosis in progress. The field either pulsates if the vibrations are synchronized to some extent, or has a rather runny character if the phases of vibrations are highly desynchronized. The results provide computational foundations for future analyses of possible mechanisms describing the effects of ultra-short electric and mechanical pulses on dividing cells. The application of such pulses is prospective for future therapy of cancer.

7 | CONCLUSIONS

7.1 CONTRIBUTION OF THE DISSERTATION

This thesis has provided novel theoretical analysis of high-frequency electric field generated by longitudinal vibration modes of individual microtubule [A1, A5] and networks formed by microtubules [A2, A3, A4]. Besides the pioneering work of Pokorný on rough estimate of the electromagnetic field of vibrating microtubule, this dissertation presents the only detailed model of this field published so far. The presented model is based on (i) a coarse-grained structure of a microtubule, (ii) approximation of longitudinal vibration modes of a microtubule by longitudinal modes of inelastic string and (iii) approximation of the electromagnetic field generated by each grain by an oscillating elementary dipole. The relevance of the model and described phenomena was discussed. Particularly, it was shown that the reported electromagnetic field of vibrating microtubule may play role in signaling for instance in neurons or separation of genetic information in dividing cells. Nevertheless, these phenomena have to be confirmed experimentally.

7.2 FUTURE DIRECTIONS

All results presented in this dissertation [A1-A3] have, more or less, theoretical nature (experimental evidence on this topic is in progress and was not included in this dissertation). The next steps should lead to verification of these ideas. The first step will be a characterization of microtubules in the microwave region on the theoretical and chiefly on the experimental level. As a following step, the measurement of oscillating electric field of cells in radio-frequency range should be performed. Future research should in conclusion follow these directions:

| Development of more detailed model which will implement (i) complete molecular structure of the microtubule, (ii) reverse coupling of the electromagnetic field to the charge of the microtubule, and (iii) detailed properties of the solvent and its interaction with the microtubule.

| Experimental characterization of microtubule properties on radio and microwave frequencies and verification of the predictions obtained using presented model.

| Elucidation of the relevance of presented electromagnetic fields in the function of microtubules.

In conclusion, we may say that goals of the thesis summarized in section 2.7 were fulfilled in candidate's papers [A1-A3].

BIBLIOGRAPHY

[1] I. Bahar, T. R. Lezon, L.-W. Yang, and E. Eyal, "Global dynamics of proteins: bridging between structure and function," *Annual Review of Biophysics*, vol. 39, p. 23, 2010.

[2] P. Ren, J. Chun, D. G. Thomas, M. J. Schnieders, M. Marucho, J. Zhang, and N. A. Baker, "Biomolecular electrostatics and solvation: a computational perspective," *Quarterly Reviews of Biophysics*, vol. 45, no. 4, pp. 427–491, 2012.

[3] J. Pokorný, F. Jelínek, and V. Trkal, "Electric field around microtubules," *Bioelectrochemistry and Bioenergetics*, vol. 45, no. 2, pp. 239–245, 1998.

[4] A. Priel, J. A. Tuszynski, and H. F. Cantiello, "Electrodynamic signaling by the dendritic cytoskeleton: toward an intracellular information processing model," *Electromagnetic Biology and Medicine*, vol. 24, no. 3, pp. 221–231, 2005.

[5] J. Pokorný, J. Hašek, and F. Jelínek, "Electromagnetic field of microtubules: Effects on transfer of mass particles and electrons," *Journal of Biological Physics*, vol. 31, no. 3, pp. 501–514, 2005.

[6] S. Hameroff, "A tale of two fields. comment on"dissipation ofdark energy'by cortex in knowledge retrieval"by capolupo, freeman and vitiello," *Physics of Life Reviews*, vol. 10, pp. 95–96, 2013.

[7] J. Pokorný, "Physical aspects of biological activity and cancer," *AIP Advances*, vol. 2, no. 1, p. 011207, 2012.

[8] J. Pokorný, J. Pokorný, and J. Kobilková, "Postulates on electromagnetic activity in biological systems and cancer," *Integrative Biology*, vol. 5, no. 12, pp. 1439–1446, 2013.

[9] B. Alberts, D. Bray, J. Lewis, M. Raff, K. Roberts, and J. D. Watson, *Molecular Biology of the Cell*. Garland, 3rd ed., 1994.

[10] R. Dallai, B. A. Afzelius, and B. Mamaev, "Flagellar axonemes with 10 microtubular doublets in spermatozoa from gall-midges (diptera, cecidomyiidae)," *Acta Zoologica*, vol. 77, no. 2, pp. 153–160, 1996.

[11] H. Sosa and R. A. Milligan, "Three-dimensional structure of ncd-decorated microtubules obtained by a back-projection method," *Journal of Molecular Biology*, vol. 260, no. 5, pp. 743–755, 1996.

[12] D. Chrétien, H. Flyvbjerg, and S. D. Fuller, "Limited flexibility of the inter-protofilament bonds in microtubules assembled from pure tubulin," *European Biophysics Journal*, vol. 27, no. 5, pp. 490–500, 1998.

[13] I. M. Jánosi, D. Chrétien, and H. Flyvbjerg, "Modeling elastic properties of microtubule tips and walls," *European Biophysics Journal*, vol. 27, no. 5, pp. 501–513, 1998.

[14] Y.-H. Song and E. Mandelkow, "Recombinant kinesin motor domain binds to beta-tubulin and decorates microtubules with a b surface lattice.," *Proceedings of the National Academy of Sciences*, vol. 90, no. 5, pp. 1671–1675, 1993.

[15] L. A. Amos, "The microtubule lattice – 20 years on," *Trends in Cell Biology*, vol. 5, no. 2, pp. 48–51, 1995.

[16] Y.-H. Song and E. Mandelkow, "The anatomy of flagellar microtubules: polarity, seam, junctions, and lattice.," *The Journal of Cell Biology*, vol. 128, no. 1, pp. 81–94, 1995.

[17] D. Chrétien and S. D. Fuller, "Microtubules switch occasionally into unfavorable configurations during elongation," *Journal of Molecular Biology*, vol. 298, no. 4, pp. 663–676, 2000.

[18] E. Nogales, S. G. Wolf, and K. Downing, "Structure of the alpha beta tubulin dimer by electron crystallography," *Nature*, vol. 391, pp. 199–203, 1998.

[19] J. Tuszyński, J. Brown, E. Crawford, E. Carpenter, M. Nip, J. Dixon, and M. Sataric, "Molecular dynamics simulations of tubulin structure and calculations of electrostatic properties of microtubules," *Mathematical and Computer Modelling*, vol. 41, no. 10, pp. 1055 – 1070, 2005.

[20] J. A. Tuszyński, E. J. Carpenter, J. T. Huzil, W. Malinski, T. Luchko, and R. F. Luduena, "The evolution of the structure of tubulin and its potential consequences for the role and function of microtubules in cells and embryos," *International Journal of Developmental Biology*, vol. 50, no. 2/3, p. 341, 2006.

[21] J. A. Tuszyński, J. A. Brown, E. J. Carpenter, E. Crawford, and M. N. A. Nip, "Electrostatic properties of tubulin and microtubules," in *Proceedings of ESA Conference*, June 2002.

[22] H. Stebbings and C. Hunt, "The nature of the clear zone around microtubules," *Cell and Tissue Research*, vol. 227, no. 3, pp. 609–617, 1982.

[23] F. Gittes, B. Mickey, J. Nettleton, and J. Howard, "Flexural rigidity of microtubules and actin filaments measured from thermal fluctuations in shape.," *The Journal of Cell Biology*, vol. 120, no. 4, pp. 923–934, 1993.

[24] P. Venier, A. C. Maggs, M.-F. Carlier, and D. Pantaloni, "Analysis of microtubule rigidity using hydrodynamic flow and thermal fluctuations.," *Journal of Biological Chemistry*, vol. 269, no. 18, pp. 13353–13360, 1994.

[25] M. Kurachi, M. Hoshi, and H. Tashiro, "Buckling of a single microtubule by optical trapping forces: direct measurement of microtubule rigidity," *Cell Motility and the Cytoskeleton*, vol. 30, no. 3, pp. 221–228, 1995.

[26] B. Mickey and J. Howard, "Rigidity of microtubules is increased by stabilizing agents.," *The Journal of Cell Biology*, vol. 130, no. 4, pp. 909–917, 1995.

[27] A. Vinckier, C. Dumortier, Y. Engelborghs, and L. Hellemans, "Dynamical and mechanical study of immobilized microtubules with atomic force microscopy," *Journal of Vacuum Science & Technology B*, vol. 14, no. 2, pp. 1427–1431, 1996.

[28] H. Felgner, R. Frank, and M. Schliwa, "Flexural rigidity of microtubules measured with the use of optical tweezers," *Journal of Cell Science*, vol. 109, no. 2, pp. 509–516, 1996.

[29] A. Kis, S. Kasas, B. Babić, A. Kulik, W. Benoit, G. Briggs, C. Schönenberger, S. Catsicas, and L. Forro, "Nanomechanics of microtubules," *Physical Review Letters*, vol. 89, no. 24, p. 248101, 2002.

[30] P. J. de Pablo, I. A. Schaap, F. C. MacKintosh, and C. F. Schmidt, "Deformation and collapse of microtubules on the nanometer scale," *Physical Review Letters*, vol. 91, no. 9, p. 098101, 2003.

[31] D. J. Needleman, M. A. Ojeda-Lopez, U. Raviv, K. Ewert, H. P. Miller, L. Wilson, and C. R. Safinya, "Radial compression of microtubules and the mechanism of action of taxol and associated proteins," *Biophysical Journal*, vol. 89, no. 5, pp. 3410–3423, 2005.

[32] J. Tuszyński, T. Luchko, S. Portet, and J. Dixon, "Anisotropic elastic properties of microtubules," *The European Physical Journal E: Soft Matter and Biological Physics*, vol. 17, no. 1, pp. 29–35, 2005.

[33] F. Pampaloni, G. Lattanzi, A. Jonáš, T. Surrey, E. Frey, and E.-L. Florin, "Thermal fluctuations of grafted microtubules provide evidence of a length-dependent persistence length," *Proceedings of the National Academy of Sciences*, vol. 103, no. 27, pp. 10248–10253, 2006.

[34] M. Kikumoto, M. Kurachi, V. Tosa, and H. Tashiro, "Flexural rigidity of individual microtubules measured by a buckling force with optical traps," *Biophysical Journal*, vol. 90, no. 5, pp. 1687–1696, 2006.

[35] M. A. Deriu, M. Soncini, M. Orsi, M. Patel, J. W. Essex, F. M. Montevecchi, and A. Redaelli, "Anisotropic elastic network modeling of entire microtubules," *Biophysical Journal*, vol. 99, no. 7, pp. 2190–2199, 2010.

[36] D. Sept and F. C. MacKintosh, "Microtubule elasticity: connecting all-atom simulations with continuum mechanics," *Physical Review Letters*, vol. 104, no. 1, p. 018101, 2010.

[37] S. Feng and H. Liang, "A coarse grain model of microtubules," *Theoretical and Applied Mechanics Letters*, vol. 2, no. 1, p. 014006, 2012.

[38] Y. Sun, Y. Tian, and K. Liew, "A multiscale model to predict the elastic property of microtubules," *Journal of Computational and Theoretical Nanoscience*, vol. 9, no. 6, pp. 789–793, 2012.

[39] H. Fröhlich, "Bose condensation of strongly excited longitudinal electric modes," *Physical Letters A*, vol. 26, pp. 402–203, 1968.

[40] H. Fröhlich, "Long-range coherence and energy storage in biological systems," *International Journal of Quantum Chemistry*, vol. 2, no. 5, pp. 641–649, 1968.

[41] H. Fröhlich, "Long-range coherence in biological systems," *Rivista del Nuovo Cimento*, vol. 7, no. 3, pp. 399–418, 1977.

[42] H. Fröhlich, "Evidence for coherent excitation in biological systems," *International Journal of Quantum Chemistry*, vol. 23, no. 4, pp. 1589–1595, 1983.

[43] J. Pokorný, F. Jelínek, V. Trkal, I. Lamprecht, and R. Hölzel, "Vibrations in microtubules," *Journal of Biological Physics*, vol. 23, pp. 171–179, 1997.

[44] J. Pokorný, J. Hašek, J. Vaniš, and F. Jelínek, "Biophysical aspects of cancer–electromagnetic mechanism," *Indian Journal of Experimental Biology*, vol. 46, pp. 310–321, 2008.

[45] F. Jelínek, M. Cifra, J. Pokorný, J. Vaniš, J. Šimša, J. Hašek, and I. Frýdlová, "Measurement of electrical oscillations and mechanical vibrations of yeast cells membrane around 1 kHz," *Electromagnetic Biology and Medicine*, vol. 28, no. 2, pp. 223–232, 2009.

[46] K. M. Tyner, R. Kopelman, and M. A. Philbert, ""Nano-sized voltmeter" enables cellular-wide electric field mapping," *Biophysical Journal*, vol. 93, pp. 1163–1174, 2007.

[47] F. Šrobár, "Impact of mitochondrial electric field on modal occupancy in the fröhlich model of cellular electromagnetism," *Electromagnetic Biology and Medicine*, vol. 32, no. 3, pp. 401–408, 2013.

[48] Y. M. Sirenko, M. A. Stroscio, and K. Kim, "Elastic vibrations of microtubules in a fluid," *Physical Review E*, vol. 53, no. 1, p. 1003, 1996.

[49] S. Portet, J. Tuszyński, C. Hogue, and J. Dixon, "Elastic vibrations in seamless microtubules," *European Biophysics Journal*, vol. 34, no. 7, pp. 912–920, 2005.

[50] C. Wang, C. Ru, and A. Mioduchowski, "Orthotropic elastic shell model for buckling of microtubules," *Physical Review E*, vol. 74, no. 5, p. 052901, 2006.

[51] C. Wang, C. Ru, and A. Mioduchowski, "Vibration of microtubules as orthotropic elastic shells," *Physica E: Low–dimensional Systems and Nanostructures*, vol. 35, no. 1, pp. 48–56, 2006.

[52] C. Wang and L. Zhang, "Circumferential vibration of microtubules with long axial wavelength," *Journal of Biomechanics*, vol. 41, no. 9, pp. 1892–1896, 2008.

[53] X. Qian, J. Zhang, and C. Ru, "Wave propagation in orthotropic microtubules," *Journal of Applied Physics*, vol. 101, no. 8, p. 084702, 2007.

[54] E. Ghavanloo, F. Daneshmand, and M. Amabili, "Vibration analysis of a single microtubule surrounded by cytoplasm," *Physica E: Low-dimensional Systems and Nanostructures*, vol. 43, no. 1, pp. 192–198, 2010.

[55] F. Daneshmand and M. Amabili, "Coupled oscillations of a protein microtubule immersed in cytoplasm: an orthotropic elastic shell modeling," *Journal of Biological Physics*, vol. 38, no. 3, pp. 429–448, 2012.

[56] K. R. Foster and J. W. Baish, "Viscous damping of vibrations in microtubules," *Journal of Biological Physics*, vol. 26, no. 4, pp. 255–260, 2000.

[57] R. K. Adair, "Vibrational resonances in biological systems at microwave frequencies," *Biophysical Journal*, vol. 82, no. 3, pp. 1147–1152, 2002.

[58] T.-M. Liu, H.-P. Chen, S.-C. Yeh, C.-Y. Wu, C.-H. Wang, T.-N. Luo, Y.-J. Chen, S.-I. Liu, and C.-K. Sun, "Effects of hydration levels on the bandwidth of microwave resonant absorption induced by confined acoustic vibrations," *Applied Physics Letters*, vol. 95, no. 17, p. 173702, 2009.

[59] T. Fukuma, "Water distribution at solid/liquid interfaces visualized by frequency modulation atomic force microscopy," *Science and Technology of Advanced Materials*, vol. 11, no. 3, p. 033003, 2010.

[60] K. Kimura, S. Ido, N. Oyabu, K. Kobayashi, Y. Hirata, T. Imai, and H. Yamada, "Visualizing water molecule distribution by atomic force microscopy," *The Journal of Chemical Physics*, vol. 132, no. 19, p. 194705, 2010.

[61] J. Pokorný, J. Hašek, F. Jelínek, J. Šaroch, and B. Palán, "Electromagnetic field generated by microtubules," in *Workshop Risk Assessment of Electromagnetic Pollution from Mobile Phone Networks. Int. School of Plasma Phys*, 2000.

[62] J. Pokorný, "Viscous effects on polar vibrations in microtubules," *Electromagnetic Biology and Medicine*, vol. 22, no. 1, pp. 15–29, 2003.

[63] J. Pokorný, "Excitation of vibrations in microtubules in living cells," *Bioelectrochemistry*, vol. 63, no. 1, pp. 321–326, 2004.

[64] J. Pokorný, J. Hašek, and F. Jelínek, "Endogenous electric field and organization of living matter," *Electromagnetic Biology and Medicine*, vol. 24, no. 3, pp. 185–197, 2005.

[65] E. C. Fuchs, J. Woisetschläger, K. Gatterer, E. Maier, R. Pecnik, G. Holler, and H. Eisenkölbl, "The floating water bridge," *Journal of Physics D: Applied Physics*, vol. 40, no. 19, p. 6112, 2007.

[66] K. Trombitás, P. Baatsen, J. Schreuder, and G. H. Pollack, "Contraction-induced movements of water in single fibres of frog skeletal muscle," *Journal of Muscle Research & Cell Motility*, vol. 14, no. 6, pp. 573–584, 1993.

[67] J. Pokorný and J. Pokorný, "Biophysical pathology in cancer transformation," *Journal of Clinical & Experimental Oncology*, p. 2, 2013.

[68] A. Samarbakhsh and J. A. Tuszyński, "Vibrational dynamics of bio-and nano-filaments in viscous solution subjected to ultrasound: implications for microtubules," *European Biophysics Journal*, vol. 40, no. 8, pp. 937–946, 2011.

[69] M. Cifra, J. Pokorný, D. Havelka, and O. Kučera, "Electric field generated by axial longitudinal vibration modes of microtubule," *BioSystems*, vol. 100, no. 2, pp. 122–131, 2010.

List of author's publications related to the doctoral thesis

All authors contributed equally, unless otherwise states.

Papers in Peer-Reviewed Journals with Impact Factor

[A1] D. Havelka, M. Cifra and O. Kučera, "Multi-mode electro-mechanical vibrations of a microtubule: In silico demonstration of electric pulse moving along a microtubule," *Applied Physics Letters*, vol. 104, no. 24, pp. 243702-1 - 243702-4, 2014. Candidate's contribution: 50 %

[A2] D. Havelka, O. Kučera, M. Deriu and M. Cifra, "Electro-acoustic behavior of the mitotic spindle: a semi-Classical Coarse-Grained Model," *PLOS ONE*, no. 1, 2014. Candidate's contribution: 60 %

[A3] D. Havelka, M. Cifra, O. Kučera, J. Pokorný, and J. Vrba, "High-frequency electric field and radiation characteristics of cellular microtubule network," *Journal of Theoretical Biology*, no. 286, pp. 31–40, 2011. Candidate's contribution: 50 %

[A4] O. Kučera and D. Havelka, "Mechano-electrical vibrations of microtubules–Link to subcellular morphology," *BioSystems*, no. 3, pp. 346 - 355, 2012. Candidate's contribution: 35 %

[A5] M. Cifra, J. Pokorný, D. Havelka, and O. Kučera, "Electric Field Generated by Axial Longitudinal Vibration Modes of Microtubule," *BioSystems*, vol. 100, no. 2, pp. 122–131, 2010.

Papers in Other Peer-Reviewed Journals

[B1] D. Havelka and M. Cifra, "Calculation of the Electromagnetic Field Around a Microtubule," *Acta Polytechnica*, vol. 49, no. 2, pp. 58–63, 2-3 2009.

Patents

We have no patents related to the doctoral thesis.

Papers and Abstracts in Conference Proceedings Listed in the Web of Knowledge

[D1]   D. Havelka, M. Cifra, and J. Vrba, "What is More Imortant for Radiated Power from Cells - Size or Geometry?" *Journal of Physics: Conference Series*, no. 329, pp. 012 014/1–012 014/9, 2011.

[D2]   M. Cifra, D. Havelka, and M. Deriu, "Electric Feld Generated by Longitudinal Axial Microtubule Vibration Modes with High Spatial Resolution Microtubule Model," *Journal of Physics: Conference Series*, no. 329, pp. 012 013/1–012 013/9, 2011.

[D3]   M. Cifra, D. Havelka, and O. Kučera, "Electric Oscillations Generated by Collective Vibration Modes of Microtubule," *Proceedings of SPIE*, vol. 7376, pp. 73 760N–1–73 760N–12, 2010.

Other Publications

[E1]   D. Havelka, M. Cifra, and J. Vrba, "Cellular Radiofrequency Electromagnetic Field can be measured only by Nanotechnological Methods," in *ISMOT Proceedings 2011*.   Praha: FEL ČVUT, 2011, pp. 307–310.

[E2]   D. Havelka and O. Kučera, "Higher vibration modes of microtubule: On how the lattice samples the field," in *POSTER 2010 - Proceedings of the 14th International Conference on Electrical Engineering*. Praha: ČVUT v Praze, FEL, 2010, pp. 1–5.

[E3]   M. Cifra, D. Havelka, O. Kučera, and J. Pokorný, "Electric Field Generated by Higher Vibration Modes of Microtubule," in *Proceedings of 15th Conference on Microwave Techniques COMITE 2010*.   Brno: VUT v Brně, FEKT, Ústav radioelektroniky, 2010, pp. 205–208.

[E4]   M. Cifra, D. Havelka, and O. Kučera, "Biophysical role of oscillatory electric field generated by undamped microtubule vibrations," in *6th International Workshop on Biological Effects of Electromagnetic Fields*.   Istanbul: Bogazici University, 2010, pp. 1–5.

[E5]   D. Havelka, O. Kučera, and J. Pokorný, and M. Cifra, "Mechano-Electrical Oscillations of Supramolecular Networks," *Technical Computing Bratislava 2010*.   Bratislava:RT systems, s.r.o , 2010, pp. 1–5.

[E6]   D. Havelka, M. Cifra, T. Vydra, and J. Vrba, "Přehled práce v oblasti buněčného elektromagnetického pole," *Sborník 9. česko-slovenské konference Trendy v biomedicínském inženýrství*.   Rožnov pod Radhoštěm: VŠB-TU Ostrava, 2011, pp. 214–217.

Citations in Web of Knowledge and SCOPUS

Citations are presented excluding autocitations.

Paper [A3]:

[A3.1]   Janca R: Neural network analysis of electrodynamic activity of yeast cells around 1 kHz. In 9TH INTERNATIONAL FROHLICH'S SYMPOSIUM: ELECTRODYNAMIC ACTIVITY OF LIVING CELLS (INCLUDING MICROTUBULE COHERENT MODES AND CANCER CELL PHYSICS), 2011. ISSN 1742-6588

[A3.2]   Daneshmand F, Amabili M: Coupled oscillations of a protein microtubule immersed in cytoplasm: an orthotropic elastic shell modeling. In JOURNAL OF BIOLOGICAL PHYSICS, 2012. ISSN 0092-0606

[A3.3]   Igamberdiev AU: Biomechanical and coherent phenomena in morphogenetic relaxation processes. In BIOSYSTEMS, 2012. ISSN 0303-2647

[A3.4] Zhao Y, Zhan QM: Electric fields generated by synchronized oscillations of microtubules, centrosomes and chromosomes regulate the dynamics of mitosis and meiosis. In THEORETICAL BIOLOGY AND MEDICAL MODELLING, 2012. ISSN 1742-4682

[A3.5] Zhao Y, Zhan QM: Electric oscillation and coupling of chromatin regulate chromosome packaging and transcription in eukaryotic cells. In THEORETICAL BIOLOGY AND MEDICAL MODELLING, 2012. ISSN 1742-4682

[A3.6] Nandi S, Johnson NF, Cohn JL: PERSISTENT PATTERNS IN MICROTUBULE DIPOLE LATTICES. In ADVANCES IN COMPLEX SYSTEMS, 2013. ISSN 0219-5259

[A3.7] Zdravkovic S, Sataric MV, Zekovic S: Nonlinear dynamics of microtubules -A longitudinal model. In EPL, 2013. ISSN 0295-5075

[A3.8] Zdravkovic S, Bugay AN, Aru GF, et al.: Localized modulated waves in microtubules. In CHAOS, 2014. ISSN 1054-1500

[A3.9] Zdravkovic S, Sataric MV, Maluckov A, et al.: A nonlinear model of the dynamics of radial dislocations in microtubules. In APPLIED MATHEMATICS AND COMPUTATION, 2014. ISSN 0096-3003

[A3.10] Zekovic S, Muniyappan A, Zdravkovic S, et al.: Employment of Jacobian elliptic functions for solving problems in nonlinear dynamics of microtubules. In CHINESE PHYSICS B, 2014. ISSN 1674-1056

Paper [A4]:

[A4.1] Cifra M: Electrodynamic eigenmodes in cellular morphology. In BIOSYSTEMS, 2012. ISSN 0303-2647

[A4.2] Igamberdiev AU: Biomechanical and coherent phenomena in morphogenetic relaxation processes. In BIOSYSTEMS, 2012. ISSN 0303-2647

[A4.3] Nawrocka-Bogusz H, Marcinkowska-Gapinska A: The effect of pulsed IR-light on the rheological parameters of blood in vitro. In BIORHEOLOGY, 2014. ISSN 0006-355X

[A4.4] Zdravkovic S, Sataric MV, Maluckov A, et al.: A nonlinear model of the dynamics of radial dislocations in microtubules. In APPLIED MATHEMATICS AND COMPUTATION, 2014. ISSN 0096-3003

Paper [A5]:

[A5.1] Ballardin M, Tusa I, Fontana N, et al.: Non-thermal effects of 2.45 GHz microwaves on spindle assembly, mitotic cells and viability of Chinese hamster V-79 cells. In MUTATION RESEARCH-FUNDAMENTAL AND MOLECULAR MECHANISMS OF MUTAGENESIS, 2011. ISSN 0027-5107

[A5.2] Plankar M, Jerman I, Krasovec R: On the origin of cancer: Can we ignore coherence?. In PROGRESS IN BIOPHYSICS & MOLECULAR BIOLOGY, 2011. ISSN 0079-6107

[A5.3] Rossi C, Foletti A, Magnani A, et al.: New perspectives in cell communication: Bioelectromagnetic interactions. In SEMINARS IN CANCER BIOLOGY, 2011. ISSN 1044-579X

[A5.4] Daneshmand F: Microtubule circumferential vibrations in cytosol. In PROCEEDINGS OF THE INSTITUTION OF MECHANICAL ENGINEERS PART H-JOURNAL OF ENGINEERING IN MEDICINE, 2012. ISSN 0954-4119

[A5.5] Daneshmand F, Amabili M: Coupled oscillations of a protein microtubule immersed in cytoplasm: an orthotropic elastic shell modeling. In JOURNAL OF BIOLOGICAL PHYSICS, 2012. ISSN 0092-0606

[A5.6] Plankar M, Del Giudice E, Tedeschi A, et al.: THE ROLE OF COHERENCE IN A SYSTEMS VIEW OF CANCER DEVELOPMENT. In THEORETICAL BIOLOGY FORUM, 2012. ISSN 0035-6050

[A5.7] Saha AA, Craddock TJA, Tuszynski JA: An investigation of the plausibility of stochastic resonance in tubulin dimers. In BIOSYSTEMS, 2012. ISSN 0303-2647

[A5.8] Zhao Y, Zhan QM: Electric fields generated by synchronized oscillations of microtubules, centrosomes and chromosomes regulate the dynamics of mitosis and meiosis. In THEORETICAL BIOLOGY AND MEDICAL MODELLING, 2012. ISSN 1742-4682

[A5.9] Zhao Y, Zhan QM: Electric oscillation and coupling of chromatin regulate chromosome packaging and transcription in eukaryotic cells. In THEORETICAL BIOLOGY AND MEDICAL MODELLING, 2012. ISSN 1742-4682

[A5.10] Plankar M, Brezan S, Jerman I: The principle of coherence in multi-level brain information processing. In PROGRESS IN BIOPHYSICS & MOLECULAR BIOLOGY, 2013. ISSN 0079-6107

[A5.11] Zdravkovic S, Sataric MV, Zekovic S: Nonlinear dynamics of microtubules -A longitudinal model. In EPL, 2013. ISSN 0295-5075

[A5.12] Ravariu C, Bondarciuc A: The sensitivity in the IR spectrum of the intact and pathological tissues by laser biophotometry. In LASERS IN MEDICAL SCIENCE, 2014. ISSN 0268-8921

[A5.13] Zdravkovic S, Sataric MV, Maluckov A, et al.: A nonlinear model of the dynamics of radial dislocations in microtubules. In APPLIED MATHEMATICS AND COMPUTATION, 2014. ISSN 0096-3003

[A5.14] Zekovic S, Muniyappan A, Zdravkovic S, et al.: Employment of Jacobian elliptic functions for solving problems in nonlinear dynamics of microtubules. In CHINESE PHYSICS B, 2014. ISSN 1674-1056

[A5.15] Zimmerman J, Parameswaran R, Tian BZ: Nanoscale semiconductor devices as new biomaterials. In BIOMATERIALS SCIENCE, 2014. ISSN 2047-4830

Paper [D1]:

[D1.1] Zdravkovic S, Bugay AN, Aru GF, et al.: Localized modulated waves in microtubules. In CHAOS, 2014. ISSN 1054-1500

[D1.2] Zdravkovic S, Sataric MV, Maluckov A, et al.: A nonlinear model of the dynamics of radial dislocations in microtubules. In APPLIED MATHEMATICS AND COMPUTATION, 2014. ISSN 0096-3003

Paper [D2]:

[D2.1] Pietak AM: Structural evidence for electromagnetic resonance in plant morphogenesis. In BIOSYSTEMS, 2012. ISSN 0303-2647

[D2.2] Zhao Y, Zhan QM: Electric fields generated by synchronized oscillations of microtubules, centrosomes and chromosomes regulate the dynamics of mitosis and meiosis. In THEORETICAL BIOLOGY AND MEDICAL MODELLING, 2012. ISSN 1742-4682

Research Projects

Study of electromagnetic processes in biomolecules, cells and tissue, SGS13/077/OHK3/1T/13, Grant Agency of the Czech Technical University in Prague, *principal investigator*.

Cellular electromagnetic field and its interactions with surrounding space, SGS11/064/OHK4/1T/13, Grant Agency of the Czech Technical University in Prague, *principal investigator*.

Research and measurements of signals generated by nanostructures, P102/11/0649, Czech Science Foundation, *member of the team*.

Non standard applications of physical fields, P102/08/H081, Czech Science Foundation, *member of the team*. Interactions of EM field with biological systems and theirs applications in medicine, SGS14/189/OHK3/3T/13, Grant Agency of the Czech Technical University in Prague, *member of the team*.

Numerical studies supporting research of biological non-thermal effects of electromagnetic field, SGS10/068/OHK4/1T/13, Grant Agency of the Czech Technical University in Prague, *member of the team*.

LIST OF AUTHOR'S PUBLICATIONS NON-RELATED TO MAIN TOPIC OF THE DOCTORAL THESIS

All authors contributed equally, unless otherwise states.

PAPERS IN PEER-REVIEWED JOURNALS WITH IMPACT FACTOR

We have no papers in peer-reviewed journals with Impact Factor non-related to main topic of the doctoral thesis.

PAPERS IN OTHER PEER-REVIEWED JOURNALS

We have no papers in other peer-reviewed journals non-related to main topic of the doctoral thesis.

PATENTS

We have no patents related non-related to main topic of the doctoral thesis.

PAPERS AND ABSTRACTS IN CONFERENCE PROCEEDINGS LISTED IN THE WEB OF KNOWLEDGE

We have no papers and abstracts in WoS conference proceedings related non-related to main topic of the doctoral thesis.

OTHER PUBLICATIONS

[E7] T. Vydra, D. Havelka, L. Výšek and J. Vrba, "An overview of Microwave Systems used for SAR Evaluation and Inspecting Effects in Biological Tissue," in *Proceedings of the 6th European Conference on Antennas and Propagation (EUCAP 2012)*. Praha: IEEE, 2012, pp. 2114–2117.

[E8] T. Vydra, D. Havelka, and J. Vrba, "Visualization of Microwave Exposure in Industrial and Medical Applications ," in *Sborník 9. česko-slovenské konference Trendy v biomedicínském inženýrství*. Rožnov pod Radhoštěm: VŠB-TU Ostrava, 2011, pp. 171–173.

[E9] J. Vrba, L. Oppl, D. Vrba, J. Vorlíček, B. Vrbová and D. Havelka, "Prospective Applications of EM Fields in Medicine," in *PIERS 2011 Marrakesh Proceedings*. Marrakesh: The Electromagnetics Academy, 2011, pp. 1816–1821.

[E10] J. Vrba, L. Oppl, J. Vorlíček, B. Vrbová, D. Vrba, T. Vydra and D. Havelka, "Electromagnetic Field Based Microwave Technologies in Medicine," in *ISMOT Proceedings 2011*. Praha: FEL ČVUT, 2011, pp. 319–323.

[E11] J. Vrba, L. Výšek, L. Oppl, D. Vrba, B. Vrbová and D. Havelka, "Microwave Exposure Systems for Research of Biological Effects of Electromagnetic Field," in *ISMOT Proceedings 2011*. Praha: FEL ČVUT, 2011, pp. 343–345.

Citations in Web of Knowledge and SCOPUS

We have no citations in WoS and SCOPUS non-related to main topic of the doctoral thesis.

Research Projects

APPENDIX

This chapter includes two papers, [A5] and [A4], and the supplementary data of Chapter 4.

A | ELECTRIC FIELD GENERATED BY AXIAL LONGITUDINAL VIBRATION MODES OF MICROTUBULE

This appendix is a version of:

Author contributions:

| Designed research: M.C. and J.P

| Performed research: M.C. and **D.H.**

| Analysed data: M.C. and O.K.

| Wrote the paper: M.C., J.P., and O.K.

| Candidate's contribution: 25%

The manuscript carries the following acknowledgements:

Electric field generated by axial longitudinal vibration modes of microtubule

M. Cifra [a,b,*], J. Pokorný [a], D. Havelka [b], O. Kučera [a,c]

[a] Institute of Photonics and Electronics, Academy of Sciences of the Czech Republic, Czech Republic
[b] Department of Electromagnetic Field, Faculty of Electrical Engineering, Czech Technical University in Prague, Czech Republic
[c] Department of Circuit Theory, Faculty of Electrical Engineering, Czech Technical University in Prague, Czech Republic

ARTICLE INFO

ABSTRACT

Microtubules are electrically polar structures fulfilling prerequisites for generation of oscillatory electric field in the kHz to GHz region. Energy supply for excitation of elasto-electrical vibrations in microtubules may be provided from GTP-hydrolysis; motor protein–microtubule interactions; and energy efflux from mitochondria. We calculated electric field generated by axial longitudinal vibration modes of microtubules for random, and coherent excitation. In case of coherent excitation of vibrations, the electric field intensity is highest at the end of microtubule. The dielectrophoretic force exerted by electric field on the surrounding molecules will influence the kinetics of microtubule polymerization via change in the probability of the transport of charge and mass particles. The electric field generated by vibrations of electrically polar cellular structures is expected to play an important role in biological self-organization.

© 2010 Elsevier Ireland Ltd. All rights reserved.

1. Introduction

Cytoskeleton, which consists of microtubules, actin filaments, and intermediate filaments, is considered to be an organizing structure of the eukaryotic cell (Alberts et al., 2008). Microtubules (MTs) are of special interest since they manifest several features that distinguish them from other subcomponents of the cytoskeleton. MTs, which consist usually of 13 protofilaments (PT), resemble hollow tubes with inner and outer diameter of 17 nm and 25 nm, respectively (Fig. 1a). The building subunits of MT are the tubulin heterodimers composed of α- and β-tubulin (Fig. 2). The heterodimers have high electric dipole moment of over 1000 Debye (10^{-26} C m) (Tuszyński et al., 2002; Mershin et al., 2004); they are responsible for the high electrical polarity of MTs. In the interphase of the cell cycle, microtubules are radially organized with their chemical minus ends embedded in a centrosome (organizing center), which is located in the center of the cell near the cell nucleus. There are several hundreds of MTs in a cell, depending on the organism and the cell type. In the interphase microtubules undergo dynamic growth (polymerization) and shrinkage (depolymerization), so-called "dynamic instability" (Fig. 1b). During the existence of mitotic spindle, MTs are subject to treadmilling, i.e. they polymerize at the plus end and depolymerize at the minus end (chemical plus and minus).

1.1. Microtubule Vibrations

Elastic and vibrational properties of MTs have been studied by several authors. Sirenko et al. (1996) analyzed vibrations of microtubules in a fluid modeled as elastic cylindrical shell with isotropic mechanical properties. Maximum frequency of tens of GHz corresponded to nonradiative elastic waves localized at the MT wall.

Pokorný et al. (1997) analyzed the vibrations of MTs modeled as one dimensional chain of mass particles with translation symmetry. Vibrations of cellular structures have been considered to be viscously overdamped in cytosol and thus not realistic (Foster and Baish, 2000; Adair, 2002). However, most of the water in the cell has different properties than bulk water (Preparata, 1995; Del Giudice et al., 2000, 2005; Zhadin and Giuliani, 2006; Zhadin et al., 2007) due to the molecular crowding and consequent large hydration surfaces. If the slip layer condition for MT longitudinal vibrations is taken into account, vibrations may be excited (Pokorný, 2004, 2003, 2005).

Portet et al. (2005) describe the microscopic dynamical properties of MTs using a discrete model based on a lattice of dimers. It was pointed out that various experimental methods yielded wide range of values of Young's and shear modulus between 1 Pa (Janmey et al., 1991; Sato et al., 1988) up to 1 GPa (Portet et al., 2005). This would be explainable by the fact that mechanical properties of microtubules are anisotropic and orthotropic.[1] This was showed by Kis et al. (2002) who obtained the most accurate values for both the Young's ($E > 100$ MPa) and shear modulus ($G = 1.4 \pm 0.4$ MPa).

---

* Corresponding author at: Institute of Photonics and Electronics, Academy of Sciences of the Czech Republic, Bioelectromagnetic Coherence Group, Chaberska 57, 18251 Prague, Czech Republic. Tel.: +420 266773528.
E-mail address: cifra@ufe.cz (M. Cifra).

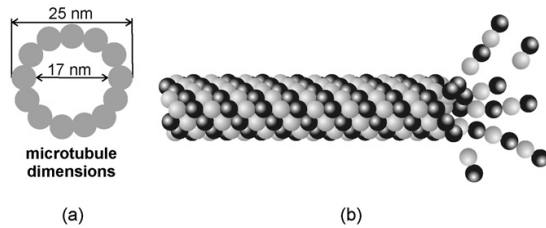[1] Orthotropic–anisotropic in the directions perpendicular to each other.

Fig. 1. (a) Cross section of microtubule. (b) Detail of chemical plus end of a microtubule undergoing dynamic instability.
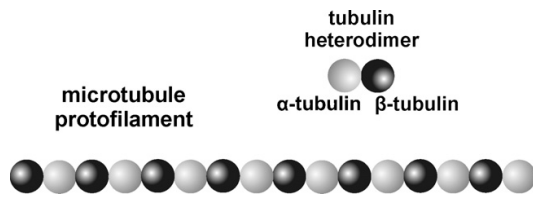

Fig. 2. Structural subunits of microtubules: protofilament composed of tubulin heterodimers.

The oscillation modes involving a change in the diameter of the MTs strongly depend on the shear modulus (Kasas et al., 2004).

Tuszyński et al. (2005) reviewed characteristic elastic properties of microtubules. Wang et al. (2006) and Wang and Zhang (2008) developed orthotropic elastic shell model to study microtubule vibrations and determined more realistic frequencies of radial and circumferential modes than that provided by Sirenko et al. (1996) which was confirmed by Qian et al. (2007).

It can be seen from above given references that frequencies of MT vibration modes may span over broad spectral range from kHz to GHz. Due to non-linearities and to mechanical anisotropy of MTs, frequency mixing and energy transfer between the modes, one may expect various frequencies of oscillations.

1.2. Energy Supply to Microtubules

Excitation of mechanical vibrations in MTs, which are electrically polar, would give rise to electrical oscillations. To excite and sustain vibrations the energy needs to be supplied. In the case when at least a part of energy supplied to MTs excites elastic vibrations of electrically polar structures, generated oscillatory electric field has the same frequency as that of elastic MT vibrations. We analyzed three possible sources of energy supply to MTs (Jelínek et al., 2009):

- Energy released from hydrolysis of guanosine triphosphate (GTP) in processes of dynamic instability of MTs (Fig. 2) is the energy supply dependent on internal MT process. β-Tubulin bound GTP is hydrolyzed to guanosine diphosphate (GDP) after polymerization of tubulin heterodimer. In the interphase the half lifetime of individual unstable MTs (subject to dynamic instability) is about 5–10 min (Alberts et al., 2008). Energy from hydrolysis of GTP stored in MT lattice is estimated to be 1.7 kcal/mol[2] (Caplow et al., 1994; Caplow, 1995; Caplow and Shanks, 1996). The corresponding power input to MT lattice due to GTP hydrolysis is about 1.8×10^{-14} W/mm of MT (if we accept 5 min as a half life of a single MT) which range roughly corresponds to the previous estimate (Pokorný, 1999; Pokorný and Wu, 1998). Assuming 100 μm total length of MT structure in a cell (the length is assumed for

---

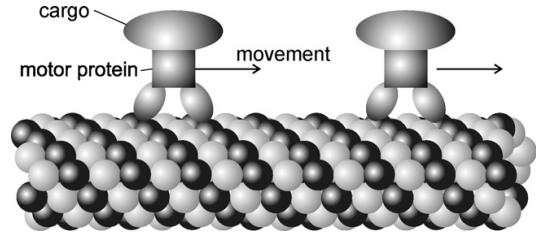[2] 1.7 kcal/mol = 7.1 kJ/mol = 118×10^{-22} J = 0.074 eV.

Fig. 3. Movement of the motor proteins on the microtubule, cargo not in scale.

yeast cell (King and Hyams, 1982; Winey et al., 1995; Sobel, 1997)), one obtains the power of about 3×10^{-18} W in whole microtubular network. In the M phase, the dynamics of polymerization and depolymerization is increased about 20-fold, for instance by treadmilling in the metaphase.

- Energy transferred from moving of motor proteins and their interaction with MTs may also contribute to excitation of vibrations in MTs (Fig. 3). Motor protein dynein moves towards the cell center (minus end of a MT) and kinesin moves towards the cell periphery (plus end of a MT). One ATP (adenosine triphosphate) molecule is hydrolyzed for each step of motor protein. One step of motor protein is ca. 8 nm long, corresponding to axial dimensions of tubulin heterodimer. Energy released during ATP hydrolysis under cellular ATP concentrations (1–10 mM) is ca. 14 kcal/mol[3] which corresponds to activation energy of motor proteins (Kawaguchi and Ishiwata, 2001, 2000; Pelling et al., 2004). Motor proteins move with a velocity ca. 0.1–2 μm/s (Alberts et al., 2008). Assuming four motor proteins on each of 100 MTs in the cell, each motor protein moving with average velocity of 800 nm/s, power exerted by all motor proteins in a cell is about 4×10^{-15} W. Assuming that 1–25% of this power excites vibrations in MTs, it corresponds to 4×10^{-17}–10^{-15} W, respectively.

- Energy released from mitochondria as "wasted" energy in the course of citric acid cycle may be the most significant energy source for excitations of MT vibrations.

 Whole metabolic turnover of *Saccharomyces cerevisiae* cell is 0.1 pW (10^{-13} W) (Lamprecht, 1980). Mitochondria are considered "power plants of the cell" generating ATP by means of energy from pyruvate and fatty acid. Less than 50% of energy is stored in ATP. The rest of the energy ("wasted" energy), i.e., more than 50%, is released to surroundings of mitochondria in the form of heat and emitted radiation (Fig. 4). Corresponding wasted power may be 0.05 pW. Since mitochondria are located near microtubules, part of the "wasted" power (we may assume 20%, i.e., 10^{-14} W) may be involved in excitation of the vibrations in MTs.

2. Method and Parameters Used for Calculation of Electric Field Around MT

First assessment of oscillating electric field around MTs has been done by Pokorný et al. (1997). Intensity of the electric field was evaluated along the lines parallel with the MT axis up to the distance of 500 nm. Their model included microtubules with heterodimers with random or coherent oscillating dipoles. Frequency of coherent excitations has been chosen as 100 MHz.

We made a preliminary assessment of MT electric field with different calculation method in Havelka and Cifra (2009a), Havelka (2008), Havelka and Cifra (2009b), but we used a higher value of dipole moment than corresponds to the real state. The complete

---

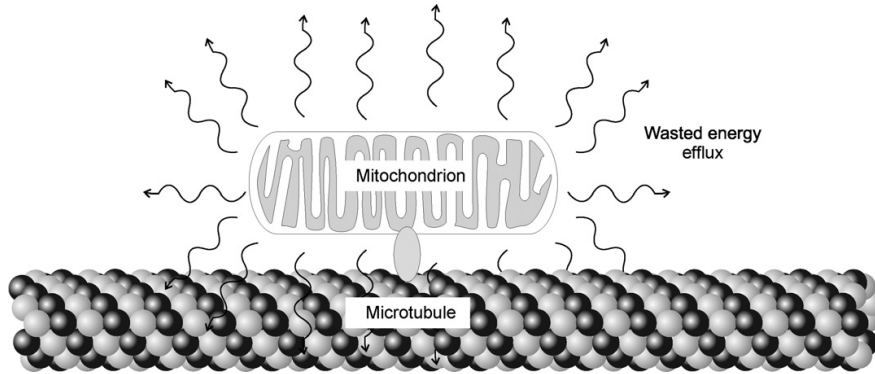[3] 58.2 kJ/mol = 0.97562×10^{-19} J = 0.609 eV.

Fig. 4. Microtubule bathed in energy efflux from a mitochondrion. The mitochondrion not in scale to microtubule.

and more realistic results are presented in this paper. We analyze electric field generated by MT longitudinal axial vibration modes. We also study the spatial distribution of electric field of MT since this has not been performed before.

Due to axial longitudinal vibrations in the MT lattice an electric dipole moment will have an oscillating component in the direction parallel to MT axis. Oscillating dipole with the dimensions much smaller than wavelength of generated electric field can be represented by elementary oscillating electric dipole (Hertz dipole).

2.1. Components of the Electric and the Magnetic Fields of the Elementary Oscillating Electric Dipole

We use standard relations for the field of oscillating electric dipole in the form as provided in Novotný (1997):

$$\vec{H}_\phi = -\frac{Id}{4\pi}k^2 \sin\theta \left(\frac{1}{jkr} + \frac{1}{(jkr)^2}\right) e^{-jkr}\vec{\phi}_0 \qquad (1)$$

$$\vec{E}_r = -\frac{Id}{4\pi}Zk^2 2\cos\theta \left(\frac{1}{(jkr)^2} + \frac{1}{(jkr)^3}\right) e^{-jkr}\vec{r}_0 \qquad (2)$$

$$\vec{E}_\theta = -\frac{Id}{4\pi}Zk^2 \sin\theta \left(\frac{1}{jkr} + \frac{1}{(jkr)^2} + \frac{1}{(jkr)^3}\right) e^{-jkr}\vec{\theta}_0 \qquad (3)$$

H is magnetic field intensity; E is electric field intensity; I is equivalent current; d is length of the dipole; k is propagation constant; Z is wave impedance; j is imaginary unit and coordinate symbols are according to Fig. 5. None of these equations is dependent on ϕ and
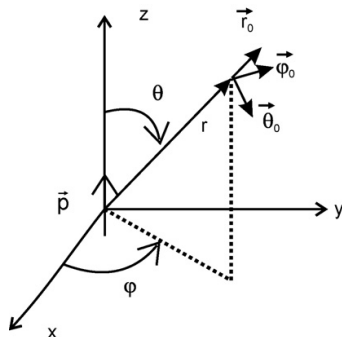

Fig. 5. A dipole in the Cartesian and spherical coordinate system.

all equations include:

$$Id = j\omega p \qquad (4)$$

ω is angular frequency, and p is dipole moment ($Id = (\partial Q/\partial t)d = j\omega Qd$, $Qd = p$, Q is charge).

2.2. Description of the Electric Field Around a Microtubule

Electric field around MT can be calculated as a vectorial sum of elementary electric components generated by individual tubulin heterodimer dipoles. Frequency of the oscillations of individual dipoles has been set to the 1 GHz which falls into the spectrum predicted by Sirenko et al. (1996), Wang et al. (2006) and Wang and Zhang (2008) and also fits almost exactly the frequency of optical branches of vibration modes of microtubule calculated by Pokorný and Wu (1998) and Pokorný et al. (1997).

The near field around electric dipole has the electric component much stronger that the magnetic one. We concentrated therefore on the electric field component.

We have rewritten the Eqs. (2) and (3) for electric field in Cartesian coordinates which can be used for arbitrarily placed and tilted dipole in lossy medium. The procedure is described thoroughly in Cifra (2009). All calculations and figures have been made in MatLab.

2.3. Shift of Protofilaments

Although the MTs are tube-like structures, their wall does not have cylindrical symmetry. This is due to longitudinal shift of protofilaments in MT lattice. Accordingly, lattice with longitudinal shift of PTs simulates more realistic organization of protofilaments in the MT. This gives us more accurate information about the spatial distribution of electric field intensity of the around MT. We have chosen the configuration in A-lattice (Song and Mandelkow, 1993, 1995; Kikkawa et al., 1994; Amos, 1995), which is a lattice with a longitudinal shift of protofilaments of 4.92 nm (Table 1 and Fig. 6).

2.4. Types of Excitation and Calculation Parameters

Geometry and orientation of tubulin dipole moments in MT is approximately known. However, the elasto-electrical waves in

Table 1
Longitudinal shift of PT in A-lattice.

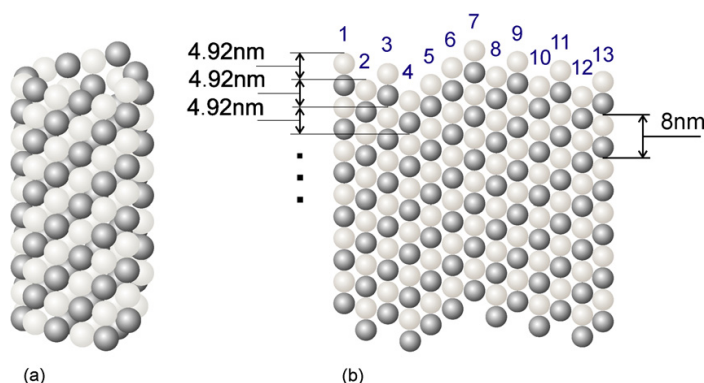| Number of PT	2	3	4	5	6	7
Shift to 1st PT (nm)	−4.92	−1.84	−6.76	−3.68	−0.6	2.48
Number of PT	8	9	10	11	12	13
Shift to 1st PT (nm)	−2.44	0.64	−4.28	−1.2	−6.12	−3.04

Fig. 6. (a) Microtubule with longitudinal shift of PT of 4.92 nm. (b) Shell of MT with longitudinal shift of protofilament.

microtubules also determine the efficiency, spatial distribution and dynamics of generated electric oscillations. There may be acoustical and optical modes of axial longitudinal oscillations. In optical modes, neighbor particles move in opposite direction. In acoustical modes, neighbor particles move in the same direction (except the end of Brillouin zone where the k-vector is large).

In the case of optical mode a component of dipole moment which is oriented along the axis would oscillate and generate electric oscillations.

Vibration modes which displace whole dipole along its axis would be significantly less efficient in generation of electric oscillations. This is due to the fact that opposite charges near each other and oscillating along the same axis with the same phase and frequency will behave as antiphase dipoles which effectively cancel each other field.

As shown in Tuszyński et al. (2002) and Mershin et al. (2004) a significant part of the tubulin dipole moment is oriented radially from MT axis. Certain kind of vibration modes involve radial oscillation of MT wall. Such kind of modes would involve displacement of rather large mass of surrounding cytosol, hence they would undergo stronger damping compared to the longitudinal optical oscillations in the direction along MT axis.

Circumferential elastic vibrations may be also connected with generation of oscillating electric field due to oscillatory changes of the distance between electric charges. Frequency of the modes depends on Young's and shear modulus. As the moduli exhibit large differences in magnitudes in different directions the frequencies of oscillations are corresponding.

Based on the discussion above, we have focused our analysis on the longitudinal optical oscillations of MT. Frequency of oscillations was chosen to be 1 GHz. It corresponds to calculations of MT vibrations of Pokorný and Wang. We estimate the oscillatory displacement of the charge in tubulin dipole moment along the MT axis to be around 0.1 nm for the vibrations in GHz region.[4] The static dipole moment (p_s) in the direction of the MT axis is accepted to be about 330 D (Tuszyński et al., 2002; Mershin et al., 2004). Length of the tubulin heterodimer is 8 nm, so the effective oscillatory component of the dipole p_a at the frequency of 1 GHz may be estimated as $p_a = (0.1/8)p_s = 4.125\,D = 1.376 \times 10^{-29}\,C\,m$.

Excitation of vibrations in our calculations was based on following models:

- Random excitation–random phase of oscillations was approximated by modulation of dipole moment of each of dipoles by function sin$(2\pi n)$, n = random number from interval $\langle 0, 1 \rangle$.
- Coherent excitation – modes with wavenumber k (k-modes) – longitudinal waves on the MT have been approximated by modulation of dipole moment of the individual heterodimers along the MT axis by function $a + b \times \sin(k_0 nz)$, z-axis corresponds to MT axis. Physically, these vibration modes belong to optical branch where neighbor particles (here α- and β-tubulin monomers in protofilaments) oscillate against each other. This corresponds to our approximation of heterodimer as an oscillating dipole. Number of mode n is provided instead of wavenumber k to indicate number of maxima. Note that direction of electric field vector is opposite in neighboring maxima as given by $\sin(k_0 nz)$ modulating function. In a special case all the dipoles may oscillate with the same phase (corresponds to $k = 0$ optical branch of longitudinal lattice vibration).

Dielectric parameters of the surrounding medium have been chosen based on experimentally obtained results from Asami et al. (1976) and Asami and Yonezawa (1996). Compared to the cited literature, we use slightly different value of the cytoplasm relative permittivity; instead 50 (Asami et al., 1976) we use 60. Slightly higher permittivity used corresponds physically to higher water content assumed (Table 2).

3. Results

Colormap figures depict MT electric field spatial distribution in the plane which contains the MT axis. White lines in the figures are contours of the MT wall. The arrows in the colormap figures denote the direction of the electric field vector. Note that neither arrow density nor arrow length is related to intensity. For greater dynamic range common logarithm of electric intensity is used for all

---

[4] This estimate is based on measurements of Pelling et al. (2004) and Pelling et al. (2005) who found oscillations of yeast cell membrane (likely excited by cytoskeleton) in the frequency range about 1 kHz and amplitudes about 1–10 nm. Microtubules associated with motor proteins are also able to vibrate at frequencies of hundreds of kHz and amplitudes up to 10 nm in cilia and flagella (Kamimura and Kamiya, 1989, 1992; Sakakibara et al., 2004).

Table 2
Fixed parameters of calculations.

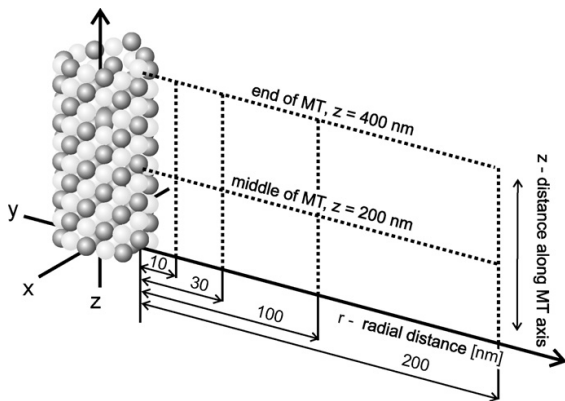|	
Frequency of vibrations	1 GHz
Number of protofilaments in MT	13
Number of heterodimers in each protofilament	50
Oscillatory component of dipole moment	$4.125\,D = 1.376 \times 10^{-29}\,C\,m$
Relative permittivity of the medium	60
Conductivity of the medium	1 S/m

Fig. 7. The lines along which the electric field intensity has been plotted.

Fig. 9. Electric field around microtubule with random excitation. Color coded electric field magnitude is in log scale ($\log(V/m)$). Arrows represent electric field vector.

graphs and figures, e.g. color on the colorbar denoted 4 corresponds to intensity 10^4 V/m.

Electric field intensity dependence on distance radially from MT axis and along MT axis in selected distances from MT axis has been plotted in separate figures for simpler comparison. See Fig. 7 for the clarification of the plotting geometry.

3.1. Coherent Excitation

First we studied the simple model of the special case of coherent excitation. The spatial distribution of electric field around MT in this case is depicted in Fig. 8.

Coherently excited (at $k = 0$) MT behaves like a giant dipole having maxima of electric field intensity at its ends. This is of no wonder since it consists of chains of in phase oscillating dipoles with the same orientation of dipole moments.

3.2. Random Excitation

Spatial distribution of electric field generated by random (thermal) excitation of MT is given in Fig. 9.

The spatial distribution depicted in the Fig. 9 is just one example which results from the certain random number sequence. Naturally, the spatial distribution of random excitation can take various forms and often exhibits local minima.

3.3. Comparison of Coherent and Random Excitation

Comparison of coherent ($k = 0$) and random excitation of electric field is provided in Fig. 10.

We clearly see the difference between the field generated by random and in phase (coherent) oscillations. Although electric field intensity is higher in the middle of the MT axis ($z = 200$ nm) at the surface of MT for random excitation, it falls off faster with the dis-
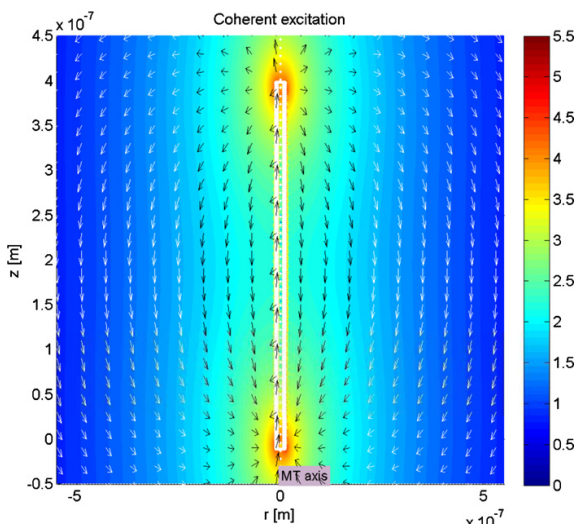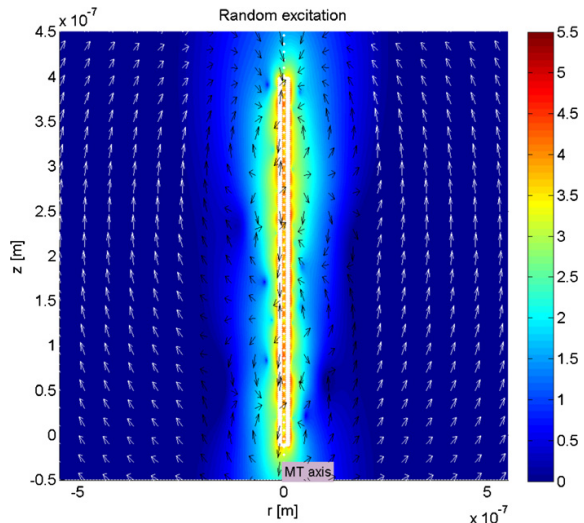

Fig. 8. Electric field around microtubule with coherent excitation ($k = 0$). Color coded electric field magnitude is in log scale ($\log(V/m)$). Arrows represent electric field vector.
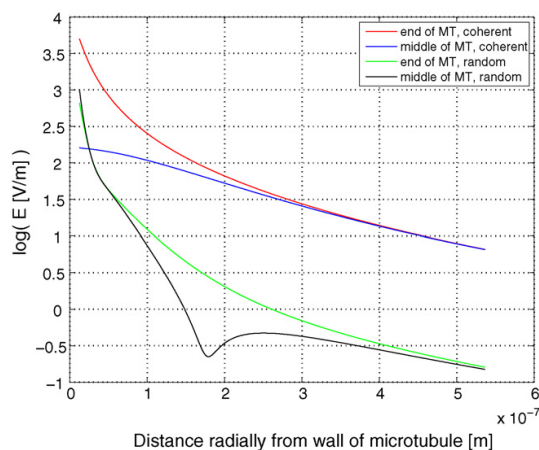

Fig. 10. Electric field intensity radial dependence from the wall of microtubule for the coherent and random excitation. From the end of MT ($z = 400$ nm) and from the middle of MT ($z = 200$ nm).
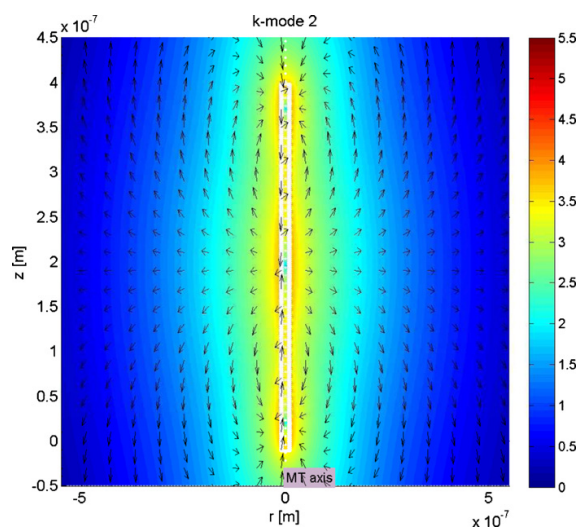
Fig. 11. Electric field distribution around MT of k-mode 2. Color coded electric field magnitude is in log scale ($\log(V/m)$). Arrows represent electric field vector.

tance compared to the in phase (coherent) excitation (Fig. 10). The electric field intensity is higher at the ends of MT ($z = 400$ nm and 0 nm[5]) for the in phase excitation compared to the random one (Fig. 10). There is a difference by one and a half orders of magnitude between the electric field intensity of randomly and in phase excited vibrations in the distance larger than ca. 100 nm.

3.4. Coherent Excitation of Higher k-modes

Normal vibration modes (termed as k-modes) can be excited in microtubules. We primarily chose to study k-modes number $n = 2$, 5 and 50 as the representative ones. We depict the spatial distribution of the k-mode 2 in Fig. 11 and zoomed in spatial distribution in 12.

Two maxima in the MT lattice are clearly discernible in Fig. 12 whereas in Fig. 11 they are not. Therefore we chose to provide only zoomed in figures when displaying spatial distribution of electric field for higher ($n > 0$) modes. Note that abscissa and ordinate have different scales in zoomed in figures; the r-axis (ordinate) is 10-fold stretched to resolve the details of electric field in direction radially from MT axis.

The zoomed in spatial distribution of electric field around MT of k-modes 5 and 50 is depicted in Figs. 13 and 14, respectively. Electric field of higher modes is depicted in figures in supplementary material.

We observed that every half-wave of k-mode of longitudinal lattice vibration produces effectively a k-mode "dipole" field[6] the maxima of which are located on the poles of the "dipole". Moreover, k-mode "dipoles" are oriented to each other with the same pole. This can be seen also from the orientation of electric field vectors (see, e.g. Fig. 12 where two k-mode "dipolar" fields are discernible in each intersection of the MT wall; the plus poles are in the middle of the MT wall, i.e. the electric field vector is oriented radially from the plus poles of the "dipole"). The effective number of maxima in

---

[5] Values are not depicted for $z = 0$ nm but they are essentially the same as for $z = 400$ nm due to the symmetry.
[6] We use term "k-mode 'dipole'" to describe an effective "dipole" field structure which appears in the MT wall due to every half wave of MT vibration. Number of mode indicates the number of k-mode "dipoles".
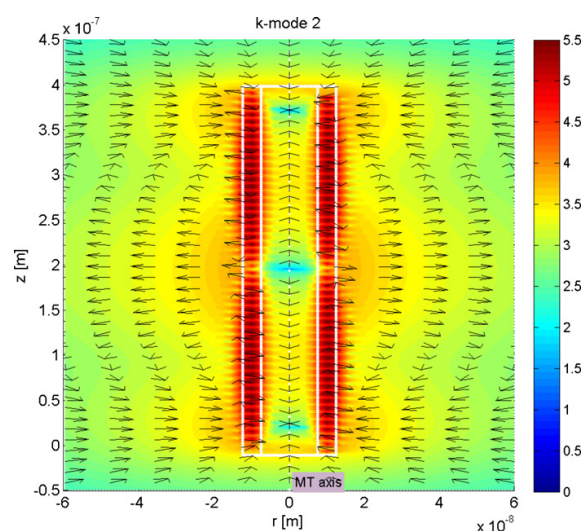

Fig. 12. Electric field distribution around MT of k-mode 2, zoomed in radial axis. Color coded electric field magnitude is in log scale ($\log(V/m)$). Arrows represent electric field vector.

the field intensity up to the distance of 10 nm from the MT wall (or more, depending on the mode number) for the k-modes $n > 0$ is actually $n + 1$ since each pole of k-mode "dipole" contributes by one maximum. The number of maxima further changes in greater distance.

Higher the mode, the total dipole moment of whole MT is split into many small k-mode "dipoles" with opposite directions. The MT obtains multipolar k-mode character with rising mode number. Multipolar character of field source distribution explains the steeper decrease of intensity from the MT for higher mode numbers (e.g. see Fig. 15).

We provide figures depicting electric field intensity radial dependence from MT end and middle of MT for k-mode 2, 5, 10, 20 and 50 in Figs. 15 and 16.
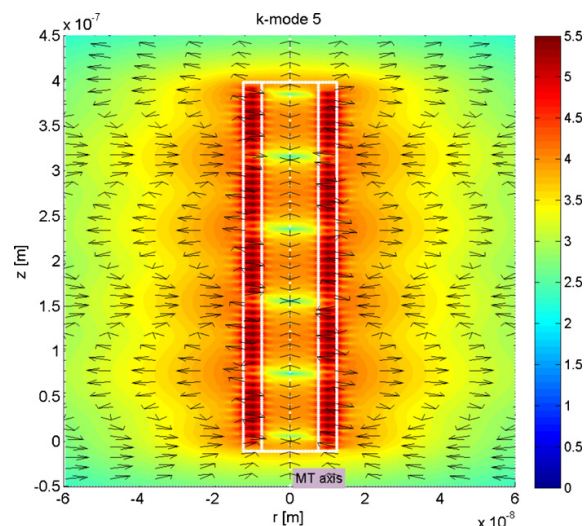

Fig. 13. Electric field distribution around MT of k-mode 5, zoomed in radial axis. Color coded electric field magnitude is in log scale ($\log(V/m)$). Arrows represent electric field vector.
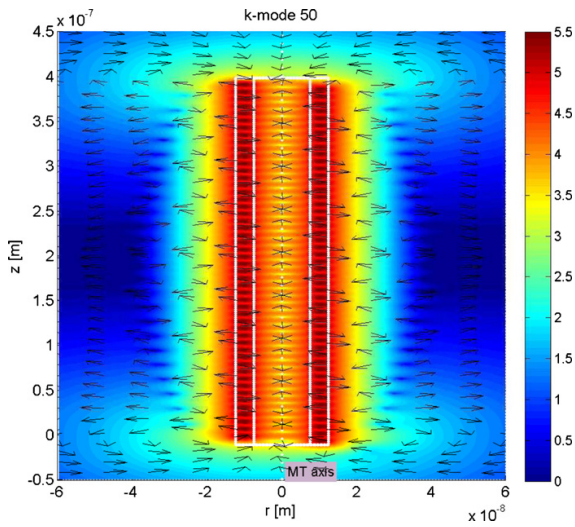
Fig. 14. Electric field distribution around MT of mode 50, zoomed in radial axis. Color coded electric field magnitude is in log scale ($\log(V/m)$). Arrows represent electric field vector.

At the close distance from the MT, for certain regions, there is a specific k-mode which has highest intensity, see Figs. 15 and 16. We see that different k-modes manifest different rate of decrease of intensity with increasing distance radially from MT wall. This resembles multipolar behavior of intensity dependence on distance: higher the multipole degree (k-mode number of MT vibrations) steeper the decrease of intensity from the multipolar source.

Following this line of thought, it is interesting to observe the profile of the intensity for various distances r from the microtubule. In Figs. 17, 18 and 19 we provide the profiles of intensity parallel to MT axis for k-mode 2, 5 and 50, respectively.

4. Discussion

First the frequency dependence will be discussed. For the frequencies up to high THz region, we can work with the microtubule generated field as near field in the distances we treat here (up
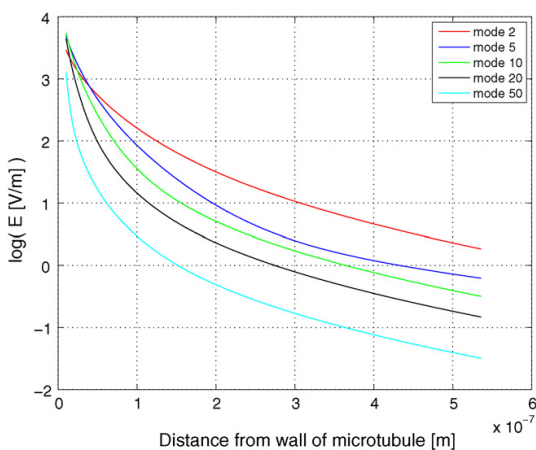

Fig. 15. Electric field intensity radial dependence from the wall of microtubule for the k-modes 2, 5, 10, 20 and 50. From the end of MT ($z = 400$ nm).
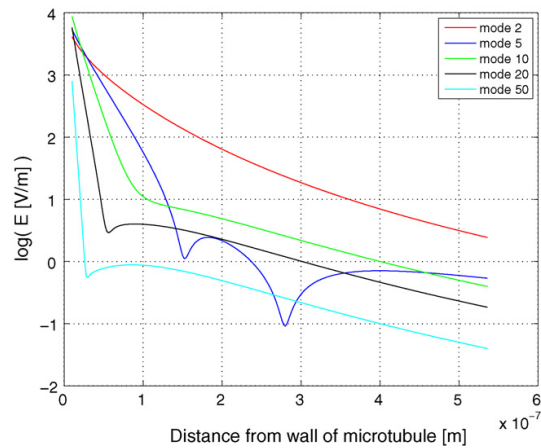

Fig. 16. Electric field intensity radial dependence from the wall of microtubule for the k-modes 2, 5, 10, 20 and 50. From the middle of MT ($z = 200$ nm).
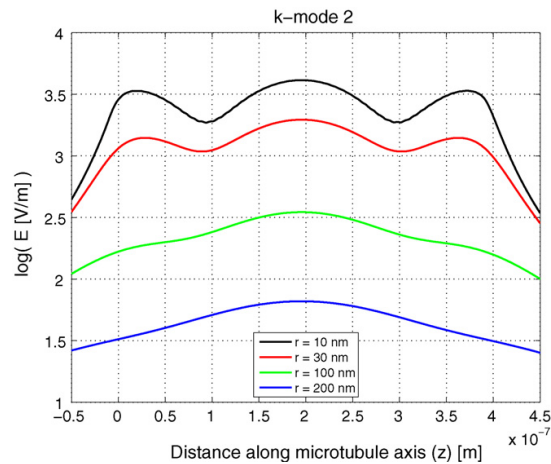

Fig. 17. Electric field intensity along the lines parallel to microtubule axis at the distance r from microtubule wall, mode 2. Microtubule is located from $z = 0$ to 400 nm.

to 1 μm from MT). So there is basically no difference in the field geometry for various frequencies.[7] With changing frequency the magnitude of the intensity may change due to permittivity and conductivity relaxations. Increasing frequency has an effect on effective current created by dipole oscillations ($Id = \omega p$), so the generated intensity would be higher if the amplitude of the vibrations does not decrease.

Discussing dipole moment separately; the generated intensity increases linearly with increasing dipole moment p magnitude. Amount of power in MT vibrations will influence effective value of dipole moment oscillating component p_a. Effective oscillating dipole moment would be increased if more power is supplied into the vibrations. If the amount of the oscillating charge is fixed,

---

[7] Actually, there would be frequency dependence of the field geometry since wavenumber of vibration modes is bound to frequency of oscillations by dispersion relations. However, in the case of optical branch of longitudinal oscillations the dispersion relation is rather flat, i.e. the function of frequency on wavenumber is almost constant.
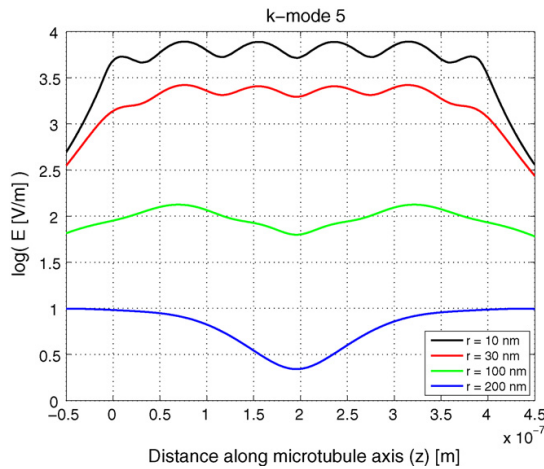
Fig. 18. Electric field intensity along the lines parallel to microtubule axis at the distance *r* radially from microtubule axis, mode 5. Microtubule is located from $z = 0$ to 400 nm.

increased dipole moment would correspond to the greater oscillating distance. However, for different frequencies, there is different amount of charge available for oscillations, given by the mobility of charge.

In a special case of strong energy condensation in certain microtubule vibration modes, electric field generated at certain frequency could be higher by several orders of magnitude and could exert force at the correspondingly greater distance. This kind of phenomenon may be transient only. Nevertheless, it may be involved in cellular interactions, if not by force interaction then by information transfer.

Only optical branches of vibrations can contribute significantly to electric field generation since in these kind of modes neighbor particles (monomers of tubulin) oscillate against each other. Actually, transverse (Kittel, 1976) and longitudinal (Berreman, 1963) optical modes in ionic crystals are responsible for electromagnetic field absorption. We can see the reciprocity of electromagnetic field
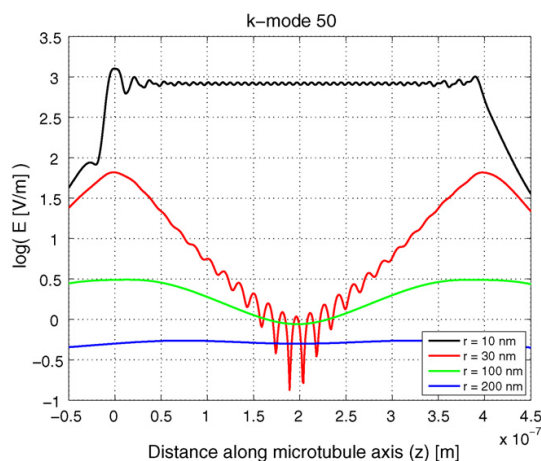

Fig. 19. Electric field intensity along the lines parallel to microtubule axis at the distance *r* from microtubule, mode 50. Microtubule is located from $z = 0$ to 400 nm. The slight asymmetry seen at the $r = 10$ nm is due to protofilament shift.

absorption and generation in these processes. Acoustic longitudinal branch could also effectively contribute to the electric field generation in the MT near the limit of the Brillouin zone, where the k vector is already large (vibration wavelength short) so that particles in the lattice oscillate against each other.

Microtubule associated proteins (MAPs) may also influence MT vibrations acting like a nodes imposing minimum of vibration amplitude (adding the mass to the binding point). This will influence generated field geometry, frequency of vibrations and the transfer of vibrations to other structures bound to the other end of MAPs.

In case of excitation of higher vibration modes, there will be regions of electric field with spatially oscillating direction of electric field vector. The dense distribution of regions with opposite field vector direction renders a problem for direct measurement of electric oscillations. Point detector needs to be used to resolve spatial regions of opposite direction of electric field vector.

We also studied the impact of the MT model with real lattice (protofilaments shifted to each other), which corresponds to realistic model of MT lattice compared to nonshifted models of MT (see supplementary material). For the low mode numbers ($n < N/2$), where *N* is the number of tubulin heterodimers in the MT, there was a small difference in the electric field around MT between the model with protofilaments (lattice) shifted and not shifted. However, the differences become significant for the growing mode number. The break in the symmetry introduced by protofilament shift changes the field geometry. The difference between the models with shifted and not shifted lattice are most pronounced for the higher mode number ($n > N/2$).

Vibrations of microtubules or of other electrically polar cellular structures may be the underlying mechanism generating the electric oscillations which were observed around living cells in kHz to MHz region (Pohl et al., 1981; Phillips et al., 1987; Hölzel, 2001; Pokorný et al., 2001; Jelínek et al., 2009).

We calculated and compared behavior of the electric field generated by random and coherent oscillations of microtubules. While random oscillations occur naturally without any special assumptions, the process where coherence of oscillations arise needs to be touched. Fröhlich's theory (Fröhlich, 1968a,b, 1980) describes a system of oscillators with energy supply, linear and nonlinear coupling with heat bath. If sufficient energy supply is provided to this system, condensation of energy occurs in lowest mode leading to its coherent excitation. Thus, coherent oscillations in microtubules described in this paper can be based on Fröhlich's theory. Numerous works have been inspired by Fröhlich's theory, for review see, e.g. Pokorný and Wu (1998), Hyland and Rowlands (2006) and Cifra (2009). Recently, Reimers et al. (2009) and McKemmish et al. (2009) presented analysis of Penrose–Hameroff orchestrated objective reduction (Orch OR) model of brain activity (Penrose and Hameroff, 1995; Hameroff, 1998; Hagan et al., 2002) with conclusion, that the model is founded on incorrect assumptions, in particular on Fröhlich's coherence, the essential requirement for Orch OR function. McKemmish et al. (2009) claimed that Fröhlich's coherence time is not long enough and that biochemical energy is too small to facilitate coherent condensation which follows from analysis in McKemmish et al. (2009). However, as described closer in comment by Pokorný (submitted for publication), authors of (McKemmish et al., 2009; Reimers et al., 2009) did not take into account the main sources of energy in the cell ("wasted" energy from mitochondria – see Section 1.2 this paper) and the fact that coherence may be strongly raised by

1. Weak damping due to organization of water (Fuchs et al., 2007, 2008, 2009; Giuliani et al., 2009) in strong static electric field around mitochondria (Tyner et al., 2007).

2. Interactions between individual Fröhlich's systems (Pokorný, submitted for publication).
3. Higher order nonlinear terms (Pokorný, 1982; Pokorný et al., 1986a,b).

If Fröhlich's theory of coherent excitations is reconsidered in the light of the facts in comment of Pokorný (submitted for publication), the disclaim of the Orch OR proposal of the brain function by Reimers et al. (2009) on the basis of insufficient coherence (McKemmish et al., 2009) does not seem to be justified.

5. Conclusions

Based on previous works (Pokorný and Wu, 1998; Pokorný, 1999; Pokorný et al., 1997, 1998; Havelka and Cifra, 2009a; Havelka, 2008), we have analyzed electric oscillations excited by vibrations of microtubule. Our model corresponds to optical branches of longitudinal vibrations.

The coherent vibrations of MT generate greater electric field in greater distance than random vibrations.

It was also found that the lattice shift of protofilaments has increasingly significant influence on the field geometry for the lattice vibration modes which wavelength is shorter than two tubulin heterodimer dipoles. This suggests necessity to model higher vibrations modes taking into account lattice shift, which is the real case.

More realistic oscillatory component of dipole moment based on experimental values of static dipole moment and amplitude of mechanical vibrations has been estimated than in previous works (Pokorný, 1999; Havelka and Cifra, 2009a).[8] Using more realistic dipole moments electric field intensity around microtubules is about two orders of magnitude lower than calculated in previous works (Pokorný and Wu, 1998; Pokorný, 1999; Pokorný et al., 1997, 1998; Havelka and Cifra, 2009a; Havelka, 2008). Nevertheless, the electric field generated by microtubules may contribute to self-organization of biological processes also under these conditions.

Acknowledgments

Appendix A. Supplementary data

Supplementary data associated with this article can be found, in the online version, at doi:10.1016/j.biosystems.2010.02.007.

References

Adair, R.K., 2002. Vibrational resonances in biological systems at microwave frequencies. Biophysical Journal 82 (3), 1147–1152.
Alberts, B., Johnson, A., Lewis, J., Raff, M., Roberts, K., Walter, P., 2008. Molecular Biology of the Cell, 5th ed. Garland.
Amos, L.A., 1995. The microtubule lattice—20 years on. Trends in Cell Biology 5 (2), 48–51, http://www.sciencedirect.com/science/article/B6TCX-40W0TW4-H/2/f5be870ff70ffdc4a7f9a3f39e0b525a.
Asami, K., Hanai, T., Koizumi, N., 1976. Dielectric properties of yeast cells. Journal of Membrane Biology 28, 169–180.
Asami, K., Yonezawa, T., 1996. Dielectric behavior of wild-type yeast and vacuole-deficient mutant over a frequency range of 10 kHz to 10 GHz. Biophysical Jour-

nal 71 (4), 2192–2200, http://www.sciencedirect.com/science/article/B94RW-4V8X9KV-1T/2/e7bf9e4fe3509087f10582c611c6ec1b.
Berreman, D.W., 1963. Infrared absorption at longitudinal optic frequency in cubic crystal films. Physical Review 130 (June (6)), 2193–2198.
Caplow, M., 1995. Correction. Journal of Cell Biology 129 (2), 549, http://jcb.rupress.org.
Caplow, M., Ruhlen, R.L., Shanks, J., 1994. The free energy for hydrolysis of a microtubule-bound nucleotide triphosphate is near zero: all of the free energy for hydrolysis is stored in the microtubule lattice. The Journal of Cell Biology 127, 779–788.
Caplow, M., Shanks, J., 1996. Evidence that a single monolayer tubulin-GTP cap is both necessary and sufficient to stabilize microtubules. Molecular Biology of the Cell 7 (4), 663–675, http://www.molbiolcell.org/cgi/content/abstract/7/4/663.
Cifra, M., 2009. Study of electromagnetic oscillations of yeast cells in kHz and GHz region. Ph.D. Thesis. Czech Technical University in Prague.
Del Giudice, E., De Ninno, A., Fleischmann, M., Mengoli, G., Milani, M., Talpo, G., Vitiello, G., 2005. Coherent quantum electrodynamics in living matter. Electromagnetic Biology and Medicine 24 (3), 199–210.
Del Giudice, E., Preparata, G., Fleischmann, M., 2000. QED coherence and electrolyte solutions. Journal of Electroanalytical Chemistry 482 (2), 110–116, http://www.sciencedirect.com/science/article/B6TGB-400WXYC-3/2/a246a1ffc5921c67c65c4a9ac6f0f8e2.
Foster, K.R., Baish, J.W., 2000. Viscous damping of vibrations in microtubules. Journal of Biological Physics 26 (4), 255–260.
Fröhlich, H., 1968a. Bose condensation of strongly excited longitudinal electric modes. Physical Letters A 26, 203–402.
Fröhlich, H., 1968b. Long-range coherence and energy storage in biological systems. International Journal of Quantum Chemistry 2, 641–649.
Fröhlich, H., 1980. The biological effects of microwaves and related questions. Advances in Electronics and Electron Physics 53, 85–152.
Fuchs, E.C., Bitschnau, B., Woisetschlager, J., Maier, E., Beuneu, B., Teixeira, J., 2009. Neutron scattering of a floating heavy water bridge. Journal of Physics D: Applied Physics 42 (6), 065502, 4 pp., http://stacks.iop.org/0022-3727/42/065502.
Fuchs, E.C., Gatterer, K., Holler, G., Woisetschlager, J., 2008. Dynamics of the floating water bridge. Journal of Physics D: Applied Physics 41 (18), 185502, 5 pp., http://stacks.iop.org/0022-3727/41/185502.
Fuchs, E.C., Woisetschlager, J., Gatterer, K., Maier, E., Pecnik, R., Holler, G., Eisenkolbl, H., 2007. The floating water bridge. Journal of Physics D: Applied Physics 40 (19), 6112–6114, http://stacks.iop.org/0022-3727/40/6112.
Giuliani, L., D'Emilia, E., Lisi, A., Grimaldi, S.,Foletti, A., Giudice, E.D., 2009. The floating water bridge under strong electric potential. Neural Network World 19 (4), 393–398.
Hagan, S., Hameroff, S.R., Tuszyński, J.A., 2002. Quantum computation in brain microtubules: decoherence and biological feasibility. Physical Review E 65 (June (6)), 061901.
Hameroff, S., 1998. Quantum computation in brain microtubules? The Penrose–Hameroff "Orch OR" model of consciousness. Philosophical Transactions Royal Society London (A) 356, 1869–1896.
Havelka, D., 2008. Electromagnetic field of microtubule (Elektromagnetické pole mikrotubulu). Bachelor Thesis (in Czech).
Havelka, D., Cifra, M., 2009a. Calculation of the electromagnetic field around microtubule. In: POSTER 2009, Prague.
Havelka, D., Cifra, M., 2009b. Calculation of the electromagnetic field around microtubule. Acta Polytechnica 49, 58–63.
Hölzel, R., 2001. Electric activity of non-excitable biological cells at radiofrequencies. Electro- and Magnetobiology 20 (1), 1–13.
Hyland, G.J., Rowlands, P. (Eds.), 2006. Herbert Fröhlich, FRS, A Physicist Ahead of His Time: A Centennial Celebration of His Life and Work. University of Liverpool.
Janmey, P., Euteneuer, U., Traub, P., Schliwa, M., 1991. Viscoelastic properties of vimentin compared with other filamentous biopolymer networks. Journal of Cell Biology 113 (1), 155–160, http://jcb.rupress.org/cgi/content/abstract/113/1/155.
Jelínek, F., Cifra, M., Pokorný, J., Hašek, J., Vaniš, J., Šimša, J., Frýdlová, I., 2009. Measurement of electrical oscillations and mechanical vibrations of yeast cells membrane around 1 kHz. Electromagnetic Biology and Medicine 28 (2), 223–232.
Kamimura, S., Kamiya, R., 1989. High-frequency nanometre-scale vibration in 'quiescent' flagellar axonemes. Nature 340, 476–478.
Kamimura, S., Kamiya, R., 1992. High-frequency vibration in flagellar axonemes with amplitudes reflecting the size of tubulin. Journal of Cell Biology 116 (6), 1443–1454, http://jcb.rupress.org/cgi/content/abstract/116/6/1443.
Kasas, S., Cibert, C., Kis, A., De Los Rios, P., Riederer, B.M., Forró, L., Dietler, G., Catsicas, S., 2004. Oscillation modes of microtubules. Biology of the Cell 96 (9), 697–700, http://www.biolcell.org/boc/096/boc0960697.htm.
Kawaguchi, K., Ishiwata, S., 2000. Temperature dependence of force, velocity, and processivity of single kinesin molecules. Biochemical and Biophysical Research Communications 272, 895–899.
Kawaguchi, K., Ishiwata, S., 2001. Thermal activation of single kinesin molecules with temperature pulse microscopy. Cell Motility and the Cytoskeleton 49, 41–47.
Kikkawa, M., Ishikawa, T., Nakata, T., Wakabayashi, T., Hirokawa, N., 1994. Direct visualization of the microtubule lattice seam both in vitro and in vivo. Journal of Cell Biology 127 (6), 1965–1971, http://jcb.rupress.org/cgi/content/abstract/127/6/1965.
King, S.M., Hyams, J.S., 1982. The mitotic spindle of *Saccharomyces cerevisiae*: assembly, structure and function. Micron 13 (2), 93–117.

---

[8] Previously, Pokorný has estimated oscillatory tubulin dipole moment at 100 MHz as $p = e \cdot d$, where e is elementary charge and d length of tubulin heterodimer (8 nm). It yields the value of $p = 1.48.10^{-27}$ C m $\simeq$ 500 D, the value of the static dipole moment. In our previous work, we have only taken the value of the total static dipole moment ∼1000 D.

Kis, A., Kasas, S., Babić, B., Kulik, A.J., Benoît, W., Briggs, G.A.D., Schönenberger, C., Catsicas, S., Forró, L., 2002. Nanomechanics of microtubules. Physical Review Letters 89 (November (24)), 248101.

Kittel, C., 1976. Introduction to Solid State Physics. John Wiley & Sons.

Lamprecht, I., 1980. Biological Microcalorimetry. Academic Press, London, pp. 43–112, Ch. Growth and metabolism in yeasts.

McKemmish, L.K., Reimers, J.R., McKenzie, R.H., Mark, A.E., Hush, N.S., 2009. Penrose–Hameroff orchestrated objective-reduction proposal for human consciousness is not biologically feasible. Physical Review E 80 (August (2)), 021912.

Mershin, A., Kolomenski, A.A., Schuessler, H.A., Nanopoulos, D.V., 2004. Tubulin dipole moment, dielectric constant and quantum behavior: computer simulations, experimental results and suggestions. Biosystems 77 (1–3), 73–85, http://www.sciencedirect.com/science/article/B6T2K-4D09KY2-1/2/0b813d32c7adf9dae706f11bae08a24d.

Novotný, K., 1997. Theory of Electromagnetic Field II (Teorie elektromagnetického pole II). Czech Technical University (in Czech).

Pelling, A.E., Sehati, S., Gralla, E.B., Gimzewski, J.K., 2005. Time dependence of the frequency and amplitude of the local nanomechanical motion of yeast. Nanomedicine: Nanotechnol. Biol. Med. 1, 178–183.

Pelling, A.E., Sehati, S., Gralla, E.B., Valentine, J.S., Gimzewski, J.K., 2004. Local nanomechanical motion of the cell wall of *Saccharomyces cerevisiae*. Science 305, 1147–1150.

Penrose, R., Hameroff, S., 1995. What 'gaps'? Reply to Grush and Churchland. Journal of Consciousness Studies 2 (2), 99–112.

Phillips, W., Pohl, H.A., Pollock, J., 1987. Evidence for a.c. fields produced by mammalian cells. Bioelectrochemistry and Bioenergetics 17 (2), 287–296, http://www.sciencedirect.com/science/article/B6TF7-458P435-TG/2/5809a327df3adccc35fa95b7735111ac.

Pohl, H.A., Braden, T., Robinson, S., Piclardi, J., Pohl, D.G., 1981. Life cycle alterations of the micro-dielectrophoretic effects of cells. Journal of Biological Physics 9, 133–154.

Pokomý, J., submitted for publication. Comment on "Penrose–Hameroff orchestrated objective reduction proposal for human consciousness is not biologically feasible". Physical Review E.

Pokorný, J., 1982. Multiple Fröhlich coherent states in biological systems: Computer simulation. Journal of Theoretical Biology 98 (1), 21–27, http://www.sciencedirect.com/science/article/B6WMD-4F1SV94-B8/2/7d7739d7ed9cf26914a7530e2fadeb46.

Pokorný, J., 1999. Conditions for coherent vibrations in cytoskeleton. Bioelectrochemistry and Bioenergetics 48 (2), 267–271.

Pokorný, J., 2003. Viscous effects on polar vibrations in microtubules. Electromagnetic Biology and Medicine 22 (1), 15–29.

Pokorný, J., 2004. Excitation of vibration in microtubules in living cells. Bioelectrochemistry 63 (1–2), 321–326.

Pokorný, J., 2005. Viscous effects on polar vibrations microtubules. In: URSI GA Delhi Proceedings.

Pokorný, J., Hašek, J., Jelínek, F., Šaroch, J., Palán, B., 2001. Electromagnetic activity of yeast cells in the M phase. Electro- and Magnetobiology 20 (1), 371–396.

Pokorný, J., Jelínek, F., Trkal, V., 1998. Electric field around microtubules. Bioelectrochemistry and Bioenergetics 48, 267–271.

Pokorný, J., Jelínek, F., Trkal, V., Lamprecht, I., Hölzel, R., 1997. Vibrations in microtubules. Journal of Biological Physics 23, 171–179.

Pokorný, J., Vacek, K., Fiala, J., 1986a. The Fröhlich kinetic equation with additional terms. Czechoslovak Journal of Physics 38 (12), 1443–1450.

Pokorný, J., Vacek, K., Fiala, J., 1986b. Multiple quantum terms in the Fröhlich kinetic equation. Physics Letters A 114 (6), 339–340, http://www.sciencedirect.com/science/article/B6TVM-46VPYF1-15/2/8a320aefb478319b232d09f89dc4c1a6.

Pokorný, J., Wu, T.-M., 1998. Biophysical Aspects of Coherence and Biological Order. Academia/Springer, Praha, Czech Republic/Berlin, Heidelberg and New York.

Portet, S., Tuszyñski, J.A., Hogue, C.W.V., Dixon, J.M., 2005. Elastic vibrations in seamless microtubules. European Biophysics Journal 34 (7), 912–920, http://www.springerlink.com/content/k23641006n0v27gg.

Preparata, G., 1995. QED Coherence in Matter. World Scientific, New Jersey/London/Hong Kong.

Qian, X.S., Zhang, J.Q., Ru, C.Q., 2007. Wave propagation in orthotropic microtubules. Journal of Applied Physics 101 (8), 084702, http://link.aip.org/link/?JAP/101/084702/1.

Reimers, J.R., McKemmish, L.K., McKenzie, R.H., Mark, A.E., Hush, N.S., 2009. Weak, strong, and coherent regimes of Fröhlich condensation and their applications to terahertz medicine and quantum consciousness. Proceedings of the National Academy of Sciences of the United States of America 106 (11), 4219–4224, http://www.pnas.org/content/106/11/4219.abstract.

Sakakibara, H.M., Kunioka, Y., Yamada, T., Kamimura, S., 2004. Diameter oscillation of axonemes in sea-urchin sperm flagella. Biophysical Journal 86 (1), 346–352.

Sato, M., Schwartz, W., Selden, S., Pollard, T., 1988. Mechanical properties of brain tubulin and microtubules. Journal of Cell Biology 106 (4), 1205–1211, http://jcb.rupress.org/cgi/content/abstract/106/4/1205.

Sirenko, Y.M., Stroscio, M.A., Kim, K.W., 1996. Elastic vibrations of microtubules in a fluid. Physical Review E 53 (January (1)), 1003–1010.

Sobel, S.G., 1997. Mini review: Mitosis and the spindle pole body in *Saccharomyces cerevisiae*. The Journal of Experimental Zoology 277 (2), 120–138.

Song, Y., Mandelkow, E., 1995. The anatomy of flagellar microtubules: polarity, seam, junctions, and lattice. Journal of Cell Biology 128 (1), 81–94, http://jcb.rupress.org/cgi/content/abstract/128/1/81.

Song, Y.H., Mandelkow, E., 1993. Recombinant kinesin motor domain binds to beta-tubulin and decorates microtubules with a B surface lattice. Proceedings of the National Academy of Sciences of the United States of America 90 (5), 1671–1675, http://www.pnas.org/content/90/5/1671.abstract.

Tuszyński, J.A., Brown, J.A., Carpenter, E.J., Crawford, E., Nip, M.N.A., 2002. Electrostatic properties of tubulin and microtubules. In: Proceedings of ESA Conference, June 2002.

Tuszyński, J.A., Luchko, T., Portet, S., Dixon, J.M., 2005. Anisotropic elastic properties of microtubules. The European Physical Journal E 17 (May (1)), 29–35, http://dx.doi.org/10.1140/epje/i2004-10102-5.

Tyner, K.M., Kopelman, R., Philbert, M.A., 2007. "Nano-sized voltmeter" enables cellular-wide electric field mapping. Biophysical Journal 93, 1163–1174.

Wang, C., Ru, C., Mioduchowski, A., 2006. Vibration of microtubules as orthotropic elastic shells. Physica E: Low-dimensional Systems and Nanostructures 35 (1), 48–56, http://www.sciencedirect.com/science/article/B6VMT-4KJTNT4-2/2/c937e65ac2d9b1c7e4f0449b66f544b0.

Wang, C., Zhang, L., 2008. Circumferential vibration of microtubules with long axial wavelength. Journal of Biomechanics 41 (9), 1892–1896, http://www.sciencedirect.com/science/article/B6T82-4SN8VB1-3/2/b00ae1dc96171994c60cd3b63102c416.

Winey, M., Mamay, C., O'Toole, E., Mastronarde, D., Giddings, T.H.J., McDonald, K., McIntosh, J., 1995. Three-dimensional ultrastructural analysis of the *Saccharomyces cerevisiae* mitotic spindle. Journal of Cell Biology 129 (6), 1601–1615, http://jcb.rupress.org/cgi/content/abstract/129/6/1601.

Zhadin, M., Barnes, F., Giuliani, L., 2007. Response to "a few remarks on 'combined action of dc and ac magnetic fields on ion motion in macromolecules'" by Binhi. Bioelectromagnetics 28 (5), 412–413.

Zhadin, M., Giuliani, L., 2006. Some problems in modern bioelectromagnetics. Electromagnetic Biology and Medicine 25 (4), 227–243.

B | Mechano-electrical vibrations of microtubules—Link to subcellular morphology

This appendix is a version of:

Author contributions:

| Designed research: O.K

| Performed research: **D.H.**

| Wrote the paper: O.K.

| Candidate's contribution: 35%

The manuscript carries the following acknowledgements:

Mechano-electrical vibrations of microtubules—Link to subcellular morphology

Ondřej Kučera [a,b,*], Daniel Havelka [a,c]

[a] *Institute of Photonics and Electronics, Academy of Sciences of the Czech Republic, Chaberská 57, 182 51 Prague, Czechia*
[b] *Department of Circuit Theory, Faculty of Electrical Engineering, Czech Technical University in Prague, Technická 2, 166 27 Prague, Czechia*
[c] *Department of Electromagnetic Field, Faculty of Electrical Engineering, Czech Technical University in Prague, Technická 2, 166 27 Prague, Czechia*

ARTICLE INFO

ABSTRACT

Spontaneous mechanical oscillations were predicted and experimentally proven on almost every level of cellular structure. Besides morphogenetic potential of oscillatory mechanical force, oscillations may drive vibrations of electrically polar structures or these structures themselves may oscillate on their own natural frequencies. Vibrations of electric charge will generate oscillating electric field, role of which in morphogenesis is discussed in this paper. This idea is demonstrated *in silico* on the conformation of two growing microtubules.

© 2012 Elsevier Ireland Ltd. All rights reserved.

1. Introduction

In spite of tremendous merit of biochemical approach, our understanding to how does the organism develop and regulate its shape and maintain its functionality is still vague. Thus, while new genetic signalling and regulation pathways are being discovered, underlying mechanism, which maintain biochemical processes extraordinarily organised in time and space, remains unknown. It is, nevertheless, evident that whatever these pathways and background mechanisms are they must result in a force acting on a matter. For that reason, we believe, the issue of morphogenesis is indeed also an issue of physics, as may be supported by works on self-organisation (Karsenti, 2008; Lehn, 2002), although they have not yet exceeded systems of several supramolecules and broader time span. Large scale coherence of biological systems, together with extraordinary variability, suggests itself an action of mechanism with longer rage than that of chemical interactions driven by thermal fluctuations. In following we will hypothesise that oscillating electric field generated by mechanical oscillations of electrically polar structures in cells – particularly microtubules – may play significant role in morphogenesis and physiology.

The reason why do we focus on oscillating electric field instead of electrostatic one is that electrostatics of biomaterials is already well explored and understood (Simonson, 2003). And more importantly, oscillating electric field seems to be more efficient for signal propagation and long range interactions under physiological conditions (Cifra et al., 2010a) because, in contrast to electrostatic field, the screening by ions takes place to lesser extent at higher frequencies.

Spontaneous mechanical oscillations of biocomponents on different levels, to which we devote Section 2, were predicted and experimentally proven. As almost all proteins and protein-composed structures are electrically polar, mechanical oscillations of the charge bound in their structure will generate oscillating electric field. Mechanical oscillations themselves have morphogenetic significance (see Kruse and Riveline, 2011 and Section 3 of this paper) but coupled electric field may potentiate this relevance even more (see Section 4). We demonstrate this idea on the conformation of two microtubules, for which we calculated electric field generated by axial longitudinal vibrations of each micrtotubule. Namely we analyse the intensity of electric field and its possibility to act on molecules under physiological conditions (Section 5). Results presented here expand on our previous work dedicated to microtubule vibrations (Cifra et al., 2010b; Havelka et al., 2011a).

2. Spontaneous mechanical oscillations in cells

In this section, starting with brief introduction to the topic, we review the phenomenon of spontaneous mechanical oscillations in cells on different levels.

Mechanics of biological object – whether it is a protein, organelle, cell, or a tissue – has gained importance since measurement and manipulation of biological samples on the scale of micro and nanometres has became technologically feasible. Besides measurement of passive mechanical properties and question of how do cells actively respond to external mechanical stimuli, there has been a number of reports concerning spontaneous mechanical oscillations in cells, including endogenous nanomechanical motion

---

* Corresponding author at: Institute of Photonics and Electronics, Academy of Sciences of the Czech Republic, Chaberská 57, 182 51 Prague, Czech Republic. Tel.: +420 605581653.

E-mail addresses: kucerao@ufe.cz (O. Kučera), havelka@ufe.cz (D. Havelka).

of the cell wall and membrane, oscillations of molecular motor proteins, or activity of myosin motors. This has been reported especially for cardiomyocytes and auditory hair cells for which oscillations are significant part of their function; however, experimental indication exists that mechanical vibrations may occur also in cells which are considered mechanically inactive and electrically non-excitable; for example yeast cells.

Generally, there are two types of oscillations. On the one hand they are result of an active process which involves transformation of chemical energy (in the form of, e.g. ATP or GDP) into mechanical one by motor proteins. Active oscillations may be attributed to the concept of nonlinear oscillator. In general words, nonlinear oscillator is able to generate spontaneous periodical output under the condition of continuous energy supply. It is important to note that the nonlinear system has the ability of spectral transformation of the energy, which means that the frequencies of generated oscillations do not necessarily need to be present in the supplied flow of energy.[1]

On the other hand, the second type of oscillations which may occur in the cells is connected with linear oscillators. In contrast to nonlinear one, periodic output of linear oscillator manifest only passive response to external feeding. The frequency of passive oscillations must be already present in the input. If the energy source stops to provide feeding at given frequencies, output of the oscillator at these frequencies will die out. From the physical point of view, every molecule or higher passive structure is a mechanical system with particular dynamical properties which may include one or more resonance frequencies. At this frequencies, the system has the maximal response to external stimuli and is able to accumulate energy. This means that the output oscillations may have significantly higher amplitude than those which feed them. Since every object is exposed at least to the thermal noise, this noise will feed oscillations of the object at its resonance frequency.[2] If the system has no resonant behaviour, then it would only transmit the feeding with some attenuation. Besides the noise, there may be a plenty of other sources of feeding of linear oscillator, including also oscillations of other oscillators, especially those which are nonlinear.

For the purpose of clarity, we will call all mechanical oscillations which originate in cells by term *spontaneous* regardless the linearity of the subcellular system they are generated by. This is contrary to the system theory convention (Franklin et al., 1994; Oppenheim et al., 1996), but in such a complex system – like living cell indeed is – it is not always easy to separate passive (linear) and active (nonlinear) oscillators.

In following, we will review spontaneous mechanical oscillations using bottom-up approach, i.e. starting at the level of chemical reactions and continuing up to the scale of whole cells.

2.1. Quantum effects and long-range correlations

Concepts and hypothesises describing generation of mechanical oscillations as a consequence of quantum effects have emerged in the past, but these hypothesises are not generally accepted nowadays. The most influential is probably the Fröhlich's hypothesis (Fröhlich, 1968; Norris and Hyland, 1997). In a nutshell, Fröhlich's hypothesis says that the energy supplied to the biological system can condense in (coherent) modes of longitudinal vibrations as a result of nonlinear interaction between elastic and polarisation fields. Although this hypothesis is far from general acceptance,

even highly sceptical authors admit that energy condensation (at least weak condensate) is biologically feasible to a certain extend (Reimers et al., 2009). Attempts to reconsider Fröhlich's hypothesis have emerged recently (Preto and Pettini, 2012; Sahu et al., in press).

There is also freshly opened question of quantum-coherent coupling of micromechanical oscillators to electromagnetic mode of a cavity (Verhagen et al., 2012) which may involve frequency transformation (Regal and Lehnert, 2011). But its relevance for biological systems was so far not discussed.

2.2. Acoustical emission of chemo-physical processes

It was experimentally shown that chemical events may emit acoustical energy in a wide range of frequencies. First, acoustic emission can be connected with chemo-physical processes like bubble formation, foam rupture or hydrodynamics of the sample. Some of these processes may be occasionally audible under certain conditions. Nevertheless, the frequency band of reported experiments span from ones of Hz up to hundreds of kHz, therefore exceeding the range of human hearing. Secondly, even chemical reactions themselves may be acoustically active in the range of 50 kHz upwards and the emission is usually attributed to phase transitions. However, the methodology of measurement of emitted power was not consistent among published reports, therefore not enabling quantitative comparison. Comprehensive review of this topic may be found in reference WR Boyd and Varley (2001). Nevertheless, acoustical emission of chemo-physical processes was not investigated to our knowledge with the attention to physiological conditions.

2.3. Eigen modes of proteins and supramolecular structures

On the range of molecules, vibration dynamics of proteins is well developed discipline (Frauenfelder et al., 2009). From the mechanical point of view, molecule may be seen as a discontinuous elastic body which may vibrate on its natural frequencies. Compared to smaller and simpler molecules, proteins have relatively low frequency of vibrations, typically in the region of THz.[3] This is because of their structure which involves a large number of atoms (which means higher mass) many of which are connected with weak bonds (e.g. hydrogen bonds) responsible for specific spatial conformation. The frequency of vibrations therefore enables investigation by means of THz and infrared spectroscopy (Barth, 2007). For review see Leitner et al. (2006), Chou (1988) and citations therein.

When proteins are bound together in supramolecules and supramolecular networks, the vibrational frequency of whole structure is accordingly lower. Based on nanomechanical measurement of elastic properties, calculations indicate that vibrations of filamentous supramolecular structures may lay in the kHz to GHz region (Wang and Zhang, 2008a; Samarbakhsh and Tuszynski, 2011). But the issue of damping becomes more important on these scales. Some authors presume that vibrations are overdamped due to viscous damping by cytosol (Foster and Baish, 2000) while others argue that the interfacial effects caused by electrical polarity of proteins may occur, making spontaneous vibrations physically plausible (Cifra et al., 2011; Pokorný et al., 2011a). However, direct experimental evidence is still missing.

---

[1] For example, electrical nonlinear oscillator may generate periodical AC (alternating) signal even if it is fed solely by DC (direct current) source.
[2] Spectrum of the noise is usually very broad so it almost certainly overlaps with the resonance frequency.

[3] It is important to note that on such high frequencies quantum concepts involving phonons are more suitable for description of vibrations.

2.4. Oscillations driven by molecular motors

Besides oscillations generated by accumulation of energy on the natural frequencies of subcellular structures there are also active mechanisms within the cell which may also generate spontaneous mechanical oscillations in the band between fractions of Hz and kHz range (Jülicher and Prost, 1997).

The active generation of mechanical force is connected with molecular motors. Among others, three families of cytoskeletal motors, which are present in eukaryote cell, play important role in cell's motility: kinesins, dyneins (both interacting with microtubules), and myosins (interacting with actin filaments). While single motor is simply walking along microtubule or actin filament, ensembles of motors may exhibit oscillative behaviour. The principle is following: let's consider a system where many motors are connected to a common rigid prop which is elastically coupled to the environment. Collective behaviour of this ensemble involves instability which, under certain conditions, may lead to spontaneous oscillations as a result of hysteresis of force–velocity relation and elastic coupling. For more details see Guérin et al. (2010).

While single motors are used for intracellular transport (cargo is attached to the one end of the motor and the other end of the motor is attached to microtubule or microfilament), collective behaviour of motor ensembles is physiologically employed for motility of higher structures, or even whole cells. Oscillatory motility of undulipodia (motile cilia and eukaryotic flagella) is based on the activity of motor-proteins ensembles contained in axoneme (a structure arranged from microtubules). Oscillations of auditory hair bundle are associated with motor proteins too (myosins in this case), but it also involves feedback loops provided by mechanosensitive ion channels. Further reading may be found in review by Kruse and Jülicher (2005).

2.5. Vibrations of whole cells

Vibrations may also occur on the level of cell wall, cell membrane or even on the scale of whole cell; however, there is usually an underlying mechanism which feeds these vibrations. It may usually be normal mode oscillations, manifestation of vibrations of subcellular parts, activity of motor proteins (Jülicher, 2001) or a combination of these.

Theoretical frequencies of mechanical resonances of bacteria are spread in a wide range of higher kHz up to higher MHz (Zinin et al., 2005). This frequency band may be significantly broader for other types of cells if one considers variability of their size, shape, and mechanical properties. Exposure to ultrasound – sonication – is widely employed for destruction of cells mainly as a result of disruption of cell membrane or disassembly of subcellular components (see for example Hrazdira et al., 1998) due to resonant accumulation of acoustical energy.

Experimental evidence of mechanical oscillations measured *in vivo* on the level of whole cells was reported starting at fractions of Hz (membrane undulations of red blood cells (Gov and Safran, 2005)) and extending to kHz range including oscillations of cardiomyocytes (Domke et al., 1999; Pelling et al., 2007a), oscillations of yeast's cell wall (Pelling et al., 2004a), and otoacoustic emission of hair cells (Hudspeth et al., 2000; Nam and Fettiplace, 2008). Generally, authors attributed these oscillations to a combination of mechanical properties of cells and particular subcellular vibrational process mentioned above.

3. Role of mechanical oscillations in morphogenesis

There is no doubt about the function of oscillations of specialised cells like cardiomyocytes, hair cells or others. The importance of oscillations of specialised sub cellular structures, like axoneme, is well understood too. However, there is a plenty of oscillations on both cellular and sub cellular level which biological relevance (or even generating mechanism) is not clear. This is, for instance, the case of oscillations of yeast's cell wall (Pelling et al., 2004a,b), sub-Hz component of human foreskin fibroblasts pulsations (Pelling et al., 2007b), vibrations of rat pheochromocytoma cells (Piga et al., 2007), or tentative report concerning cancer cells oscillations (He et al., 2008). On the one hand, some authors claim that these oscillations are only manifestation or a side effect of other processes – like the noise of an engine – so they themselves do not have any biological relevance. On the other hand, other authors hypothesised about the importance of these oscillations in biophysical processes.

Possible role of mechanical oscillations during development was speculated by Kruse and Riveline (2011). Authors suggested that cells may probe surrounding mechanical environment by oscillations of stress fibres. Using this mechanism, cells may gain information about elastic and viscous properties of their surroundings and react to these properties by reorganising themselves and by changes in development. Hypothetically, there is also a possibility that acoustic wave propagating along cytoskeletal filaments or cytosol may induce specific pattern of organisation (like the particles arranged in the pattern of standing wave), as may be supported by recent work by Sumino et al. (2012).

Plenty of experimental work revealing response of a cell to mechanical load at the nanoscale has emerged in last years (Charras and Horton, 2002; Silberberg et al., 2008). If we replace external load with vibrations originating in a cell, we may expect some kind of morphological response as well. Martin et al. (2008) have shown that apical constriction is driven by pulsed contractions (in the sub-Hz range), demonstrating that spontaneous mechanical oscillations may results in the changes of morphology. On the other hand, Reed et al. (2009) have reported pulsatile motion of zebrafish embryonic eye (with frequencz of few Hz) due to cardiovascular pressure pulsations. Morphogenetic significance of such a common load is disputable; however, it can not be simply ruled out.

Interestingly, spontaneous mechanical oscillations may bring evidence for Beloussov's hyper-restoration (HR) hypothesis (Beloussov, 2008). HR hypothesis suggest overshoot of cellular response to the stress and postulates its role in mechanical regulation of morphogenesis. Overshot behaviour may lead to instabilities (Taber, 2008) which under specific conditions may generate oscillations, but this issue goes beyond the range of interest of this paper.

As we have shown, the general role of mechanical oscillations in morphogenesis is not yet satisfactory understood, but there are some specific cases proving its morphogenetic significance. Below we discuss another morphogenetic role of mechanical oscillations in cells. If the structures which undergo oscillations are electrically polar, the oscillating electric field in their vicinity may constitute an important part of morphogenetic regulation pathway (Pokorný, 2001; Pokorný et al., 2005b) which itself may act with force on matter or mediate the information transfer. As mechanical signals themselves are more efficient than diffusion-based signalling system (Ingber et al., 1994), they may become even more powerful in combination with interaction through electric field.

4. Electrical oscillations in living matter

Existence of electric field is coupled to electric charge. Almost all proteins are electrically polar[4] and electrostatic properties

---

[4] Electric field changes vibrational spectrum of molecules (vibrational Stark effect) which helps to map internal electric field in proteins (Bublitz and Boxer, 1997; Park et al., 1999).
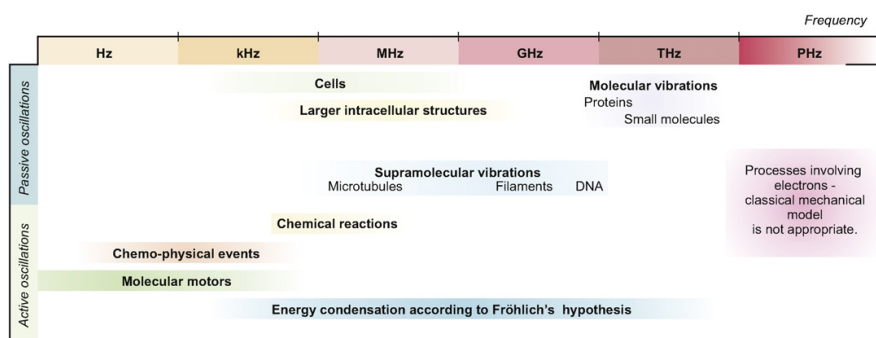
Fig. 1. Schematic position of spontaneous mechanical oscillations in cells within the frequency spectrum. Passive and active oscillations are connected with the concept of linear and nonlinear oscillator, respectively.

of proteins oftentimes play essential role in their function. Interaction between proteins or protein–ligand interactions are often of electrostatic nature because they involve contact between charged or polar groups. Charge transfer or separation is usually involved in local chemical events in proteins (Simonson, 2003) and electrostatics contributes to local mechanical properties and function of proteins (e.g. properties of bacteriorhodopsin; Voïtchovsky et al., 2007). Electrostatic interaction is also important for assembly of supramolecules (e.g. polymerisation of actin; Tang et al., 1997) and electrostatic environment influences reactivity of their subunits (e.g. cysteine reactivity of tubulin; Britto et al., 2002). On the higher level, electrostatics contribute to mechanics of tissues (e.g. compressive modulus of cartillage is strongly influenced by negative charges of proteoglycans; Canal Guterl et al., 2010). For more details on electromechanical coupling in biomaterials see Kalinin et al. (2007).

Below we proceed from electrostatics to oscillating electric field. Oscillating electric component of electromagnetic field may spring from oscillative motion of free or quasi-free electrons, ions, or bounded charge. It may be also radiated by excited electron during its fall to lower energetic level.

Oscillations of electric field caused by flow of ions through ion channels (which may be, among other mechanisms, driven by electric field or mechanical pressure) are well known basis of electrophysiology. There is also *in vivo* evidence for mechanical oscillations of a layer of ions separated by a membrane (Mosbacher et al., 1998). Quantum effects resulting in photon emission or excitation of electrons into conductive band were reported too (Cifra et al., 2011; Sahu et al., in press); however, we will focus solely on oscillating electric field generated by oscillations of bound charge in living matter, particularly microtubules.

4.1. Mechano-electrical oscillations of supramolecular structures

For their electrical polarity, proteins are good candidates for mechano-electrical oscillations. As we have shown in Section 2, there are spontaneous mechanical oscillations of proteins, and probably also protein-composed structures. Moreover, there are other mechanisms described above which are most likely able to drive their vibrations. Therefore we consider it worth asking how the pattern of oscillating electric field will look like and what effect it may have.

Electromechanical coupling is poorly explored on the nanoscale, especially when talking about biomaterials (Kalinin et al., 2007), and mechano-electrical oscillations of supramolecular structures remain relatively unresearched. This fact may be attributed to doubts that arose about their feasibility *in vivo* and, more importantly, the experimental difficulty connected with attempts to prove their existence. To our knowledge, there is no direct experiment regarding mechanical and electrical oscillations of supramolecular structures measured simultaneously or even separately. So we have to rely on computations and deduce from what is known about mechanical, electrical, and energetic circumstances. In what follows, some simplifications will be therefore necessary. Most importantly, we will at first separate dynamics of a supramolecule and its electrical properties, although they are mutually connected because force interaction on the level of atoms is of electromagnetic nature. We find it advantageous for our argumentation, because the plenty of experimental work regarding mechanical oscillations in cells (although not regarding supramolecular structures) is in deep contrast with almost none reports regarding electrical oscillations, although they are coupled with the former.[5]

5. Mechano-electrical vibrations of microtubules

Microtubules (MTs) constitute important part of eukaryotic cytoskeleton. In contrast to the skeleton of a body, cytoskeleton is not only a mechanical support of the cell but also an active network responsible for self-organisation of a cell. MTs are present in a cell most frequently in the form of single cylindrical tubes (inner diameter 17 nm and outer diameter 25 nm) consisting of 13 protofilaments (see Fig. 2). More complicated shapes are also possible; however, the protofilament is their primary building block. Protofilament is assembled from alternating monomers of α-tubulin and β-tubulin (together forming heterodimer of tubulin). The number of MTs in a cell is strongly dependent upon the cell type and the phase of the cell cycle.

What attracts attention to MTs, when talking about mechano-electrical vibrations, are their electrical and mechanical properties. Heterodimer of tubulin is strong electrical multipole with axial component constituing static dipole moment as strong as 1.12×10^{-27} C m (Tuszyński et al., 2005a). MT is therefore highly electrically polar structure. Mechanical properties of MT are extraordinarily anisotropic, which is the reason of extremely large variation of published values of its mechanical moduli (Tuszyński et al., 2005b).

5.1. Origin of MT's vibrations

There is a number of sources of energy which may drive vibrations of MTs. In their detailed analysis, Cifra et al. (2010b) suggest three types of energy sources. First, the energy released from

---

[5] Or, with less physical exactness but according to the way of our argumentation, they are implied by the former.
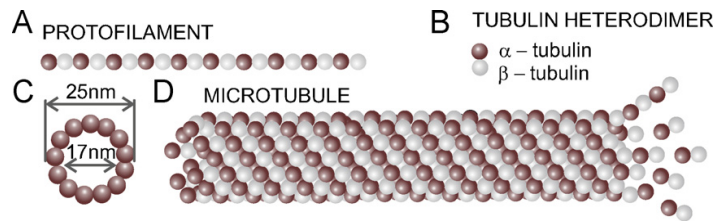
Fig. 2. Schematic depiction of a microtubule, showing one protofilament (A), heterodimer of tubulin, its building block (B), cross-section of microtubule (C), and side view of one microtubule (D) which undergo dynamic instability on its right end.

hydrolysis of GTP (guanosine triphosphate) during polymerisation of MT; secondly, the energy originating in the movement of motor proteins along MT; and thirdly, the "wasted energy" form mitochondria. Here we would like to add kind of fourth, indirect, source of vibrational energy from other sources mentioned in Section 2 of this paper, because this energy may be transmitted through mechanical environment of a cell to MTs.

If the process is linear, or quasi-linear, then MT may be viewed as linear oscillator with two possible regimes of operation. On the one hand, the system may be overdamped (quality factor, $Q < 0.5$) and dissipate energy without resonance. Then the amplitude of vibrations of MT will be lower or theoretically equal to the amplitude of the feeding mechanism. Frequencies of the feeding and MT vibrations will be equal. As a result, MT will behave like transmitter of external vibrations. We may expect that it will behave like a low-pass filter (Boresi et al., 2002; Oppenheim et al., 1996). This means that only frequencies between zero and so called cut-off frequency will be transmitted. On the second hand, the system may be underdamped (quality factor, $Q > 0.5$) and exhibit resonant behaviour. Then it would selectively accumulate energy on its resonance frequencies. The source of energy then does not necessarily need to have purely vibrational character, but it just need to have frequency spectrum wide enough to overlap with resonance frequency. MT will thus behave like resonator. As we already mentioned in Section 2.2, the issue of damping is crucial for vibrations of supramolecules. Foster and Baish (2000) and Adair (2002) argued that vibrations of supramolecular structures are overdamped by cytosol. This claim excludes resonant behaviour of MT; however, its function like an attenuating transmitter is not affected. If interfacial effects take place (Cifra et al., 2011; Pokorný et al., 2011a), then vibrations may become underdamped.

In fact, MT is not object which may be represented by lumped element model of oscillator. It is a body with a number of vibrational modes. However, the analogy with oscillator is suitable for each mode of vibrations. Many theoretical models of how does the MT transmit and accumulate vibrational energy were published. Here we do not go to details – interested readers may find detailed information in references Sirenko et al. (1996), Pokorný et al. (1997), Portet et al. (2005), Kasas et al. (2004), Wang et al. (2006, 2009), Wang and Zhang (2008b), Qian et al. (2007), Deriu et al. (2010), Samarbakhsh and Tuszynski (2011).

As may be seen in Fig. 1, vibrational energy exists in a cell in entire frequency spectrum. This energy may be transmitted over and/or accumulated in MT. Generally, the most efficient mechanism of generation of MT vibrations is that which involves resonance. In this particular case, the frequency of driving force is identical or very close to natural frequency of MT. Since MT has a large number of vibration modes and high variability of its length, the range of possible resonance frequencies is very broad. The problem becomes even more complicated if we consider protein complexes coupled to MT and boundary conditions generally. If we accept theoretical range of higher kHz to GHz as a real range of possible resonance modes of MT, then following sources have similar frequencies.

First coupling of passive oscillations of cells body and larger intracellular structures fits to this range. Partial frequency overlap is also achieved for vibrational emission from chemical reactions and entire range is covered by thermal noise and Fröhlich's hypothetical condensation. Possibility also exists that non-vibrational events with broad spectrum may provide energy for driving of natural modes. All other sources very probably do not allow resonant driving. Then the forced vibrations of MT are also possible, but energetic demands become more substantial. An example *par excellence* of such forced vibrations of MT are oscillations driven by motor proteins in axoneme.

However, if the process of generation of vibrations is nonlinear, then such a simple analysis is out of the question. In this case, the generating mechanism must be precisely identified. Otherwise, the variability of parameters to be chosen leads to a vast number of dramatically different solutions. Although some authors speculate about nonlinearity, this idea is almost unexplored with the exception of Fröhlich's condensation. In general words, vibrational energy may be then coupled between modes and different frequencies in such a way that almost each process mention in Fig. 1 will allow efficient driving of MT vibrations. Such a conclusion was also drawn by Cifra et al. (2010b).

Needless to say, excitation of particular vibrational mode depends strongly on the spatial character of feeding mechanism. One may gain opposing results when considering local feeding or excitation by plane wave, etc. In our model below, we do not deal with any specific kind of generating mechanism. We simply assume that the vibrational energy, which is present in the cell, was delivered to particular vibration mode. We are aware that this issue requires thorough analysis in the future, but now it appears to be outside of the scope of this manuscript.

5.2. Electric field generated by vibrations of MT

Mechanical vibrations of MT will be coupled with oscillating electric field. Pioneering estimate of the electric field generated by axial longitudinal vibrations of MT was published by Pokorný et al. (1997). More accurate calculation was performed by Cifra et al. (2010a) using what we suggest to call the Microtubule Resonance Dipole-Network Approximation (MRDNA) method. This method was also used for simulation of power radiated from entire network of MTs (Havelka et al., 2011a).

Detailed description of MRDNA method is given in Cifra et al. (2010a). Here we only briefly summarise its principle and parameters used in calculations. Electric field of each tubulin heterodimer was approximated by elementary electric dipole. This dipole moment is the projection of total electric multipole moment of the tubulin heterodimer into the direction of vibrations. Since amplitude of vibrations is smaller than the length of the dipole, only a part of total dipole moment will contribute to oscillations. In our model we used one eighth of total dipole moment. Resulting oscillating dipole moment is modulated according to the local direction of vibrations of the MT. The electric field of whole MT or MTs'
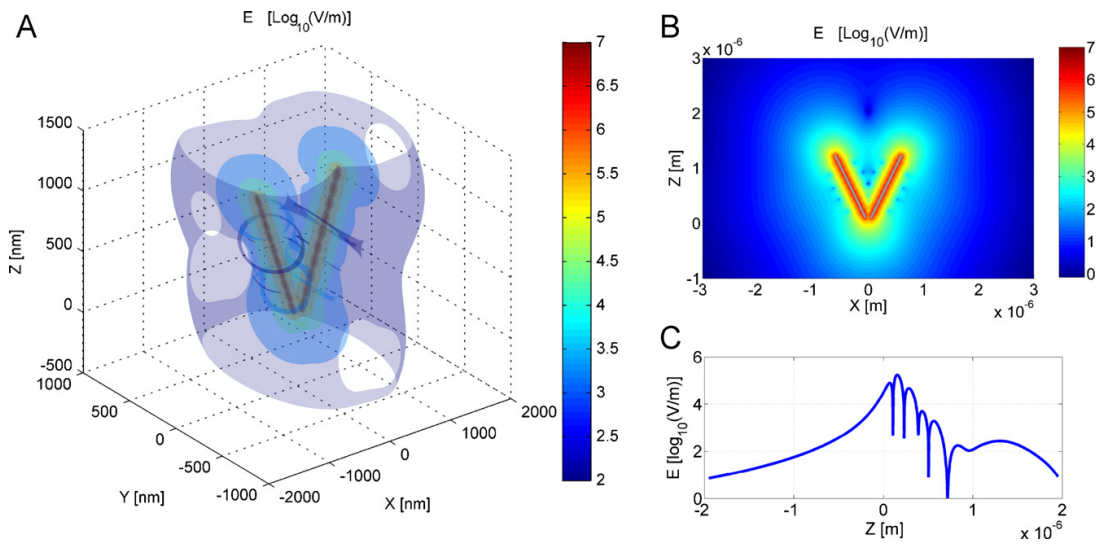
Fig. 3. Results of the calculation of electric field generated by vibrations of two equally long MTs vibrating in phase. Isosurface of the intensity of electric field (A) evince local minima with the shape of a ring. Section through the field in the plane which contains axes of both MTs is shown in part (B) and (C) shows detailed shape of the intensity of electric field along vertical axis of section (B).
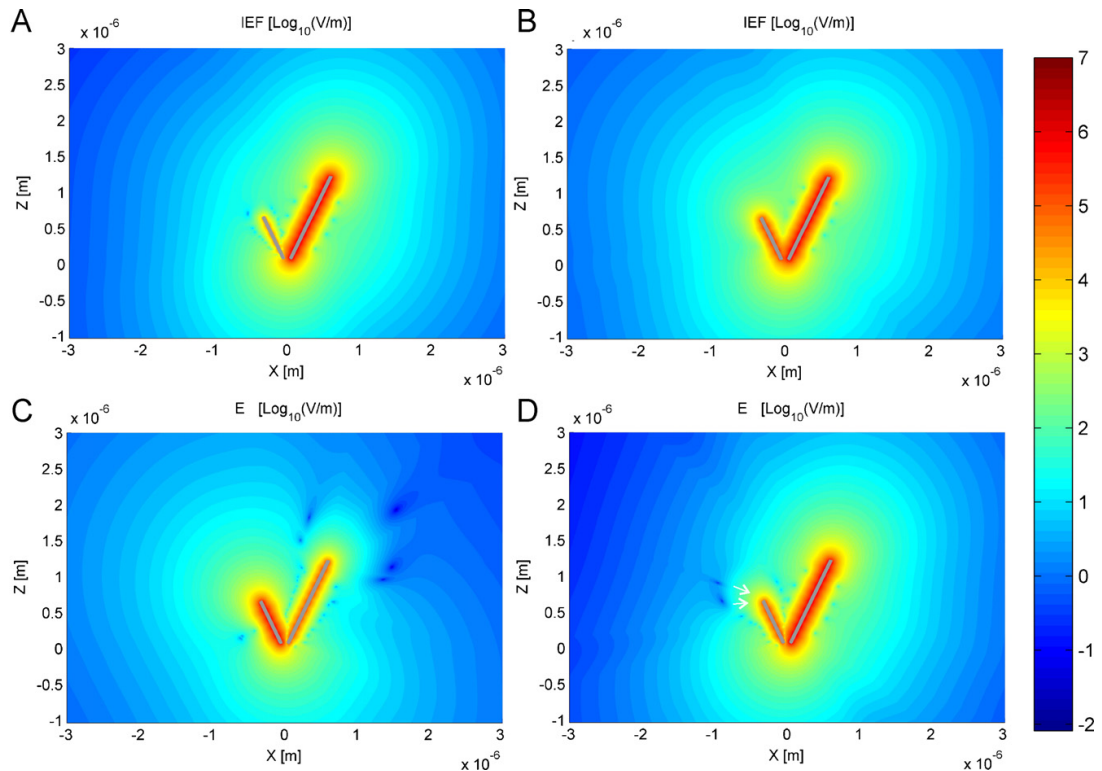

Fig. 4. Electric field generated by $\pi/2$ radians shifted vibrations of two MTs of different length. Parts (A–D) depicts the intensity of electric field in the plane which contains axes of both MTs. Direction of movement of local minima is indicated by arrows in part (D). Time-locks were acquired in the phase of $358°$ (A), $18°$ (B), $276°$ (C), and $348°$ (D) of vibrations of the longer MT.

network is calculated as a vector summation of contributions from all heterodimers. The dipole–dipole interactions are not taken into account.

Here we use MRDNA method to demonstrate electric field which establishes between two vibrating MTs. The V-shape conformation of MTs (angle between their axes was 52°) was chosen in order to resemble two MTs growing from the centrosome. Results with different angle are provided in supplementary material. Two cases were studied. In the first case, both MTs had the same length of 156 heterodimers (1.248 μm). In the second case, one of MTs was shorter (88 heterodimers = 0.624 μm) than the other. Acoustic branch of axial longitudinal vibrations was investigated. Frequency of oscillations was 250 GHz which corresponds to mode number 10 for the longer MT and mode number 5 for the shorter one. Following parameters were used in our calculations. We have chosen MTs lattice B, which means that the shift between protofilaments in MT is 0.92 nm. Relative permittivity of the surrounding medium was $\varepsilon_r = 6.3626$, and conductivity was $\sigma = 72, 52$ S/m (Kaatze and Feldman, 2006). The amplitude of vibrations was 0.1 nm. Concerning the phase of vibrations, we focused on two special cases. The case where vibrations of both MTs are in phase corresponds to common coherent feeding. The other case where the phase of vibrations is shifted for $\pi/2$ radians may be attributed to elastic coupling between MTs.

Results of the calculation are presented in Figs. 3 and 4. Fig. 3 shows the case of equally long MTs. It presents only time-lock of oscillating field. A movie may be found in supplementary material. Isosurface of intensity of electric field generated by equally long MTs is depicted in Fig. 3A. It shows the contour of the field in the space. Section through the field in the plane containing axes of both MTs is presented in Fig. 3B and detailed curve in the vertical axis of the conformation is shown in Fig. 3C. Fig. 4 is dedicated to the case when one MT is shorter. It shows different time-locks of the shape of the field in the plane containing axes of both MTs.

We observed local minima of the intensity of electric field. These minima have shape of a ring in the space (see Fig. 3A). Minima change their position during the period of vibrations. We indicate this movement by arrows in Fig. 4D.

6. Discussion

6.1. Implications for experiments

The very first thought of results presented here naturally leads to the possibility of their experimental verification. As we have already mentioned, no experimental work unifying mechanical and electrical vibrations of supramolecules has been published yet. In the case of electrical oscillations, there have however been reports of resonant interaction of MTs with external oscillating electric field. This indicates the existence of oscillation states in MTs alone (Sahu et al., in press).

Some authors also tried to explain their experimental results obtained on the level of whole cells by vibrations of MTs. Pokorný et al. (2011b) attributed discovered resonant interaction between nonlinear electromagnetic oscillator and tumours to vibrations of MTs. Pokorný et al. (2001) also found correlation between electromagnetic activity of yeast cells and formation of mitotic spindle during M phase of the cell cycle. Pelling et al. (2004b, 2005) demonstrated a local oscillatory nanomechanical motion of the cell wall of yeast cells (frequency was about 1 kHz) and attributed it to concerted activity of motor proteins. Measurement of such oscillations was partially reproduced by Jelínek et al. (2009), who afterwards attempted to measure electric field generated by these vibrations. Jelínek et al. (2009) concluded that there were significant differences of measured power between different phases of the cell

cycle. Janča (2011) analysed this data using neural networks and identified significant frequencies in electrical signal. However, the issue of sensitivity of the measurement system remains unsolved as mechanical and electrical signals were not measured simultaneously. Other results concerning electrical oscillations of living cells and non-thermal effects of electromagnetic irradiation may be attributed to mechano-electrical vibrations of MTs too (Pohl et al., 1981; Grundler and Keilmann, 1983).

Technical aspects of measurement of electrical component of mechano-electrical oscillations in radio-frequency range were analysed by Kučera et al. (2010), but only on the level of whole cells. Limitations for mechanical measurements in range up to tens of kHz were discussed also by Gittes and Schmidt (1998). Combining these experimental prerequisites seems to be rather complicated, because we may expect spontaneous mechano-electrical oscillations to take place only *in vivo* due to presence of appropriate energy feeding[6] and coupling. Then the question is: How to bring the probe inside the cell? Although advances have been made in this direction (Rohrbach et al., 2004; Tian et al., 2010; Duan et al., 2011; Robinson et al., 2012), more realistic at the beginning seems to be measurement from the outside of a cell along recommendations presented in references Kučera et al. (2010), Gittes and Schmidt (1998) (for instance by using some branch of scanning probe microscopy (Kalinin et al., 2007; Gan, 2009; Parot et al., 2007)) with the awareness of unspecificity arising from the high number of intracellular sources of oscillations. Calculations indicate (Havelka et al., 2011b) that electromagnetic power emitted from a cell as a result of vibrations of whole microtubular network is on the level of thermal noise; however, the magnitude of intensity of electric field is still sufficient for detection.

Mechano-electrical oscillations of MT *in vitro* may be obtained by driving of the MT by electric field and measuring the mechanical response and *vice versa*. But to our knowledge, no experiment in this direction has been published yet.

6.2. Implications for morphogenesis

Relevance of electric component of mechano-electrical oscillations of MTs for morphogenesis may be, according to our opinion, reduced to the question of force effects of electric field. These force effects may be employed for the purpose of information transfer or directed motion of the matter.

The role of endogenous electromagnetic forces in transfer of reaction components was discussed by Pokorný (2001). He distinguishes three different stages of chemical reactions: translation of reaction components to the region where the reaction takes place; short range motion of components in order to adjust appropriate space position; and the formation of chemical bonds. We will analyze this force effects on the case of tubulin dimer. The idea behind this choice is that oscillating electric field may govern transport of tubulin dimers towards the plus-end of growing MT.

The model we used has shown that directional transport of single tubulin dimers by generated electric field does not seem to be efficient under parameters we considered. The translational force, $\mathbf{F}_d$, acting on the electric dipole of free tubulin dimer (with moment $\mathbf{p} = 1.12 \times 10^{-27}$ C m), $\mathbf{F}_d = \nabla (\mathbf{p} \cdot \mathbf{E})$, reaches its maximum in the order of about 10^{-19} N. Moreover, this maximum is tied together with the position of maximal gradient of intensity of electric field. As may be seen in Fig. 3C, the local maximum of this gradient is located between neighbouring local minima and maxima of the intensity of electric field. As this position is dramatically changing during the period of vibrations, the effective force

---

[6] Remember that energy in chemical form constitute only minor part of possible feedings presented in this paper.

acting on the dipole is even lower. Truly feasible translational effect on tubulin dimer may be observed under these conditions only for resonant interaction. However, recent findings suggest that MT elongation and nucleation involves interactions of short tubulin oligomers rather than dimers (Mozziconacci et al., 2008). The dipole moment is defined as $\mathbf{p} = q\mathbf{d}$, where $\mathbf{d}$ is the displacement vector (with the size of the length of the moment) and q is the charge. When dipole moments are arranged in a line, then the neighbouring charges with opposite sign compensate each other. Only charges on the ends of the oligomer contribute to the resulting dipole moment and the total charge of the oligomer is then equal to the charge of a dimer. But what is changed is the length of the dipole, $\mathbf{d}$, which is lengthened. The resulting force is then proportional to the number of dimers in the oligomer. As we may expect this number to be in the order of ones, then the force, $\mathbf{F}_d$, is still too small to exert efficient translational effect. However, this claim is based on the results of our calculations parameters of which may not entirely correspond to physiological reality. More optimistic results should be expected for different boundary conditions and spatial conformations. This direction should be therefore followed in the future research.

Translational effects may be also caused by dielectrophoretic force, i.e. the force acting on the polarisable dielectric particle in the inhomogeneous electric field. This force is proportional to the volume of the particle (V), the difference between permittivity of the particle (ε_p) and the medium (ε_m), and the gradient of the square of the intensity of electric field, so $\mathbf{F}_\varepsilon \approx sV(\varepsilon_p - \varepsilon_m)\nabla \mathbf{E}^2$. Besides the properties of the field and the particle, the force, $\mathbf{F}_\varepsilon$, is also governed by dielectric properties of the ambient medium. Very important parameter is also the shape of the particle, here expressed by the parameter s. In general words, the larger is the asymmetry of the shape of the particle, the larger is the value of s. Tubulin dimer or oligomer is extraordinarily inhomogeneous material and its dielectric properties were not satisfactorily documented so far. If we adopt elliptical homogenous model inspired by works on viruses (Ermolina et al., 2006; Morgan and Green, 1997), we gain approximately identical results like in the previous case of force $\mathbf{F}_d$. As we mentioned therein, different parameters of the model and resonant interaction may lead to values of average force that is capable to overcome thermal fluctuations. Novel discoveries concerning Brownian motion (Franosch et al., 2011) may also change our view on thermal fluctuations of the particle in the fluid. Influence of deterministic force on this particle can therefore be larger then in recent models involving Stokes drag.

Achievement of appropriate space position of components implies short range motion which is supposed to be of rotational or deformational character rather than translational nature. Electrorotational torque, $\boldsymbol{\tau} = \mathbf{p} \times \mathbf{E}$, will act on the particle with dipole moment in order to align it with the external field. However, electrostatic interaction due to static dipole moment seems to be more efficient at this scale. Oscillating part of the field may, nevertheless, help with achieving of desired position.

The most promising therefore seems to be the influence of oscillating electric field on the charge transfer. Pokorný et al. (2005a,b) analysed transport of electrons in the molecular chains outside the regions of redox potential under the presence of deterministic force. They conclude that electrons may be shifted to the target as far as 20 nm in the time scale under 1 ns (which corresponds to frequency of 1 GHz) with probability almost equal to 1 if the intensity of electric field is 10^6 V m. Maximal values of the intensity of electric field in our calculations are of the same order and they are distributed in the vicinity of the MT. Profound effect of the electric field in regions far from MT is also possible, but it requires longer time to reach the same probability.

Information transport by means of oscillating electric field is possible only under the condition that there is a mechanism capable of detection of this field. Oscillating electric field generated by vibrations of MTs has, according to our model, relatively low magnitude. It is therefore evident, that the efficient and instant information transfer on a large distance (i.e. within a cell) would be possible only for the case of resonant interaction or electron transfer as a detection mechanism.

6.3. Implications for cancerogenesis

Cytoskeleton in cancer cells undergoes disintegration which results in disordered morphology and altered mechanical properties of cancer cells (Suresh, 2007). These changes are not only consequence of cancer process but also significant part of its patophysiology. There is extensive experimental evidence that mechanical properties of metastatic cancer cells significantly differ from that of healthy cells or even non-metastatic cancer cells and that the metastatic potential of a cell is well correlated with its stiffness. All these properties are essential for uncontrolled growth and metastatic proliferation.

From the point of view of mechanics, such a dramatic change in structure and stiffness must be also accompanied with change of dynamic properties, for example frequency of spontaneous oscillations or response to external vibrations.

Pokorný (2009, 2012) developed theory which unifies mechano-electrical vibrations of microtubules with recently revisited role of mitochondrial dysfunction in cancer cells (Warburg effect). Dysfunction of mitochondria implies decline of the zone of the strong static electric field and of the space charge layer of protons around mitochondria. It was shown that this changes are followed by disruption of the level of water ordering. This, together with decreased efflux of the non utilized energy from mitochondria, changes damping of mechano-electrical vibrations of microtubules. This effect was employed in diagnostics by Pokorný et al. (2011b).

Implications of this phenomenon for cancer transformation pathways and cancerogenesis may be following. Increased damping of microtubule vibrations will manifest itself in the drop of amplitude of spontaneous oscillations. The resulting oscillating electric field will be weaker and any effect of this field as well, so the contribution to organisation, information transfer and negative entropy production will be lower which well corresponds with disorganisation of cancer cells.

7. Conclusions

In this paper, we reviewed spontaneous mechanical oscillations in cells and discussed them as a feeding of mechano-electrical vibrations of microtubule. We demonstrated calculations of generated oscillating electric field and we speculated about its role in morphogenesis. The model we used is simplified, and also very special case of physical reality. Our results however, together with recent experimental findings (Sahu et al., in press), indicate that the effect of generated electric field is suitable for mass transport in the case of resonant interaction. The effect on the charge transfer is physically feasible too.

We are far from overestimating the role of mechano-electrical oscillations in cell biology and morphogenesis, but we are convinced that it must be, along with electrostatic and stochastic processes, incorporated into complex scene of intracellular interactions.

Contributions

OK designed the research and wrote the paper and DH performed calculations.

Acknowledgments

Appendix A. Supplementary data

Supplementary data associated with this article can be found, in the online version, at http://dx.doi.org/10.1016/j.biosystems.2012.04.009. Videos showing the time evolution of the intensity of electric field during one period of vibrations are provided. Time-locks of the intensity of electric field for different angles of MTs are provided too.

References

Adair, R.K., 2002. Vibrational resonances in biological systems at microwave frequencies. Biophys. J. 82 (3), 1147–1152.

Barth, A., 2007. Infrared spectroscopy of proteins. Biochim. Biophys. Acta (BBA)-Bioenergetics 1767 (9), 1073–1101.

Beloussov, L., 2008. Mechanically based generative laws of morphogenesis. Phys. Biol. 5, 015009.

Boresi, A., Schmidt, R., Sidebottom, O., 2002. Advanced Mechanics of Materials, 6th ed. Wiley.

Britto, P., Knipling, L., Wolff, J., 2002. The local electrostatic environment determines cysteine reactivity of tubulin. J. Biol. Chem. 277 (32), 29018–29027.

Bublitz, G., Boxer, S., 1997. Stark spectroscopy: applications in chemistry, biology, and materials science. Annu. Rev. Phys. Chem. 48 (1), 213–242.

Canal Guterl, C., Hung, C., Ateshian, G., 2010. Electrostatic and non-electrostatic contributions of proteoglycans to the compressive equilibrium modulus of bovine articular cartilage. J. Biomech. 43 (7), 1343–1350.

Charras, G., Horton, M., 2002. Single cell mechanotransduction and its modulation analyzed by atomic force microscope indentation. Biophys. J. 82 (6), 2970–2981.

Chou, K., 1988. Low-frequency collective motion in biomacromolecules and its biological functions. Biophys. Chem. 30 (1), 3–48.

Cifra, M., Fields, J., Farhadi, A., 2011. Electromagnetic cellular interactions. Prog. Biophys. Mol. Biol. 105 (3), 223–246.

Cifra, M., Pokorny, J., Havelka, D., Kucera, O., 2010a. Electric field generated by axial longitudinal vibration modes of microtubule. BioSystems 100 (2), 122–131.

Cifra, M., Pokorný, J., Havelka, D., Kučera, O., 2010b. Electric field generated by axial longitudinal vibration modes of microtubule. BioSystems 100 (2), 122–131.

Deriu, M.A., Soncini, M., Orsi, M., Patel, M., Essex, J.W., Montevecchi, F.M., Redaelli, A., 2010. Anisotropic elastic network modeling of entire microtubules. Biophys. J. 99 (7), 2190–2199, URL http://www.sciencedirect.com/science/article/B94RW-515K8MN-V/2/b04f67bbda5123dade8927db98c5cb93.

Domke, J., Parak, W., George, M., Gaub, H., Radmacher, M., 1999. Mapping the mechanical pulse of single cardiomyocytes with the atomic force microscope. Eur. Biophys. J. 28 (3), 179–186.

Duan, X., Gao, R., Xie, P., Cohen-Karni, T., Qing, Q., Choe, H., Tian, B., Jiang, X., Lieber, C., 2011. Intracellular recordings of action potentials by an extracellular nanoscale field-effect transistor. Nat. Nanotechnol.

Ermolina, I., Milner, J., Morgan, H., 2006. Dielectrophoretic investigation of plant virus particles: cow pea mosaic virus and tobacco mosaic virus. Electrophoresis 27 (20), 3939–3948.

Foster, K., Baish, J., 2000. Viscous damping of vibrations in microtubules. J. Biol. Phys. 26 (4), 255–260.

Franklin, G., Powell, J., Emami-Naeini, A., Powell, J., 1994. Feedback Control of Dynamic Systems, vol. 2. Addison-Wesley Reading, MA.

Franosch, T., Grimm, M., Belushkin, M., Mor, F., Foffi, G., Forró, L., Jeney, S., 2011. Resonances arising from hydrodynamic memory in Brownian motion. Nature 478 (7367), 85–88.

Frauenfelder, H., Chen, G., Berendzen, J., Fenimore, P., Jansson, H., McMahon, B., Stroe, I., Swenson, J., Young, R., 2009. A unified model of protein dynamics. Proc. Natl. Acad. Sci. U.S.A. 106 (13), 5129.

Fröhlich, H., 1968. Long-range coherence and energy storage in biological systems. Int. J. Quant. Chem. 2, 641–649.

Gan, Y., 2009. Atomic and subnanometer resolution in ambient conditions by atomic force microscopy. Surf. Sci. Rep. 64 (3), 99–121.

Gittes, F., Schmidt, C., 1998. Thermal noise limitations on micromechanical experiments. Eur. Biophys. J. 27 (1), 75–81.

Gov, N., Safran, S., 2005. Red blood cell membrane fluctuations and shape controlled by ATP-induced cytoskeletal defects. Biophys. J. 88 (3), 1859–1874.

Grundler, W., Keilmann, F., 1983. Sharp resonances in yeast growth prove nonthermal sensitivity to microwaves. Phys. Rev. Lett. 51 (13), 1214–1216.

Guérin, T., Prost, J., Martin, P., Joanny, J., 2010. Coordination and collective properties of molecular motors: theory. Curr. Opin. Cell Biol. 22 (1), 14–20.

Havelka, D., Cifra, M., Kucera, O., Pokorny, J., Vrba, J., 2011a. High-frequency electric field and radiation characteristics of cellular microtubule network. J. Theor. Biol.

Havelka, D., Cifra, M., Kučera, O., Pokorný, J., Vrba, J., 2011b. High-frequency electric field and radiation characteristics of cellular microtubule network. J. Theor. Biol. 286, 31–40, URL http://www.sciencedirect.com/science/article/pii/S0022519311003511.

He, H., Kong, S., Chan, K.,2008. First Optical Observation of Periodic Motion of Native Human Cancer Cells. In: CLEO. Optical Society of America.

Hrazdira, I., Skorpikova, J., Dolnikova, M., 1998. Ultrasonically induced alterations of cultured tumour cells. Eur. J. Ultrasound 8 (1), 43–49.

Hudspeth, A., Choe, Y., Mehta, A., Martin, P., 2000. Putting ion channels to work: mechanoelectrical transduction, adaptation, and amplification by hair cells. Proc. Natl. Acad. Sci. U.S.A. 97 (22), 11765.

Ingber, D., Dike, L., Hansen, L., Karp, S., Liley, H., Maniotis, A., McNamee, H., Mooney, D., Plopper, G., Sims, J., et al., 1994. Cellular tensegrity: exploring how mechanical changes in the cytoskeleton regulate cell growth, migration, and tissue pattern during morphogenesis. Int. Rev. Cytol. 150, 173–224.

Janča, R., 2011. Neural network analysis of electrodynamic activity of yeast cells around 1 kHz. In: Journal of Physics: Conference Series, vol. 329. IOP Publishing, p. 012037.

Jelínek, F., Cifra, M., Pokorný, J., Hašek, J., Vaniš, J., Šimša, J., Frýdlová, I., 2009. Measurement of electrical oscillations and mechanical vibrations of yeast cells membrane around 1 kHz. Electromagn. Biol. Med. 28 (2), 223–232.

Jülicher, F., 2001. Mechanical oscillations at the cellular scale. Comptes Rendus de l'Académie des Sciences-Series IV-Physics 2 (6), 849–860.

Jülicher, F., Prost, J., 1997. Spontaneous oscillations of collective molecular motors. Phys. Rev. Lett. 78 (23), 4510–4513.

Kaatze, U., Feldman, Y., 2006. Broadband dielectric spectrometry of liquids and biosystems. Meas. Sci. Technol. 17, R17.

Kalinin, S., Rodriguez, B., Jesse, S., Karapetian, E., Mirman, B., Eliseev, E., Morozovska, A., 2007. Nanoscale electromechanics of ferroelectric and biological systems: a new dimension in scanning probe microscopy. Annu. Rev. Mater. Res. 37, 189–238.

Karsenti, E., 2008. Self-organization in cell biology: a brief history. Nat. Rev. Mol. Cell Biol. 9 (3), 255–262.

Kasas, S., Cibert, C., Kis, A., De Los Rios, P., Riederer, B.M., Forró, L., Dietler, G., Catsicas, S., 2004. Oscillation modes of microtubules. Biol. Cell 96 (9), 697–700, URL http://www.biolcell.org/boc/096/boc0960697.htm.

Kruse, K., Jülicher, F., 2005. Oscillations in cell biology. Curr. Opin. Cell Biol. 17 (1), 20–26.

Kruse, K., Riveline, D., 2011. Spontaneous mechanical oscillations: implications for developing organisms. Curr. Top. Dev. Biol. 95, 67–91.

Kučera, O., Cifra, M., Pokorný, J., 2010. Technical aspects of measurement of cellular electromagnetic activity. Eur. Biophys. J. 39 (10), 1465–1470.

Lehn, J., 2002. Toward self-organization and complex matter. Science 295 (5564), 2400.

Leitner, D., Havenith, M., Gruebele, M., 2006. Biomolecule large-amplitude motion and solvation dynamics: modelling and probes from thz to X-rays. Int. Rev. Phys. Chem. 25 (4), 553–582.

Martin, A., Kaschube, M., Wieschaus, E., 2008. Pulsed contractions of an actin-myosin network drive apical constriction. Nature 457 (7228), 495–499.

Morgan, H., Green, N., 1997. Dielectrophoretic manipulation of rod-shaped viral particles. J. Electrostat. 42 (3), 279–293.

Mosbacher, J., Langer, M., Horber, J., Sachs, F., 1998. Voltage-dependent membrane displacements measured by atomic force microscopy. J. Gen. Physiol. 111 (1), 65–74, URL http://jgp.rupress.org/cgi/content/abstract/111/1/65.

Mozziconacci, J., Sandblad, L., Wachsmuth, M., Brunner, D., Karsenti, E., 2008. Tubulin dimers oligomerize before their incorporation into microtubules. PLoS ONE 3 (11), e3821.

Nam, J., Fettiplace, R., 2008. Theoretical conditions for high-frequency hair bundle oscillations in auditory hair cells. Biophys. J. 95 (10), 4948–4962.

Norris, V., Hyland, G., 1997. Microcorrespondence: do bacteria sing? Mol. Microbiol. 24 (4), 879–880.

Oppenheim, A., Willsky, A., Nawab, S., 1996. Signals and Systems, 2nd ed. Prentice-Hall.

Park, E., Andrews, S., Hu, R., Boxer, S., 1999. Vibrational stark spectroscopy in proteins: a probe and calibration for electrostatic fields. J. Phys. Chem. B 103 (45), 9813–9817.

Parot, P., Dufrêne, Y., Hinterdorfer, P., Le Grimellec, C., Navajas, D., Pellequer, J., Scheuring, S., 2007. Past, present and future of atomic force microscopy in life sciences and medicine. J. Mol. Recogn. 20 (6), 418–431.

Pelling, A., Nicholls, B., Silberberg, Y., Horton, M., 2007a. Approaches for investigating mechanobiological dynamics in living cells with fluorescence and atomic force microscopies. Modern Res. Educ. Top. Microsc. 3, 3–10.

Pelling, A., Sehati, S., Gralla, E., Valentine, J., Gimzewski, J., 2004a. Local nanomechanical motion of the cell wall of *Saccharomyces cerevisiae*. Science 305 (5687), 1147.

Pelling, A., Veraitch, F., Pui-Kei Chu, C., Nicholls, B., Hemsley, A., Mason, C., Horton, M., 2007b. Mapping correlated membrane pulsations and fluctuations in human cells. J. Mol. Recogn. 20 (6), 467–475.

Pelling, A.E., Sehati, S., Gralla, E.B., Gimzewski, J.K., 2005. Time dependence of the frequency and amplitude of the local nanomechanical motion of yeast. Nanomed.: Nanotechnol. Biol. Med. 1, 178–183.

Pelling, A.E., Sehati, S., Gralla, E.B., Valentine, J.S., Gimzewski, J.K., 2004b. Local nanomechanical motion of the cell wall of *Saccharomyces cerevisiae*. Science 305, 1147–1150.

Piga, R., Micheletto, R., Kawakami, Y., 2007. Acoustical nanometre-scale vibrations of live cells detected by a near-field optical setup. Opt. Expr. 15 (9), 5589–5594.

Pohl, H.A., Braden, T., Robinson, S., Piclardi, J., Pohl, D.G., 1981. Life cycle alterations of the micro-dielectrophoretic effects of cells. J. Biol. Phys. 9, 133–154.

Pokorný, J., 2001. Endogenous electromagnetic forces in living cells: implication for transfer of reaction components. Electro- Magnetobiol. 20 (1), 59–73.

Pokorný, J., 2009. Biophysical cancer transformation pathway. Electromagn. Biol. Med. 28 (2), 105–123.

Pokorný, J., 2012. Physical aspects of biological activity and cancer. AIP Advances 2 (1), 011207.

Pokorný, J., Hašek, J., Jelínek, F., 2005a. Electromagnetic field in microtubules: effects on transfer of mass particles and electrons. J. Biol. Phys. 31 (3-4), 501–514.

Pokorný, J., Hašek, J., Jelínek, F., 2005b. Endogenous electric field and organization of living matter. Electromagn. Biol. Med. 24 (3), 185–197.

Pokorný, J., Hašek, J., Jelínek, F., Šaroch, J., Palán, B., 2001. Electromagnetic activity of yeast cells in the M phase. Electro- Magnetobiol. 20 (1), 371–396.

Pokorný, J., Jelínek, F., Trkal, V., Lamprecht, I., Hölzel, R., 1997. Vibrations in micro-tubules. J. Biol. Phys. 23, 171–179.

Pokorný, J., Vedruccio, C., Cifra, M., Kučera, O., 2011a. Cancer physics: diagnostics based on damped cellular elastoelectrical vibrations in microtubules. Eur. Bio-phys. J., 1–13.

Pokorný, J., Vedruccio, C., Cifra, M., Kučera, O., 2011b. Cancer physics: diagnostics based on damped cellular elastoelectrical vibrations in microtubules. Eur. Bio-phys. J. 40 (6), 747–759.

Portet, S., Tuszyński, J.A., Hogue, C.W.V., Dixon, J.M., 2005. Elastic vibrations in seam-less microtubules. Eur. Biophys. J. 34 (7), 912–920.

Preto, J., Pettini, M., 2012. Long-range resonant interactions in biological systems. Arxiv preprint arXiv:1201.5187.

Qian, X.S., Zhang, J.Q., Ru, C.Q., 2007. Wave propagation in orthotropic microtubules. J. Appl. Phys. 101 (8), 084702, URL http://link.aip.org/link/?JAP/101/084702/1.

Reed, J., Ramakrishnan, S., Schmit, J., Gimzewski, J., 2009. Mechanical interferometry of nanoscale motion and local mechanical properties of living zebrafish embryos. ACS Nano 3 (8), 2090–2094.

Regal, C., Lehnert, K., 2011. From cavity electromechanics to cavity optomechanics. In: Journal of Physics: Conference Series, vol. 264. IOP Publishing, p. 012025.

Reimers, J.R., McKemmish, L.K., McKenzie, R.H., Mark, A.E., Hush, N.S., 2009. Weak, strong, and coherent regimes of Fröhlich condensation and their applications to terahertz medicine and quantum consciousness. Proc. Natl. Acad. Sci. U.S.A. 106 (11), 4219–4224, URL http://www.pnas.org/content/106/11/4219.abstract.

Robinson, J., Jorgolli, M., Shalek, A., Yoon, M., Gertner, R., Park, H., 2012. Vertical nanowire electrode arrays as a scalable platform for intracellular interfacing to neuronal circuits. Nat. Nanotechnol.

Rohrbach, A., Tischer, C., Neumayer, D., Florin, E., Stelzer, E., 2004. Trapping and tracking a local probe with a photonic force microscope. Rev. Sci. Instrum. 75, 2197.

Sahu, S., Ghosh, S., Hirata, K., Fujita, D., Bandyopadhyay, A. Ultra-fast condensation of tubulins into microtubule unravels a generic resonance engineering. Nat. Mater., in press.

Samarbakhsh, A., Tuszynski, J., 2011. Vibrational dynamics of bio- and nano-filaments in viscous solution subjected to ultrasound: implications for microtubules. Eur. Biophys. J., 1–10.

Silberberg, Y., Pelling, A., Yakubov, G., Crum, W., Hawkes, D., Horton, M., 2008. Mito-chondrial displacements in response to nanomechanical forces. J. Mol. Recogn. 21 (1), 30–36.

Simonson, T., 2003. Electrostatics and dynamics of proteins. Rep. Progr. Phys. 66, 737.

Sirenko, Y.M., Stroscio, M.A., Kim, K.W., Jan 1996. Elastic vibrations of microtubules in a fluid. Phys. Rev. E 53 (1), 1003–1010.

Sumino, Y., Nagai, K.H., Shitaka, Y., Tanaka, D., Yoshikawa, K., Chate, H., Oiwa, K., 2012. Large-scale vortex lattice emerging from collectively moving micro-tubules. Nature 483 (7390), 448–452.

Suresh, S., 2007. Biomechanics and biophysics of cancer cells. Acta Mater. 55, 3989–4014.

Taber, L., 2008. Theoretical study of beloussov's hyper-restoration hypothesis for mechanical regulation of morphogenesis. Biomech. Model. Mechanobiol. 7 (6), 427–441.

Tang, J., Szymanski, P., Janmey, P., Tao, T., 1997. Electrostatic effects of smooth muscle calponin on actin assembly. Eur. J. Biochem. 247 (1), 432–440.

Tian, B., Cohen-Karni, T., Qing, Q., Duan, X., Xie, P., Lieber, C., 2010. Three-dimensional, flexible nanoscale field-effect transistors as localized bioprobes. Science 329 (5993), 830.

Tuszyński, J., Brown, J., Crawford, E., Carpenter, E., Nip, M., Dixon, J., Sataric, M., 2005a. Molecular dynamics simulations of tubulin structure and cal-culations of electrostatic properties of microtubules. Math. Comput. Model. 41 (10), 1055–1070, URL http://www.sciencedirect.com/science/article/B6V0V-4HBSKN3-2/2/696be29f0574687723502f8017c628c5.

Tuszyński, J.A., Luchko, T., Portet, S., Dixon, J.M., may 2005. Anisotropic elastic properties of microtubules. Eur. Phys. J. E 17 (1), 29–35, URL http://dx.doi.org/10.1140/epje/i2004-10102-5.

Verhagen, E., Deléglise, S., Weis, S., Schliesser, A., Kippenberg, T., 2012. Quantum-coherent coupling of a mechanical oscillator to an optical cavity mode. Nature 482 (7383), 63–67.

Voïtchovsky, K., Contera, S.A., Ryan, J.F., 2007. Electrostatic and Steric Interactions Determine Bacteriorhodopsin Single-Molecule Biomechanics. Biophys. J. 93 (6), 2024–2037.

Wang, C., Li, C., Adhikari, S., 2009. Dynamic behaviors of microtubules in cytosol. J. Biomech. 42 (9), 1270–1274.

Wang, C., Ru, C., Mioduchowski, A., 2006. Vibration of microtubules as orthotropic elastic shells. Phys. E: Low-dimension. Syst. Nanostruct. 35 (1), 48–56, URL http://www.sciencedirect.com/science/article/B6VMT-4KJTNT4-2/2/c937e65ac2d9b1c7e4f0449b66f544b0.

Wang, C., Zhang, L., 2008a. Circumferential vibration of microtubules with long axial wavelength. J. Biomech. 41 (9), 1892–1896.

Wang, C., Zhang, L., 2008b. Circumferential vibration of microtubules with long axial wavelength. J. Biomech. 41 (9), 1892–1896, URL http://www.sciencedirect.com/science/article/B6T82-4SN8VB1-3/2/b00ae1dc96171994c60cd3b63102c416.

WR Boyd, J., Varley, J., 2001. The uses of passive measurement of acous-tic emissions from chemical engineering processes. Chem. Eng. Sci. 56 (5), 1749–1767.

Zinin, P., Allen III, J., Levin, V., 2005. Mechanical resonances of bacteria cells. Phys. Rev. E 72 (6), 061907.

C | SUPPLEMENTARY DATA OF CHAPTER 4

This chapter include the supplementary data of Chapter 4.

Supplementary material to "High frequency electric field and radiation of cellular microtubule network"

D. Havelka[a], M. Cifra[b], O. Kučera[b,c], J. Pokorný[b,c], J. Vrba[a]

[a]*Department of Electromagnetic Field, Faculty of Electrical Engineering, Czech Technical University in Prague*
[b]*Institute of Photonics and Electronics, Academy of Sciences of the Czech Republic*
[c]*Department of Circuit Theory, Faculty of Electrical Engineering, Czech Technical University in Prague*
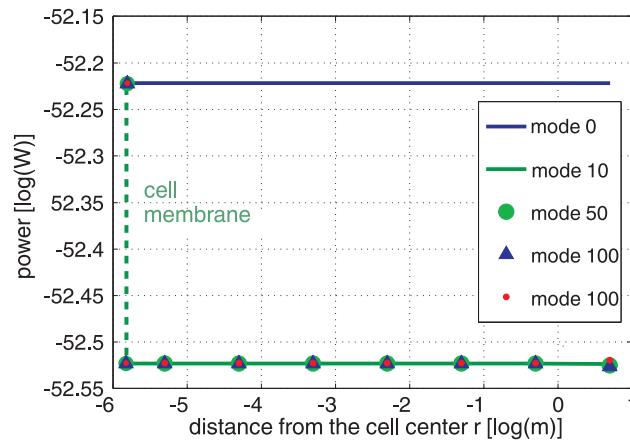
Figure 1: Power calculated from the cell membrane to the distance of 1 m for modes 0, 10, 50, 100 and 150. (symmetric model, frequency 1 kHz and lossless medium)
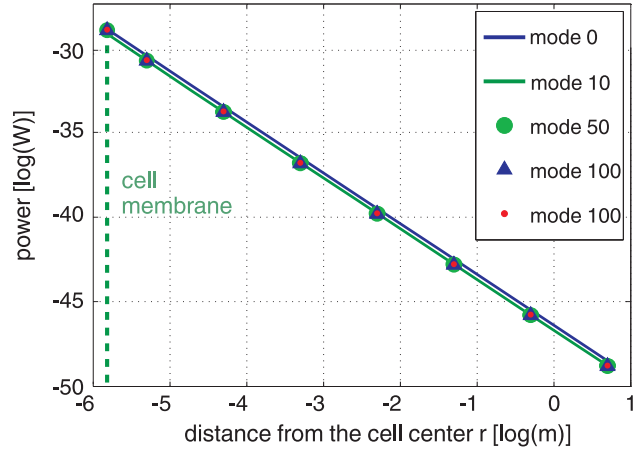
Figure 2: Power calculated from the cell membrane to the distance of 1 m for modes 0, 10, 50, 100 and 150. (symmetric model, frequency 1 kHz and lossy medium)
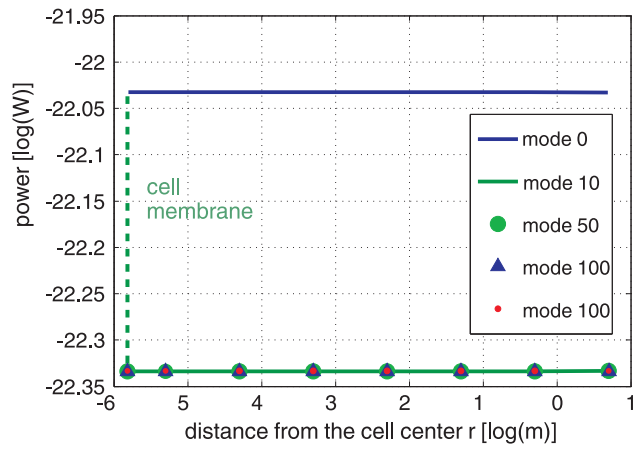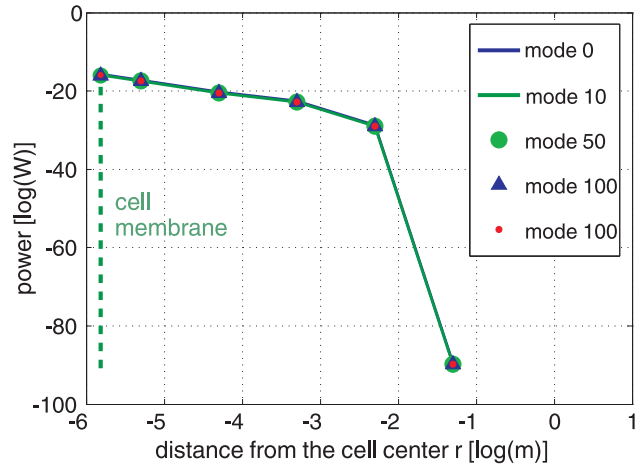

Figure 3: Power calculated from the cell membrane to the distance of 1 m for modes 0, 10, 50, 100 and 150. (symmetric model, frequency 42 GHz and lossless medium)

2

Figure 4: Power calculated from the cell membrane to the distance of 1 m for modes 0, 10, 50, 100 and 150. (symmetric model, frequency 42 GHz and lossy medium)
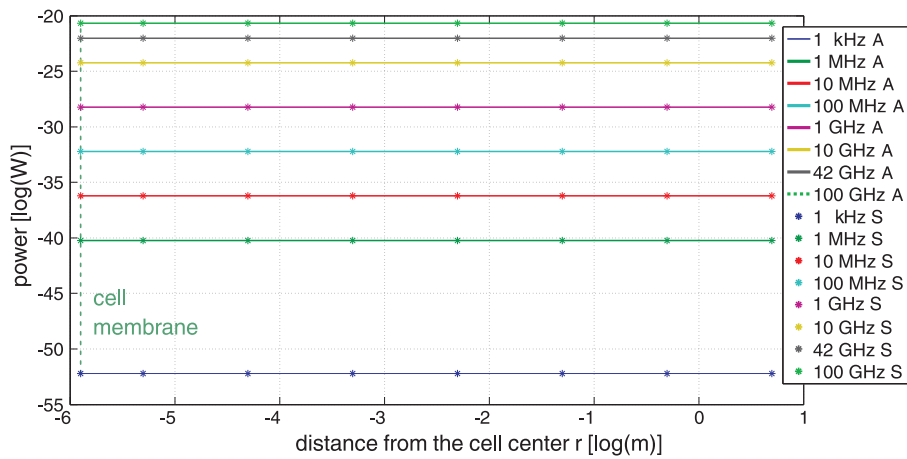

Figure 5: Comparison of asymmetric (A) and symmetric (S) models. Power calculated from the cell membrane to the distance of 1 m for 8 frequencies in lossless medium
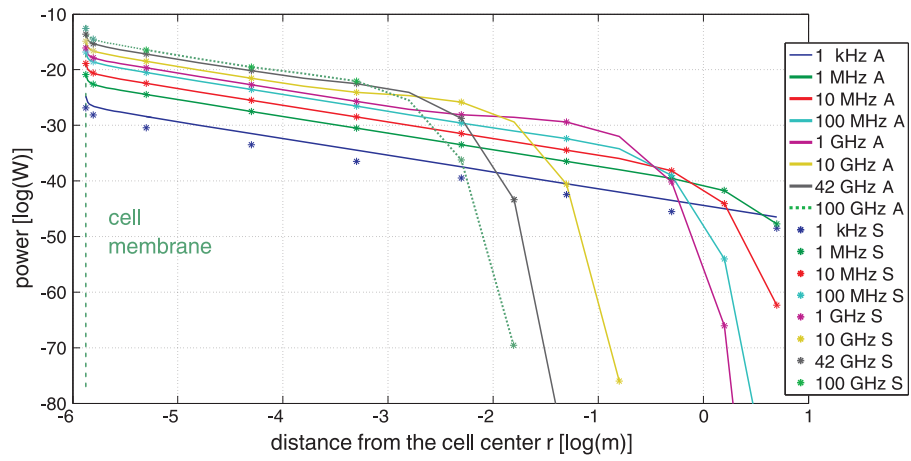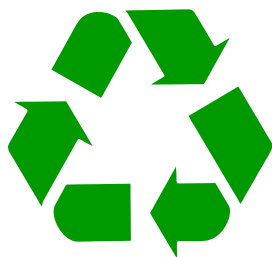
3

Figure 6: Comparison of asymmetric (A) and symmetric (S) models. Power calculated from the cell membrane to the distance of 1 m for 8 frequencies in lossy medium

4

CURRICULUM VITAE

1. March 1982
| Born, Dvůr Kálové nad Labem, Czechia

2001 – 2008
| Bc. (B.S.) Electronics and Communication Technology
Czech Technical University in Prague
Prague, Czechia

2005 – 2006
| Supervisor
House Services Ltd. and Clean Attack Ltd.
Prague, Czechia

2008 – 2010
| Ing. (MSc. with Honors) Telecommunications and Radio-engineering: High-frequency and Microwave Technology
Czech Technical University in Prague
Prague, Czechia

2010
| Dean's Prize for the outstanding diploma thesis

2010
| Werner von Siemens Excellence Award in the category "The best diploma thesis"

2010
| The Prize of the MTT/AP/ED/EMC chapter of the Czechoslovak section of the IEEE for the outstanding diploma thesis

2010
| Diploma (3rd place) from Natural Sciences section of the 14th International Student Conference on Electrical Engineering - POSTER 2010

2010 – 2014
| Doctoral study program: Electrical Engineering and Information Technology
Czech Technical University in Prague
Prague, Czechia

2011
| Principal investigator
Grant No. SGS11/064/OHK4/1T/13 *Cellular electromagnetic field and its interactions with surrounding space*, Grant Agency of the Czech Technical University in Prague

2011
| Member of the Organizing Committee
EDALC11 conference
Prague, Czechia

2011
| Member of the Organizing Committee and Editing Committee
ISMOT 2011 conference,
Prague, Czechia

2012 – present
| Research staff
Institute of Photonics and Electronics, Academy of Sciences of the Czech Republic
Prague, Czechia

2013
| Principal investigator
Grant No. SGS13/077/OHK3/1T/13 *Study of electromagnetic processes in biomolecules, cells and tissue*, Grant Agency of the Czech Technical University in Prague

Až dosloužím, chci do sběru!